Naval Research Laboratory
Stennis Space Center, MS 39529-5004

NRL/MR/7320--13-9476

Model Verification and Validation Using Graphical Information Systems Tools

Timothy R. Keen
James D. Dykes

Ocean Dynamics and Prediction Branch
Oceanography Division

July 31, 2013

Approved for public release; distribution is unlimited.

REPORT DOCUMENTATION PAGE

Form Approved
OMB No. 0704-0188

Public reporting burden for this collection of information is estimated to average 1 hour per response, including the time for reviewing instructions, searching existing data sources, gathering and maintaining the data needed, and completing and reviewing this collection of information. Send comments regarding this burden estimate or any other aspect of this collection of information, including suggestions for reducing this burden to Department of Defense, Washington Headquarters Services, Directorate for Information Operations and Reports (0704-0188), 1215 Jefferson Davis Highway, Suite 1204, Arlington, VA 22202-4302. Respondents should be aware that notwithstanding any other provision of law, no person shall be subject to any penalty for failing to comply with a collection of information if it does not display a currently valid OMB control number. **PLEASE DO NOT RETURN YOUR FORM TO THE ABOVE ADDRESS.**

1. REPORT DATE *(DD-MM-YYYY)*	**2. REPORT TYPE**	**3. DATES COVERED** *(From - To)*
31-07-2013	Memorandum Report	

4. TITLE AND SUBTITLE

Model Verification and Validation Using Graphical Information Systems Tools

5a. CONTRACT NUMBER

5b. GRANT NUMBER

5c. PROGRAM ELEMENT NUMBER
0601153N

6. AUTHOR(S)

Timothy R. Keen and James D. Dykes

5d. PROJECT NUMBER

5e. TASK NUMBER

5f. WORK UNIT NUMBER
73-4261-02-5

7. PERFORMING ORGANIZATION NAME(S) AND ADDRESS(ES)

Naval Research Laboratory
Oceanography Division
Stennis Space Center, MS 39529-5004

8. PERFORMING ORGANIZATION REPORT NUMBER

NRL/MR/7320--13-9476

9. SPONSORING / MONITORING AGENCY NAME(S) AND ADDRESS(ES)

Office of Naval Research
One Liberty Center
875 North Randolph Street, Suite 1425
Arlington, VA 22203-1995

10. SPONSOR / MONITOR'S ACRONYM(S)

ONR

11. SPONSOR / MONITOR'S REPORT NUMBER(S)

12. DISTRIBUTION / AVAILABILITY STATEMENT

Approved for public release; distribution is unlimited.

13. SUPPLEMENTARY NOTES

14. ABSTRACT

This report is the Software Development Plan (SDP) for an ArcGIS module called Model Verification and Validation (MVV). The software's purpose is to assist an expert analyst in evaluating the accuracy of model forecasts of currents in coastal areas. The MVV module is implemented as part of the Geospatial Analysis and Model Evaluation Software (GAMES) library. This report describes the components of the SDP: (1) conceptual model (data structures and theory); (2) logical model (methods); (3) physical model (code); and (4) demonstrations. The data structure utilizes ocean and coastal features that are instantiated from model predictions and validation data sources. The logical model implements computer-based tools to compare these instantiations. The software consists of modular code that is compatible with other GAMES modules (e.g., ARCOAS). The system is demonstrated for models of the northern Gulf of Mexico and Yellow Sea.

15. SUBJECT TERMS

Coastal currents
ArcGIS
Computer software
Model validation

16. SECURITY CLASSIFICATION OF:			**17. LIMITATION OF ABSTRACT**	**18. NUMBER OF PAGES**	**19a. NAME OF RESPONSIBLE PERSON**
a. REPORT	**b. ABSTRACT**	**c. THIS PAGE**			Timothy Keen
Unclassified Unlimited	Unclassified Unlimited	Unclassified Unlimited	Unclassified Unlimited	108	**19b. TELEPHONE NUMBER** *(include area code)* (228) 688-4950

Standard Form 298 (Rev. 8-98)
Prescribed by ANSI Std. Z39.18

Table of Contents

Executive Summary

The Model Verification and Validation (MVV) project was tasked with developing an algorithm, and the necessary software components, to assist a subject matter expert (SME) in verifying and validating the predicted currents from a coastal model forecast. Here we intend that verification is a confirmation of the competency of the forecast (i.e., realistic and consistent) whereas validation is meant as an official statement of its accuracy. This task is addressed through the following objectives: (1) identify potential validation data sources; (2) develop a methodology to validate the currents from a forecast model; (3) develop the necessary software tools; and (4) demonstrate its applicability and demonstrate the MVV procedure for several regions. This document addresses objectives (1), (2), and (5) by outlining the overall conceptual model being used to develop the methodology and software, and demonstrating it with examples. This document is the software development plan (SDP) for the developers of the software system. A user guide is included as an appendix.

The MVV algorithm and software are based on a feature data model. The data model is employed to document and organize the data and processes within the system, and improve communication between the developers. The data model is thus primarily intended for the use of the system designers and programmers but it may also prove helpful for MVV software users. The data model consists of three components: a conceptual data model; a logical process model; and a physical process model.

The problem of verifying the realism of a forecast model is simplified by the use of features. We define a feature to be a distinctive attribute or aspect of the ocean. Although ocean features are 3D in general (e.g., an eddy), they are treated as primarily 2D for MVV. We also introduce the concept of a time-dependent feature, such as a time series of tidal currents. We extend this concept to meteorological features like frontal systems, and geographic features like the shoreline. Features are useful because they simplify superimposed processes that are not naturally comparable in space and time. MVV uses three categories of ocean features: circular flows like eddies and island wakes; linear flows like squirts, filaments, fronts, and shelf currents; and special flows like river plumes, coastal currents, and tidal currents. Features are the basic entity of MVV because they can be identified in model-predicted fields and in validation data.

Ocean features are incompletely sampled by most ocean observations; this may also be true of a numerical model, even though it calculates gridded fields of variables, because the feature may be weak or poorly represented in the model. This introduces the concept of a feature instantiation, which is a concrete or tangible example of the abstract concept referred to by a feature name (e.g., a river plume). Features may be instantiated using multiple ocean variables (e.g., temperature and currents) from validation data or model fields. MVV is accomplished by comparing the validation and model feature instantiations.

The conceptual data model represents the physical relationships between currents and ocean features. Ocean currents must often be estimated from features because they are infrequently measured as fields that can be directly compared to a model. Ocean flows, which are organized

current systems, transport heat and salinity and cause water to pile up as a water surface anomaly. The general nature of the transporting flow can be inferred from the resulting features although the exact currents cannot be known. This transfer of information from small-scale currents to large-scale ocean features is accompanied by a loss of detail. This gap is bridged by the user (e.g., SME), who must infer the original flow characteristics from the feature instantiations using the MVV software. An additional complexity that is handled by the user with the help of the MVV software is the impact of meteorological and geographic features on ocean features and their associated currents.

The logical process model focuses on the relationships between currents and features (ocean, atmosphere, and geographic). A time/location-stamped dataset from a model or validation source is an entity that is related to other entities by processes that are understood, at least conceptually. For example, currents transport heat in a rotating flow to form an eddy. The following relationships (i.e., processes) are implemented in the MVV system: (i) shoreline impacts; (ii) shelf seafloor profiles, which influence subsurface ocean currents; (iii) geographic effects on estuarine flows; (iv) changing water depths with tidal flow; (v) eddies and fronts; (vi) upwelling flows; (vii) river plumes and coastal jets; (viii) random processes that are represented by statistical analyses; and (ix) coastal meteorology. The applicable relationships are applied to multiple data entities to instantiate a validation feature, which is then compared to the model instantiation. The MVV system uses a set of rules to compare the model and validation features. The rules are implemented as instructions for feature instantiation and guides to interpretation of the resulting comparison. They are applied sequentially in order of the decreasing impacts of the data used to instantiate a validation feature (e.g., shoreline->bathymetry->in-situ observations->satellite images->historical observations->supplementary models->weather analysis).

The physical process model consists of the tools and functions to accomplish the tasks required for processes (i) through (ix). Many of these functions are available through ArcGIS software. New functions are included within a validation box tool, a shoreline/seafloor profile tool, toolkits for satellite images, historical data, feature instantiation, and weather analysis, a model grid transform tool, and a process flow tool. The MVV software generates a model validation file (*.mvv) for later reference.

The method has been developed using a model simulation for the Mississippi Bight in the northern Gulf of Mexico. The primary interest of this model simulation was the response of the sounds within this area to spring cold fronts, although the entire year was simulated as part of another project. No concurrent validation data were available. An accurate shoreline was digitized from Google Earth. Historical observations consisted of time series of currents from March 1997 and water levels from December 2005, satellite images from March 2005 and 2008, and tidal elevations from the International Hydrographic Office. There were also predictions from other models for March 1997, as well as hurricanes in 1947 and 1969. These data and the model results were used to create instantiations of the shoreline, filaments, tidal elevation, and water patches in the sounds, eddies offshore, and plume-like flows through tidal passes. MVV was applied to three regional boxes with common characteristics: (A) deep water in the bight; (B) Mississippi sound in the north; and (C) the bird-foot delta in the SW. The model instantiation rules were applied to each box independently and an optional scoring system was used to rank the model currents as follows. Though there were very little validation data for comparison, Box

A received a perfect score, mainly because it has a coastline only along the Chandeleur Islands, which was accurate in the model grid. Box B was okay (score = 0.5), because tidal heights were low and the postfrontal flow was meteorologically unrealistic (probably because of the low-resolution model wind). Box C was ranked poor with a score of 0.25, because of multiple shoreline and water depth problems and even worse tidal height prediction.

This software is intended to improve the consistency of validation for models applied to coastal areas. The use of a quantitative score is valuable in assuring consistency in model ranking; two potential scoring methods are demonstrated. A multiplicative score is sensitive to poor performance but does not account for a lack of validation data; thus, a model with no validation receives a high score. An alternative additive score penalizes the model where no validation data are available but it is more subjective. The goal of consistency is also supported by the use of a unique file for each validation. The contents and appropriate archive and reuse of this file should be discussed by users. There are a number of semi-dynamic feature models that could be considered, but none have been implemented because of the potential for a substantial effort with minimal improvement in the ranking. The weighting of validation data should be examined by users.

Section 1: Project Overview

Introduction

The motion within the littoral zone (continental shelf) is the result of complex interactions between oceanic flows, the seafloor, the shoreline, water input from rivers, and the atmosphere. In order to make sense of the resulting observable flows, it is convenient to use feature models that can be easily identified from multiple observations. These compound realizations can then be used to validate the model-instantiated features, which are embedded in sometimes poorly reproduced flows in the models. We have reduced the set of features to a small subset to simplify this analysis. Part of the motivation is to use features that can be readily used in model validation. For example, we can identify circular, linear, and oscillating patterns. The superpositioning of these multiple processes makes the reproduction of shelf currents an important validation tool for a coastal model (e.g., Dzwonkowski and Park, 2010; Matano et al., 2010). This interaction makes interannual variability (Flagg et al., 2006) of currents in the shelf-break frontal region an important consideration in evaluating model performance as well.

This list includes the Wiki pages that comprise the on-line version of this document. These pages are listed in the order in which they are printed as an NRL Memorandum Report.

Upon observing the ocean, whether from space or on an office globe, it is apparent that its surface is represented by features of different types and sizes (*e.g.*, western boundary currents, eddies, river plumes). These features result from the interaction of atmospheric, terrestrial, biological, and oceanographic processes. The fundamental (and implicit) goal of ocean modeling is to reproduce these features. This is nowhere more important than in the coastal ocean (*i.e.*, continental shelf, estuaries, and bays). In order to validate numerical model predictions of coastal flows and their causative currents, it is thus necessary to evaluate how well they reproduce these features.

Objectives

Develop a methodology for analyzing forecasts from high-resolution regional ocean models including verification and validation of modeled currents, especially in areas where validation data are not readily available. For useful information in the analysis, various data sources are identified for mining and may include but are not limited to published data, ocean observations, remotely sensed measurements, and climatology. We will identify applications of the various forms of data, *e.g.* bathymetry from other sources compared to the bottom boundary conditions of the model to determine the probability of model error due to coastal/bathymetry errors and problematic morphology. Some data may require processing for application--*e.g.* calculation of long-term and seasonal statistics of historical data collected in the area of interest to identify seasonal and diurnal patterns, and annual scales of predominant ocean features. Software is developed as necessary to assist the model analyst in using tide and velocity data and/or methods in determining model accuracy for currents. Three domains from a high-resolution ocean model

Manuscript approved July 2, 2013.

are targeted for analysis and used for demonstration of the methodology. The primary focus is on the modeled parameters of currents including phase, speed and direction.

Oceanographic Feature Data Model

A data model is an abstract concept that documents and organizes processes and data for communication between system components, and which is used as a plan for developing applications. The main aim of the data model is to support development of the analysis system by providing the definition and format of the data. This improves communication between developers and also increases precision in applying the rules that govern the data model.

There are several approaches that can be used to validate simulated currents using sparse data. Whichever is used, it is necessary to bring the validation and model data into a common data model, which incorporates the data types, the data formats, and the software environment (*e.g.*, ARCOAS) that is to be used for the comparison. This effort is based on the common occurrence of current fields in the ocean associated with *oceanographic features.* The data model applied to the verification and validation of ocean currents in coastal areas is thus based on *features*. The feature model that is used for this effort will incorporate three perspectives:

- Conceptual Data Model: describes the types of data and their relationships.
- Logical Process Model: semantics of the model (e.g., processing steps).
- Physical Process Model: program units, etc.

In this document, a database is used in reference to a unique set of data inputs and analysis results be used for a specific model analysis task. General archives of model results or geophysical data are referred to using a specific name. This nomenclature is adopted in order to focus on the unique combination of data sources as well as derived data types that are necessary for the analysis activity. These mixed data types are inserted into a specific (time and place) model analysis database, which is only one realization of the many such analyses that can be generated. This database will then be stored for future reference. This database is thus analogous to a "Project File".

Document Organization

This document contains the Software Development Plan (SDP) for the MV&V software in addition to several examples and applications. It consists of the following sections:

- Section 1: Background, schedule, and overview of the system approach
- Section 2: Description of the Conceptual Data Model, which is the foundation of the software
- Section 3: Description of the Logical Process Model, the method by which the validation procedure is accomplished
- Section 4: Description of the Physical Process Model, the actual programs and functions that accomplish the work
- Section 5: Applications
- Section 6: Appendices

References

Dzwonkowski, B., and K. Park (2010), Influence of wind stress and discharge on the mean and seasonal currents on the Alabama shelf of the northeastern Gulf of Mexico, *J. Geophys. Res.*, 115, C12052, doi:10.1029/2010JC006449.

Flagg, C. N., M. Dunn, D.-P. Wang, H. T. Rossby, and R. L. Benway (2006), A study of the currents of the outer shelf and upper slope from a decade of shipboard ADCP observations in the Middle Atlantic Bight, *J. Geophys. Res.*, 111, C06003, doi:10.1029/2005JC003116.

Matano, R. P., Palma, E. D., and Piola, A. R.: The influence of the Brazil and Malvinas Currents on the Southwestern Atlantic Shelf circulation, *Ocean Sci.*, 6, 983-995, doi:10.5194/os-6-983-2010, 2010.

Section 2: Conceptual Data Model

Introduction

The conceptual data model discussed in this section is the foundation of the MV&V software. It comprises the fundamental entities and processes that are used in identifying and evaluating useful features in the ocean.

The motion within the littoral zone (continental shelf) is the result of complex interactions between oceanic flows, the seafloor, the shoreline, water input from rivers, and the atmosphere. In order to make sense of the resulting observable flows, it is convenient to use feature models that can be easily identified from multiple observations. These compound realizations can then be used to validate the model-instantiated features, which are embedded in sometimes poorly reproduced flows in the models. We have reduced the set of features to a small subset to simplify this analysis. Part of the motivation is to use features that can be readily used in model validation. For example, we can identify circular, linear, and oscillating patterns.

The superpositioning of these multiple processes makes the reproduction of shelf currents an important validation tool for a coastal model (e.g., Dzwonkowski and Park, 2010; Matano et al., 2010). This interaction makes interannual variability (Flagg et al., 2006) of currents in the shelf-break frontal region an important consideration in evaluating model performance as well.

The Data Structure Diagram

The model validation software system implements a data model for a data processing activity (i.e., sequential data analysis). The data entities processed by the system are either model data or validation data. Model validation fundamentally consists of a comparison of geophysical features as represented by these two data types. For our purposes, there are three kinds of such feature: weather patterns, ocean features, and geographic (i.e., geomorphological) features like coastlines. Our analysis will attempt to use the practical relationships between these features to estimate the validity of the forecast model's currents. This is problematic because currents are one of the basic data elements in the data structure. The Data Structure Diagram or DSD (Figure 2.1) is an abstraction that is *instantiated* for each data source to be used in the analysis. This report uses instantiation and realization interchangeably. These sources can be any available ocean data such as model results, satellite images, or glider observations. The top level of the DSD contains geophysical features: atmospheric flows, ocean flows, and coastal geomorphology.

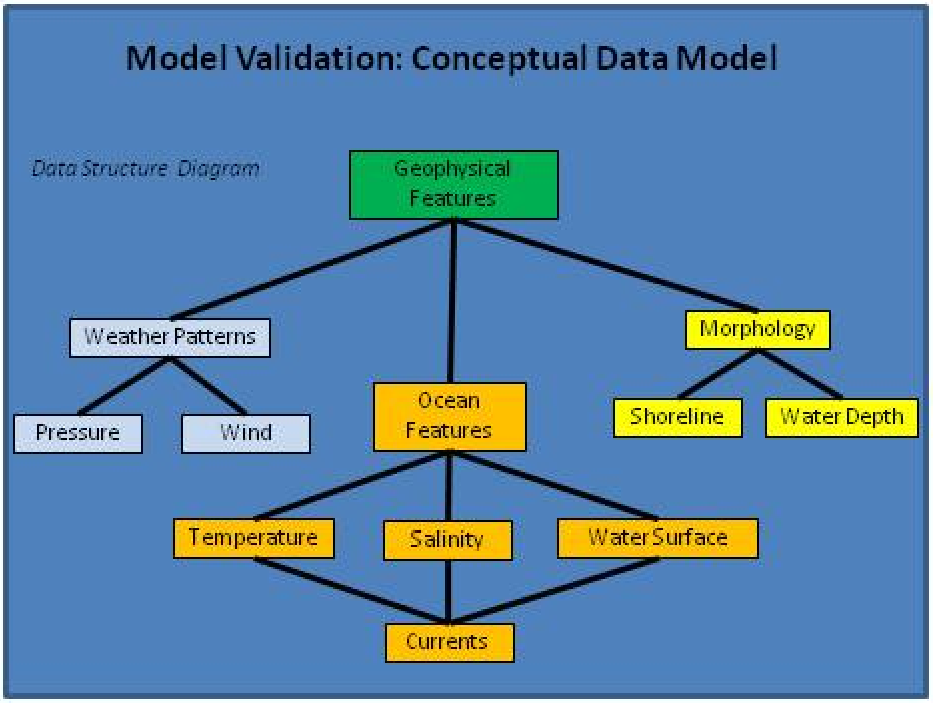

Figure 2.1. Data structure diagram for ocean data elements used for the analysis system.

The geophysical feature elements are built of sub-elements that can be directly measured by different means: the shoreline and water depth; water level; water temperature and salinity; atmospheric pressure; and wind speed and direction. The ocean feature sub-elements are themselves the result of mass conservation through hydrodynamics (*i.e.*, currents). In order to validate the currents predicted by a forecast model, we must use the relationships between these elements to construct a process model of the ocean domain of interest. For this we must define the processes (relationships) that have the highest potential for success.

Oceanographic Features

Circular Features

Eddies are common in the ocean, and range in diameter from centimeters, to hundreds of kilometers. The smallest scale eddies may last for a matter of seconds, while the larger features may persist for months to years.

Mesocale eddies are between about 10 and 500 km in diameter. The persist for periods of days to months. A mesoscale eddy may be formed when an ocean current, such as the Gulf Stream, develops an instability, which grows, causing the current to meander, and eventually forming an eddy that is pinched off from the meander. These eddies have been observed in many of the major ocean currents, including the Gulf Stream, the Agulhas Current, the Kuroshio Current, and the Antarctic Circumpolar Current, amongst others. Mesoscale eddies are characterized by currents which flow in a roughly circular motion around the center of the eddy. The rotation may be either cyclonic or anticyclonic. Oceanic eddies are also usually made of water masses that are different to those outside of the eddy, i.e. the water within an eddy usually has different temperature and salinity characteristics to the water outside of the eddy. There is a direct link between the water mass properties of an eddy and its rotation. Warm eddies rotate anti-cyclonically, while cold eddies rotate cyclonically.

A gyre is any large system of rotating ocean currents, particularly those involved with large wind movements. Gyres are caused by the Coriolis Effect; planetary vorticity along with horizontal and vertical friction, which determine the circulation patterns from the wind curl (torque). Major gyres that exist in the worlds' oceans are 1)Indian Ocean Gyre, 2)North Atlantic Gyre, 3)North Pacific Gyre, 4)South Atlantic Gyre, and 5)South Pacific Gyre. Other gyres include tropical gyres, subtropical gyres, and subpolar gyres.

Tropical gyres are less unified and tend to be mostly east-west with minor north-south extent.

- Atlantic Equatorial Current System (two counter-rotating circulations)
- Pacific Equatorial Current System
- Indian Monsoon Gyres (two counter-rotating circulations in northern Indian Ocean)

The center of a subtropical gyre is a high pressure zone. Circulation around the high pressure is clockwise in the northern hemisphere and counterclockwise in the southern hemisphere, due to the Coriolis effect. The high pressure in the center is due to the westerly winds on the northern side of the gyre and easterly trade winds on the southern side of the gyre. These cause frictional surface currents towards the latitude at the center of the gyre. The build-up of water in the center of the gyre creates equatorward flow in the upper 1,000 to 2,000 m (3,300 to 6,600 ft) of the ocean, through rather complex dynamics. This equatorward flow is returned poleward in an intensified western boundary current.

The intensified western boundary current of the North Atlantic Gyre is the Gulf Stream, in the North Pacific it's the Kuroshio Current, in the South Atlantic it's the Brazil Current, in the South Pacific it's the East Australian Current, and in the Indian Ocean it's the Agulhas Current.

Subpolar gyres form at high latitudes (around 60°). Circulation of surface wind and ocean water is anticlockwise in the Northern Hemisphere, around a low-pressure area, such as the persistent Aleutian Low and the Icelandic Low. Surface currents generally move outward from the center of the system. This drives the Ekman transport, which creates an upwelling of nutrient-rich water from the lower depths.

Subpolar circulation in the southern hemisphere is dominated by the Antarctic Circumpolar Current, due to the lack of large landmasses breaking up the Southern Ocean. There are minor gyres in the Weddell Sea and the Ross Sea, the Weddell Gyre and Ross Gyre, which circulate in a clockwise direction.

Vortices are the disturbances that occur due to turbulent flow when a fluid flows past an object. In the course of their formation, a row of vortices (*i.e.* von Karman vortex street) is generated downstream of the obstacle. The diameters of these vortices are from centimeters to kilometers. This phenomenon is associated with strong currents past islands. This is most common for small islands because of the limitations of the Rossby number on vortex generation (Gryanik et al., 2004). They have important implications on ecosystems (Haseqawa et al., 2009) and water properties (Burk et al., 2003), and can be observed from satellites (Caldeira et al., 2002). This makes it a useful validation feature when it can be observed and/or reproduced in a model (Dietrich et al.,1996).

Linear Flows

Linear flow features can be subdivided into those that are perpendicular to the coast (e.g., filaments) and those parallel to depth contours (e.g., shelf currents and fronts). Filaments, which are commonly associated with coastal upwelling, have been referred to as tongues (Ramp et al., 1991), plumes, and squirts (Flament, et al., 1985). These features are narrow jets that originate near the coast and transport cold, upwelled water several hundred kilometers offshore. They have been described on the California shelf (Brink, 1983) as well as South America (Figure 2.2).

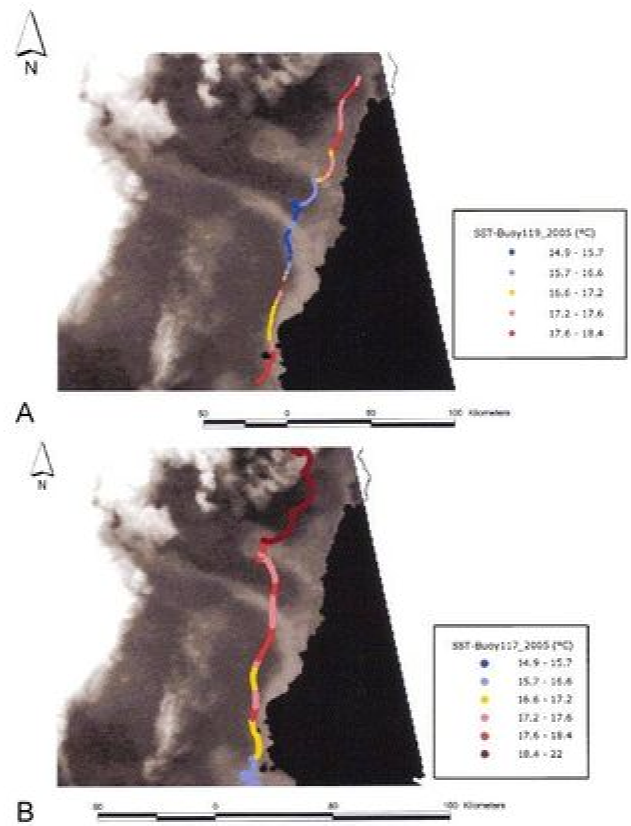

Figure 2.2. Satellite images of development of a cold-water squirt along the Chile coast (Marine et al., 2007).

Squirts are transverse jets (Matthews et al., 1993) that have been observed in surface currents and [Chl] from satellites. They are associated with eddy generation along fronts and convergence zones (Stern, 1986), and during coastal upwelling strongly controlled by coastal morphology (Zhurbas et al., 2008; Marin et al., 2003; Marin and Delgado, 2007). As such, they can be very important indicators of model performance if sufficient validation data are available to construct a feature. They can be identified in satellite images and with Lagrangian drifters like buoys.

These ageostrophic currents are associated with strong upwelling and thus can be difficult to reproduce in a primitive-equation (hydrostatic) circulation model. This makes them a good test of the model's applicability in regions where these processes have been observed.

Ocean flows and their associated currents occur at all depths at a range of time scales on the continental shelf. This section focuses on flows that are generally parallel to the depth contours at the shelf-break. These can be surface or bottom currents (Signorini et al., 1983; Johnson et al., 1975). These flows can develop a significant across-shelf component where they coincide with astronomical tides (Lam et al., 2004). Because of the expense of collecting 3D ADCP data of this type, these observations are most useful as historical records that indicate the seasonality of these currents.

There are many scales of motion on the continental shelf. Subtidal currents are low-frequency movement generated by shallow-water waves propagating in a direction determined by the Coriolis force. The coast is to the right of the direction of travel for the northern hemisphere. These waves include continental shelf waves (i.e., free waves) and coastal Kelvin waves. Shelf waves are generated by the alongshore component of the wind stress (Adams and Buchwald, 1969). The wind stress is important in generating shelf waves and their associated currents in shallower water on the shelf. Complex current systems are also associated with Rossby waves that are generated where deep-sea eddies interact with bottom topography (Zhang et al., 2011).

Oceanic fronts are boundaries between water masses with different characteristics, such as temperature, salinity, [Chl], nutrients, and currents. They commonly occur in these locations: (1) the boundary between a warm and a cold current; (2) the boundary between coastal and oceanic waters; (3) off estuaries; (4) along the margins of areas of upwelling; and (5) around banks, reefs, shoals, islands, and the shelf edge (Fearnhead, 1975). This makes them good candidates for validating coastal currents.

A thermal front is a zone with a pronounced horizontal temperature gradient (Ullman and Cornillon, 2001), whereas a haline front (Melling, 2003) exhibits a horizontal salinity gradient. Ocean fronts can extend from the surface to the very deep layers of the ocean and be semi-permanent or vary seasonally (Park and Chu, 2006; Hill and Simpson, 1989). The most useful fronts for validating coastal currents in forecast models are shelf sea fronts, which tend to be the boundaries between stratified and well-mixed regimes (Simpson and Bowers, 1981).

Fronts in shallow water are proposed to form when there is enough bottom-generated turbulence to prevent the formation of a seasonal thermocline. If the transition from stratified to mixed water occurs over a short distance, a geostrophic shear may be produced, which further strengthens the gradient. The source of turbulence is often tidal currents. These fronts display complex dynamics as tides and eddies interact with river discharge in variable water depths (Lwiza et al., 1991; Yanagi and Takahashi, 1988; Le Boyer et al., 2008).

The flow field associated with shelf fronts is highly variable and these features need to be used with some knowledge of the environment being considered. It is important to examine instantiations from multiple data sources before assigning a skill level to the simulated currents. For example, the predicted model currents can be evaluated in the context of the likelihood of a shelf front being present (Figure 2.3).

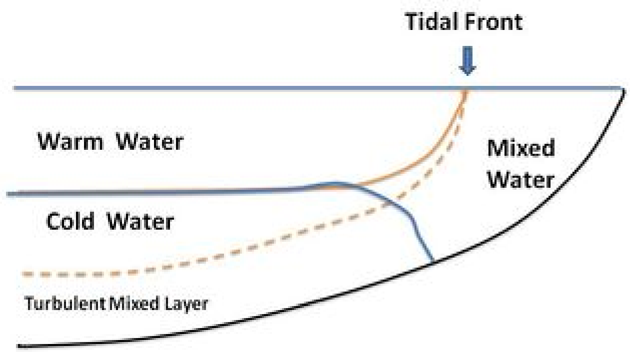

Figure 2.3. Schematic of water masses associated with a tidal front.

Special Flow Features

The most variable of these special flows is the predictable but complex flow associated with the freshwater inflow from rivers. These features can be persistent but they are intimately related to the coastal currents that are constrained to the inner shelf. There is a special class of oscillatory motion associated with the astronomical tides. These flows become more pronounced as they interact with geomorphology features like the shoreline.

Internal waves are also an important mechanism for generating strong currents on the shelf (Wang et al., 2004). However, they are not described in detail because of the difficulty of identifying them in the available validation data and the difficulties of reproducing them in the numerical models (Xu et al., 2011; Li and Farmer, 2011; Zhang et al., 2011; Lai et al., 2011). It is straightforward to construct an *Internal Wave Field* feature for comparison if this appears useful.

RIVER PLUMES AND COASTAL CURRENTS

River water flowing out of a river mouth or delta into the ocean does not immediately mix with the usually denser seawater. Instead, it forms a plume that is transported by the coastal flows as it gradually mixes. The inflow water of a differing density from the larger water mass into which it flows may be characterized by lower salinity and warmer temperatures resulting in a distinct signature that can be seen from aerial photography or satellites. Many times these plumes transport dissolved and suspended material that can be used to identify the plume in remote sensing or *in situ* data (Figure 2.4).

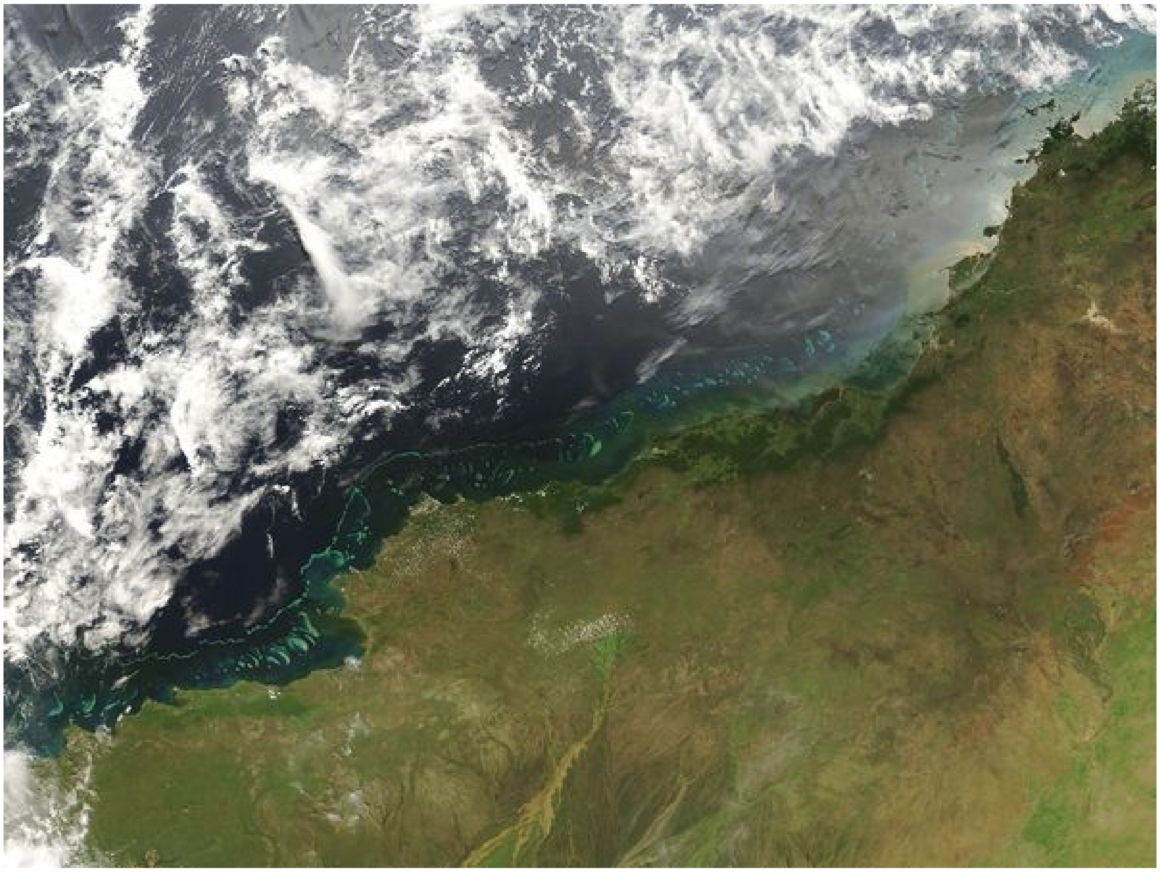

Figure 2.4. This image was captured by Moderate Resolution Imaging Spectroradiometer (MODIS) instrument onboard the Terra satellite on February 9, 2007. The image shows the sediment plumes coming from the inland rivers.

The lower-density water from rivers frequently forms and merges into a coastal current (Wiseman and Garvine, 1995). The behavior of a plume is sensitive to wind forcing and river discharge. The resulting evolution of the plume and the creation of a coastal plume has been measured in the Hudson River using HF radar (Figure 2.5). These studies are ideal for model validation but these observations are costly and not generally available. However, the resulting surface current map clearly shows the convergence pattern to be expected in the vicinity of the plume front.

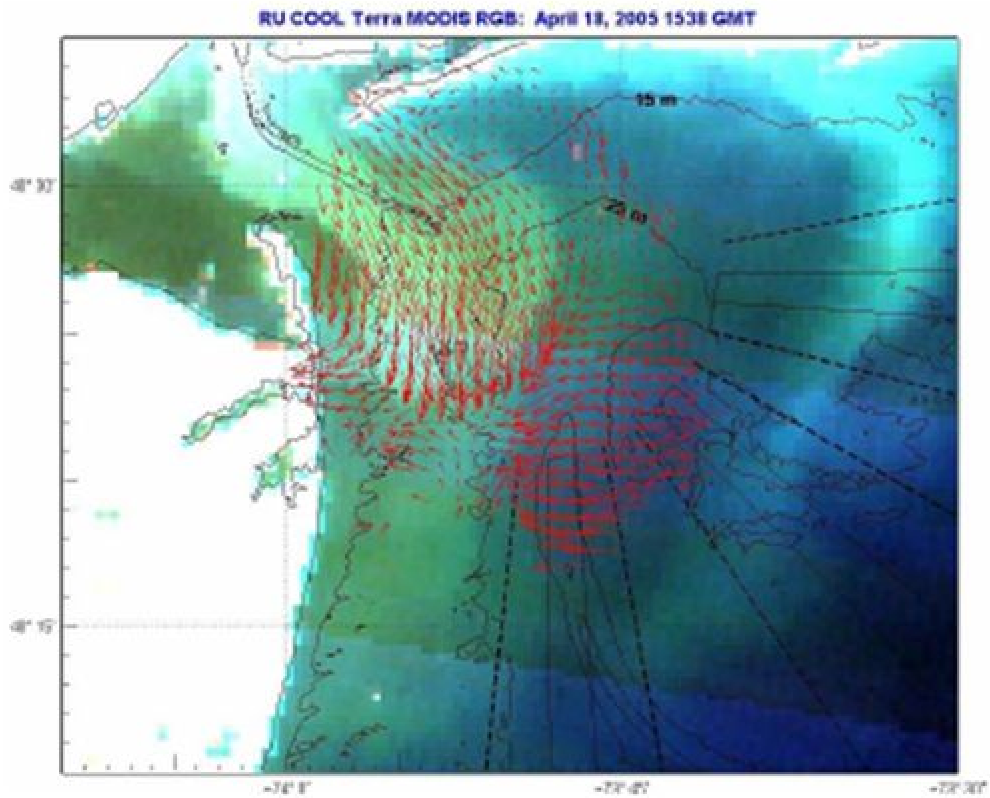

Figure 2.5. Overlay of HF radar surface currents on MODIS RGB image (Kohut et al. 2005; Chant, et al., 2008).

Hetland (2004) provides a nice examination of a river plume using an idealized numerical model of fresh water discharging from an estuary into a continental shelf. The coastal current is determined by the Coriolis force. Thus, these flows become more intense at high latitude and the largest river in the world (Amazon) is at the equator and forms no coastal current.

River plumes are also impacted by tidal currents (Gao et al., 2009; Isobe, 2005). Because of the difficulty of observing the surface expression of plumes and coastal currents, they have been examined mostly with numerical models. These results can be used for inter-model comparisons for validation. These models can be used in conjunction with satellite images to build an instantiation of a plume. It is possible to measure plumes with ship-mounted instruments as has been done with eddies, but the platforms are necessarily smaller as are the resulting study areas (O'Donnell, 1997).

Coastal currents are ubiquitous because of the tendency of fresh water to remain trapped at the coast much of the time. This water only moves offshore under seaward winds. Coastal currents can extend to hundreds of meters (Skagseth et al., 2011) and tens of kilometers offshore (Manning et al., 2008). In addition to seasonal cycles of runoff and coastal current development, interannual variability must also be considered (Shenoi, 2010) because these data will typically be used as historical instantiations of coastal currents. The response of coastal currents can also be examined in light of atmospheric forcing because of Ekman veering, but this analysis should be used for geometric comparison only because of the unknown impacts of bottom stress and stratification (Kim et al., 2009). A full realization of a coastal current requires remote sensing, 3D currents, and knowledge of coastal water levels (Ebuchi et al., 2009). These data bases are extremely rare but they can be used to evaluate the 3D structure of a model instantiation of a comparable feature as historical data.

TIDAL CURRENTS

The currents associated with the flood and ebb of the diurnal and semidiurnal astronomical tides are a special case of coastal currents because they are repeated every ~14 days. The currents that result from the periodic water level changes are not themselves features. However, they can form many of the other features described in this section as well as abstract features that we will discuss here.

Tidal flow can form semi-permanent eddies as it passes headlands and other geomorphological features Li et al., 2006). Tidal currents are important contributors to Langmuir circulation Kukulka et al., 2011). These features can be very useful for evaluating the general computation of tidal flow in light of the difficulty of getting tidal currents exactly right.

Tidal currents can also be compared using abstract features that are instantiated by manipulating currents at a point. Two such useful entities are: (1) residual currents; and (2) tidal ellipses (Carbajal and Pohlmann, 2004). These constructs allow the degrees of dimensionality of the tidal flow features to be reduced, thus enhancing the recognition of the base flow. Residual tidal currents can be important in estuaries (Cheng et al., 2010), along open coasts (Moreira et al., 2009), in marginal seas (Fukumoto et al., 1992), in straits (Juang, 2006) and over the shelf break (Lam et al., 2004).

Validation Data

Observations

There are multiple sources of data for model validation, including remotely sensed observations and derived data. The usefulness of validation data depends on their applicability to instantiating an ocean feature. Direct observations from satellites (e.g., altimeters, AVHRR, and scatterometers) are spatially large but limited in time and problematic for inferring ocean currents. In-situ observations made from buoys, ships, floats, and gliders can directly include current measurements but they are more limited in space. There are additional problems with instantiating ocean features from these restricted observations.

Mathematical and numerical methods can be used to construct more complete instantiations of ocean features from incomplete observations. The most direct type of such a feature instantiation is derived from assimilated data using statistical models based on covariance. This approach is represented by the multivariate method used in NCODA (Cummings, 2005). Hydrodynamic models can be used to extend this method to produce a more geophysically robust instantiation using variational assimilation methods (e.g, Puri, 1983; Smedstad and O'Brien, 1991; Marchuk and Zalesny, 2012). Numerical ocean models initialized with these fields are able to fully instantiate ocean features but they have uncertainties, which make them more useful for validating the consistency of a model being validated.

There is necessarily some overlap in discussing individual feature data and remote sensing, since all surface features are visible from satellites. This section is included to differentiate geomorphological features from oceanic features, partly because these tend to be static in satellite databases.

Geomorphic Measurements

The primary source of shoreline data is an existing vector shoreline database. There are vector shoreline databases available at different resolutions. These have been compiled from a number of sources over the years and they reflect different methods and sources themselves (WVS). However, if from a trusted source with a known error, they are the most direct approach. A vector shoreline can also be created by digitizing the shoreline as observed in an image. The georeferencing of satellite data has progressed to the point where they are probably the best data available for areas with low tidal variations. The most globally available database comes from many sources. The justification is that the satellite images are generally updated frequently and thus have identified errors corrected on a more-or-less continuous basis.

The seafloor is an integral part of the geomorphological seascape. This feature is thus 3D in nature. It can be sampled in 3D using high-resolution multibeam and sidescan sonar. This is time-consuming and expensive. It is becoming more common, however, as part of the exploration of the seafloor for economic development. Using these methods for the nearshore seafloor is restricted by water depth; thus, airborne surveys are made with LIDAR for clear/shallow water. For special regions, these methods have been compiled into high-resolution Digital Elevation Models.

NRL has created a standard 2 minute global bathymetry data base, (DBDB2). Some of the data are from charts, but these remain a source for updated depth values in coastal areas, where nautical charts are critical for transportation. These data consist of individual points rather than paths. Bathymetry data improves in both horizontal and vertical resolution with time, as seen in two bathymetry maps (Figure 2.6) for the Yellow Sea from 2008 (left) and 1999 (right). Note how much further from the shoreline the 10 m isobath is in Laizhou Bay from the 2008 data.

Changes in Bathymetry, 1999-2008

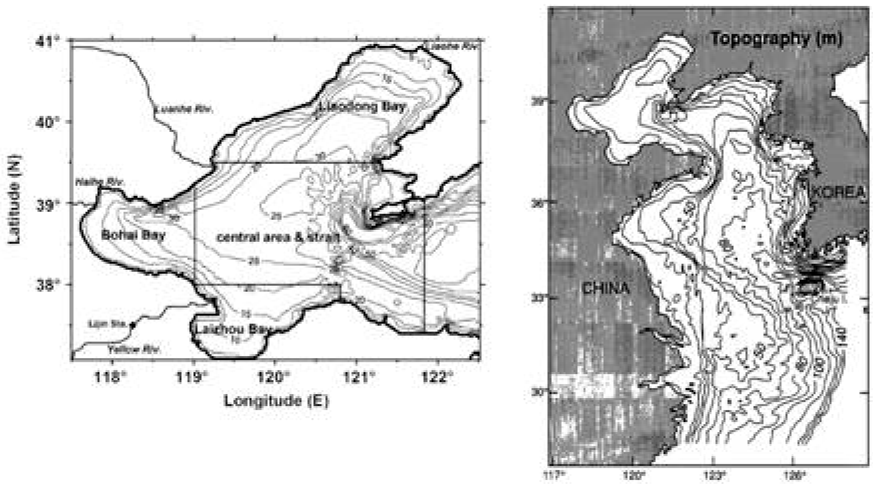

Figure 2.6. Contour maps of Yellow Sea from research papers describing model simulations.

Even higher resolution data are sometimes available as swaths rather than gridded fields. Depending on the region, this could be critical in validating model currents.

Historical Data

There are several sources of historical data. Archives of satellite images are historical but they are being treated as a specific database because of their importance. There have been many oceanographic studies in different parts of the world, which have generated a wealth of observations and model results. The model results are included in another category. There are several ways in which the historical oceanographic data can be available. The most useful and easiest to access is through on-line data bases. Coastal data are available through NOAA, as well as data portals like *OPD* (Ocean Data Portal). In addition, there are derived surface currents from altimeter and scatterometer data. Since these are derived data, they are not necessarily found in satellite image libraries. Other databases of currents are hosted at individual institutions (e.g., U. Miami).

A less convenient source of coastal currents is from publications in scientific journals, conference proceedings, and technical reports. It is becoming relatively simple to find data in papers through the Web of Science. These data are not digital, however, and must be used either qualitatively or digitized in some manner. This is somewhat time consuming but it can allow use of foreign data that may not be available through an ocean data portal like ODP. We will give several examples of historical data use in this report.

The historical data also include instantiations of ocean and geomorphology features. Standard topographic databases like DBDB2

Supplemental Model Simulations

This includes model results from historical sources like published scientific papers as well as other operational models that may be available to the model analyst. The U.S. has invested tremendous effort into operational forecast systems, with 11 systems currently available through NOAA, NOCMP (National Operational Coastal Modeling Program). Other countries have similar ocean forecasting systems like the U.K. National Centre for Ocean Forecasting (NCOF). There are also regional systems operated by educational institutions like the Oregon Coastal Ocean Observing System (OrCOOS). There are fewer such systems outside the U.S. and U.K., however. There are French systems, (Mercator, and PREVIMER). There has been substantial growth recently in coastal ocean forecasting in Asia as well (e.g., special conferences and regional collaborations like SARCCM (Sino-Australian Research Centre for Coastal Management). Coastal forecasting has also spread to the Eastern Mediterranean in the Cyprus Coastal Ocean Forecasting and Observing System (CYCOFS) as well as larger models like MOON (Mediterranean Operational Oceanography Network). There are also potential supplemental models in the Indian Ocean (e.g., Indian National Centre for Ocean Information Services). The SimOcean initiative further seeks to expand coastal modeling to Africa through multi-institutional collaborations.

These operational models may be available through official channels. Many of these systems were preceded by modeling studies that may be available through library services. These research models can be an excellent source of validation data because they are often validated with unpublished observations. They are often accompanied by a discussion of current features that can be used confirm an operational model result. For example, common analyses for coastal scales (<100 km) are tides and the residual flow. These are excellent for verifying if an operational model is capturing the most fundamental features of the coastal flow.

The specific databases used to compile the validation instantiations of the meteorological/ocean/geomorphological features (Figure 2.1) are assembled from many sources of data. The conventional method of storing data by how it is collected or how an application (e.g. a model) outputs data will still exist, but target features are identified, located and timed. The information generated through this process of identification (which could be manual or automatic) is cataloged in a searchable database. Then these features are found again much like gas stations or hotels are found on Google Earth.

Some important properties of the geophysical data that describes its quality:

- relevance: the usefulness of the data in the context of war fighter support.
- clarity: clearly defined parameter, e.g. tides in reference to what, MLLW?.
- consistency: the compatibility of the same type of data from different sources, e.g. altimeter height anomaly is not the same thing as modelled sea surface heights.
- timeliness: the availability of data at the time required and how up to date that data is, e.g. before the mission.

- accuracy: represented quantitatively with an error value.
- completeness: how much of the required data is available (this could be never ending).
- accessibility: where, how, and to whom the data is available or not available e.g. classified access.
- cost: the cost incurred in obtaining the data, and making it available for use, including time to move it.

References

Adams, J.K. and V.T. Buchwald (1969), The generation of continental shelf waves, *J. Fluid Mechanics*, 35 (4), 815-826.

Brink, K.H. (1983), The near-surface dynamics of coastal upwelling, *Progress In Oceanography*, 12 (3), 223-257, ISSN 0079-6611, 10.1016/0079-6611(83)90009-5.

Burk, S. D., T. Haack, L. T. Rogers, L. J. Wagner (2003), Island Wake Dynamics and Wake Influence on the Evaporation Duct and Radar Propagation. *J. Appl. Meteor.*, 42, 349–367.

Caldeira, R.M.A. , S. Groom, P. Miller, D. Pilgrim, N.P. Nezlin (2002), Sea-surface signatures of the island mass effect phenomena around Madeira Island, Northeast Atlantic, *Remote Sensing of Environment*, 80 (2), 336-360.

Carbajal, N. and T. Pohlmann (2004), Comparison between measured and calculated tidal ellipses in the German Bight, *Ocean Dynamics*, 54 (5), 520-530, DOI: 10.1007/s10236-004-0096-5.

Chant, R., J. Wilkin, et al. (2008), Dispersal of the Hudson River Plume in the New York Bight Synthesis of Observational and Numerical Studies During LaTTE. *Oceanography,* 21(4): 148-161.

Cheng, Peng, Arnoldo Valle-Levinson, Huib E. de Swart (2010), Residual Currents Induced by Asymmetric Tidal Mixing in Weakly Stratified Narrow Estuaries. *J. Phys. Oceanogr.*, 40, 2135–2147. doi: 10.1175/2010JPO4314.1

Dietrich, DE; Bowman, MJ; Lin, CA; Mestas Nunez, A (1996), Numerical studies of small island wakes in the ocean; *Geophys. and Astrophys. Fluid Dyn.*, 83 (3-4), 195-231 DOI: 10.1080/03091929608208966.

Dzwonkowski, B., and K. Park (2010), Influence of wind stress and discharge on the mean and seasonal currents on the Alabama shelf of the northeastern Gulf of Mexico, *J. Geophys. Res.*, 115, C12052, doi:10.1029/2010JC006449.

Ebuchi, N; Fukamachi, Y; Ohshima, K; Wakatsuchi, M (2009), Subinertial and seasonal variations in the Soya Warm Current revealed by HF ocean radars, coastal tide gauges, and bottom-mounted ADCP; *J. Oceanogr.*, 65 (1), 31-43 DOI: 10.1007/s10872-009-0003-2 Published: FEB.

Fearnhead, P.G. (1975), On the formation of fronts by tidal mixing around the British Isles, *Deep Sea Research and Oceanographic Abstracts,* 22, (5), 311-321.

Flagg, C. N., M. Dunn, D.-P. Wang, H. T. Rossby, and R. L. Benway (2006), A study of the currents of the outer shelf and upper slope from a decade of shipboard ADCP observations in the Middle Atlantic Bight, *J. Geophys. Res.*, 111, C06003, doi:10.1029/2005JC003116.

Flament, P., Armi, L., and Washburn, L. (1985), The evolving structure of an upwelling filament. *J. Geophys. Research*, 90 (C6), 11,765-11,778.

Fukumoto, T; Nakamura, T; Togashi, H (1992), Tidal Residual current in Omura Bay; *Hydraulic and Env. Modeling: Coastal Waters*, 79-87.

Gao, Lei, Dao-Ji Li, Ping-Xing Ding (2009), Quasi-simultaneous observation of currents, salinity and nutrients in the Changjiang (Yangtze River) plume on the tidal timescale, *Journal of Marine Systems*, 75 (1-2), 265-279, DOI: 10.1016/j.jmarsys.2008.10.006.

Gryanak, V.M., Borth, H., and Olbers, D. (2004). The theory of quasi-geostrophic von Kármán vortex streets in two-layer fluids on a beta-plane. *Journal of Fluid Mechanics*, 505, 23-57 doi:10.1017/S0022112004008122.

Hasegawa, D., M. R. Lewis, and A. Gangopadhyay (2009), How islands cause phytoplankton to bloom in their wakes, *Geophys. Res. Lett.*, 36, L20605, doi:10.1029/2009GL039743.

Hetland, R. D., (2005) Water mass structure of wind forced river plumes, *J. Phys. Oceanogr*, 35 (9), 1667-1688.

Hill, A.E. and J.H. Simpson (1989), On the interaction of thermal and haline fronts: The Islay front revisited, Estuarine, *Coastal and Shelf Science,* 28 (5), 495-505.

Isobe, Atsuhiko (2005), Ballooning of River-Plume Bulge and Its Stabilization by Tidal Currents. *J. Phys. Oceanogr*., 35, 2337–2351. doi: 10.1175/JPO2837.1

Johnson, J. A., P. D. Killworth (1975): A Bottom Current Along the Shelf Break. *J. Phys. Oceanogr.*, 5, 185–188.

Juang, W.J. (2006), Morphological impacts of tidal residual currents in the Taiwan Strait, *Second Sino-German Joint Symposium on Coastal and Ocean Engineering,* 249-260.

Kim, Sung Yong, Bruce D. Cornuelle, and Eric J. Terrill (2009): Anisotropic Response of Surface Currents to the Wind in a Coastal Region. *J. Phys. Oceanogr.*, 39, 1512–1533. doi: 10.1175/2009JPO4013.1

Kohut, J.T., Roarty, H.J., Glenn, S.M., and Chant, R.J. (2005), Surface current response of Hudson River plume to wind forcing. *Oceans 2005*, Vols. 1-3 Book Series: Oceans-IEEE , pp. 2540-2542.

Kukulka, T., A. J. Plueddemann, J. H. Trowbridge, and P. P. Sullivan (2011), The influence of crosswind tidal currents on Langmuir circulation in a shallow ocean, *J. Geophys. Res.*, 116, C08005, doi:10.1029/2011JC006971.

Lai, Z., C. Chen, G. W. Cowles, and R. C. Beardsley (2010), A nonhydrostatic version of FVCOM: 2. Mechanistic study of tidally generated nonlinear internal waves in Massachusetts Bay, *J. Geophys. Res.*, 115, C12049, doi:10.1029/2010JC006331.

Lam, Frans-Peter A., Leo R. M. Maas, Theo Gerkema (2004), Spatial structure of tidal and residual currents as observed over the shelf break in the Bay of Biscay, *Deep Sea Research Part I: Oceanographic Research Papers*, 51 (8), 1075-1096, DOI: 10.1016/j.dsr.2004.03.008.

Le Boyer, A., G. Cambon, N. Daniault, S. Herbette, B. Le Cann, L. Marié, P. Morin (2009), Observations of the Ushant tidal front in September 2007, *Continental Shelf Research*, 29, (8), 1026-1037.

Li, C ; Armstrong, S; Willlams, D. (2006), Residual eddies in a tidal channel. *Estuaries and Coasts*, 29, (1), 147-158.

Li, Qiang, David M. Farmer (2011), The Generation and Evolution of Nonlinear Internal Waves in the Deep Basin of the South China Sea. *J. Phys. Oceanogr.*, 41, 1345–1363. doi: 10.1175/2011JPO4587.1

Lwiza, K.M.M., D.G. Bowers, J.H. Simpson (1991), Residual and tidal flow at a tidal mixing front in the North Sea, *Continental Shelf Research*, 11 (11), 1379-1395.

Manning, J.P., D.J. McGillicuddy Jr., N.R Pettigrew, J.H. Churchill, L.S. Incze (2009), Drifter observations of the Gulf of Maine Coastal Current, *Continental Shelf Research*, 29 (7), 835-845.

Marin, V.H. and Delgado, L.E. (2007), Lagrangian observations of surface coastal flows north of 30S in the Humboldt current system. *Cont. Shelf Research*, 27, 731-743.

Marin, V.H., Delgado, L.E., and Luna-Jorquera, G. (2003), S-chlorophyll squirts at 30S off the Chilean coast (eastern South Pacific): Feature-tracking analysis. *J.Geophys. Research*, 108 (C12), doi:10.1029/2003JC001935.

Marchuk, G. I. and Zalesny, V. B. (2012), Modeling of the world ocean circulation with the four-dimensional assimilation of temperature and salinity fields. *Izvestiya Atmospheric and Oceanic Physics*, 48 (1), 15-29.

Matano, R. P., Palma, E. D., and Piola, A. R. (2010), The influence of the Brazil and Malvinas Currents on the Southwestern Atlantic Shelf circulation, *Ocean Sci.*, 6, 983-995, doi:10.5194/os-6-983-2010.

Matthews, J.P., A.D. Fox, D. Prandle. (1993), Radar observation of an along-front jet and transverse flow convergence associated with a North Sea front, *Continental Shelf Research*, 13 (1), 109-130.

Melling, H. (1993), The formation of a haline shelf front in wintertime in an ice-covered arctic sea, *Continental Shelf Research*, 13 (10), 1123-1147.

Moreira Diego; Simionato Claudia G.; Dragani Walter C., et al. (2009), Tidal and Residual Currents Observations at the San Matias and San Jose Gulfs, Northern Patagonia, Argentina, *J. Coastal Res.*, 25 (4), 957-968 DOI: 10.2112/08-1035.1.

O'Donnell, J. (1997), Observations of near-surface currents and hydrography in the Connecticut River plume with the surface current and density array, *J. Geophys. Res.*, 102(C11), 25, 021–25, 033.

Park, S., Chu, P.C. (2006), Thermal and haline fronts in the Yellow/East China Seas: Surface and subsurface seasonality comparison, *J. Oceanogr.*, 62 (5), 617-638, DOI: 10.1007/s10872-006-0081-3.

Puri, K. (1983), Some experiments in variational normal mode initialization in data assimilation. *Monthly Weather Review*, 111 (6), 1208-1218.

Petus, C., Guillem Chust, Francis Gohin, David Doxaran, Jean-Marie Froidefond, Yolanda Sagarminaga (2010), Estimating turbidity and total suspended matter in the Adour River plume (South Bay of Biscay) using MODIS 250-m imagery, *Continental Shelf Research*, 30 (5), DOI: 10.1016/j.csr.2009.12.007.

Ramp, S.R., Jessen, P.F., Brink, K.H., Niiler, P.P., Daggett, F.L., and Best, J.S. (1991), The physical structure of cold filaments near Point Arena, California, during June 1987. *J. Geophys. Res.*, 96, (C8), 14,859-14,883.

Shenoi, S. S. C. (2010), Intra-seasonal variability of the coastal currents around India: A review of the evidences from new observations, *Indian J. Mar. Sci.*, 39 (4) Special Issue, 489-496.

Signorini, Sérgio R., Luiz B. De Miranda (1983), Tidal and Low-Frequency Currents Near the Shelf-Break: Northeastern Coast of Brazil. *J. Phys. Oceanogr.*, 13, 2107–2115.

Simpson, J.H. and D. Bowers (1981). Models of stratification and frontal movement in shelf seas. *Deep-Sea Research*, 28A (7), 727-738.

Skagseth, Ø., K. F. Drinkwater, and E. Terrile (2011), Wind- and buoyancy-induced transport of the Norwegian Coastal Current in the Barents Sea, *J. Geophys. Res.*, 116, C08007, doi:10.1029/2011JC006996.

Smedstad, O. M. and O'Brien, J. J. (1991), Variational data assimilation and parameter estimation in an equatorial Pacific Ocean model. *Progress in Oceanogr.*, 26 (2), 179-241.

Ullman, David S. and Peter C. Cornillon (2001), Continental shelf surface thermal fronts in winter off the northeast US coast, *Continental Shelf Research*, 21 (11-12), 1139-1156.

Wang, Gang, Fangli Qiao, Dejun Dai and Yijun Hou (2011), A possible generation mechanism of the strong current over the northwestern shelf of the South China Sea, *Acta Oceanologica Sinica*, 30 (3), 27-32, DOI: 10.1007/s13131-011-0116-5.

Wiseman, W.J. and Garvine, R.W. (1995), Plumes and coastal currents near large river mouths, *Estuaries*, 18 (3), 509-517 DOI: 10.2307/1352368.

Xu, Jiexin, Jieshuo Xie, Shuqun Cai (2011), Variation of Froude number versus depth during the passage of internal solitary waves from the in-situ observation and a numerical model, *Continental Shelf Research*, 31 (12), 1318-1323.

Yanagi, Tetsuo, Satoru Takahashi (1988), A tidal front influenced by river discharge, *Dynamics of Atmospheres and Oceans*, 12 (2), 191-206.

Zhang, Z., O. B. Fringer, and S. R. Ramp (2011), Three-dimensional, nonhydrostatic numerical simulation of nonlinear internal wave generation and propagation in the South China Sea, *J. Geophys. Res.*, 116, C05022, doi:10.1029/2010JC006424.

Zhang, Yu, Joseph Pedlosky, Glenn R. Flierl (2011), Shelf Circulation and Cross-Shelf Transport out of a Bay Driven by Eddies from an Open-Ocean Current. Part I: Interaction between a Barotropic Vortex and a Steplike Topography. *J. Phys. Oceanogr.*, 41, 889–910. doi:

Zhurbas, V., Laanemets, J., and Vahtera, E. (2008), Modeling of the mesoscale structure of coupled upwelling/downwelling events and the related input of nutrients to the upper mixed layer in the Gulf of Finland, Baltic Sea., *J. Geophys. Research*, 113, doi:10.1029/2007JC004280.

Section 3: Logical Process Model

Introduction

The logical process model (LPM) is the implementation and extension of the conceptual model. It represents the task requirements of the validation process. This section defines the data structures and processes that bind them. We will loosely follow general guidelines for LPM development and use software design principles (*e.g.*, entities, attributes, key groups, and relationships) to represent the geophysical features (data structures) and the validation algorithm (analysis processes).

We can use the data structure diagram in combination with physical relationships between the data elements (entities) to construct an entity-relationship diagram (ERD) (Figure 3.1). The ERD will permit the physical processes that govern the interrelationships between our data elements to be visualized, thus identifying potential validation data from the large number of oceanographic data types. We will construct the ERD using the notation of Chen (1976). Surface currents transport water with different heat content in rotational flows that produce circular features like eddies.

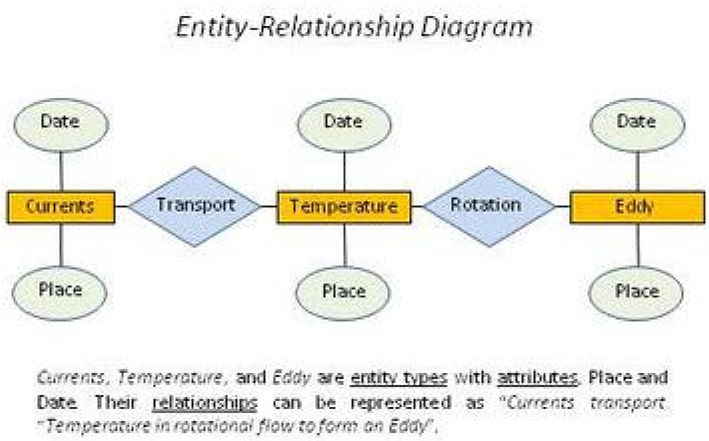

Figure 3.1. Example Entity-Relationship Diagram for currents, temperature, and eddy data entities.

The primary keys, *Place* and *Time*, are used to identify specific instantiations (specific examples) of these data entities. This entity relationship can produce instantiations of the same eddy using different data elements that are themselves instantiations of (possibly) multiple data sources (*e.g.*, SST and altimetry). These types of data relationships are known as many-to-one. They are represented in the Data Structure Diagram (DSD) by several lines connecting the **Ocean Feature** data element to its sub-elements. The one-to-many relationship for **Currents** to **Temperature**, *etc.*, is also problematical for the validation of currents in a coastal model.

The validation process consists of multiple components, including:

- Model output
- Validation data
- Individual comparisons between validation and model instantiations (*i.e.*, tasks)

- Decisions that determine the model performance
- Movement of data between tasks
- The analyst who performs the model validation

The flow of data follows a series of steps (comparisons) that are designed to result in a specific confidence outcome. These steps can be manual or automated, fully documented or simply knowledge in the mind of the analyst. They can be simple or complex. They can be formal, requiring exact adherence to all details, or flexible. Finally, they can be optional or mandatory.

The logical process model details all of the activities associated with the validation from data collection to assigning a confidence score to the forecast model. The LPM includes the following activities:

- Gathering the data
- Controlling access to the data during validation
- Determining work flow
- Delivering appropriate subset of data for each analysis
- Assuring data availability and completion of each analysis
- Providing a mechanism to indicate acceptance of the validation, such as a *signature*

The LPM consists of data structures that are associated with features, as shown in the DSD, and validation processes that are composed of basic sequential processes. These major components are briefly described in this section. Details of the data structures and analysis processes are given in later sections.

The model validation is completed using the feature entity type for all validation data. This approach is used to simplify the overall procedure and avoid multiple algorithm development and learning. Thus, even simple statistical analyses are performed using the *Feature* data entity. Several approaches to feature analysis have been used in oceanography but this is not the primary thrust of our algorithm. These methods are incorporated where appropriate.

An example ERD can be constructed for an eddy (Figure 3.2) by accounting for the impact of currents in producing circular features. These forecast features can then be compared to whatever instantiations can be constructed from available validation data.

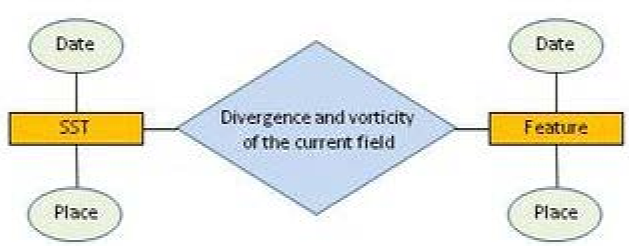

Figure 3.2. Entity-relationship diagram for an eddy feature.

Divergence and vorticity are characteristics of the current vector field, which can be used to represent this field in a fundamental way. They could then be used to sample the original field at any location where another data instantiation (e.g., a satellite image) may be available. However, we cannot compute them from the SST field from the satellite because it is a scalar. We need to find a proxy for our analysis. It does not need to incorporate physics. This approach could potentially produce a first-guess vector field overlaid on a model output image.

Validation Process Model

The validation process model is represented by a series of steps that can be completed in sequence or independently. Model validation is the highest level activity for this project, which we will refer to as a *Function*. The *Validation* function consists of several *Processes*: (1) data input; (2) feature identification; (3) feature instantiation; (4) model validation; (5) output; and (6) user interface. These processes are discrete (with a beginning and an end) and in-turn consist of sub-processes and *Sequential Processes*, which are specific tasks that cannot be decomposed further. Many of these sequential processes are performed by the underlying *GIS* software.

Much of the data input and preprocessing is completed using Geospatial Analysis and Model Evaluation Software (GAMES) modules. Additional data input operations (Figure 3.3) are described on the Model Validation Page. These new capabilities include a data import feature to allow more validation data sources, as well as formats for satellite images. *Instantiating* geophysical features is accomplished using the Feature Instantiation Function.

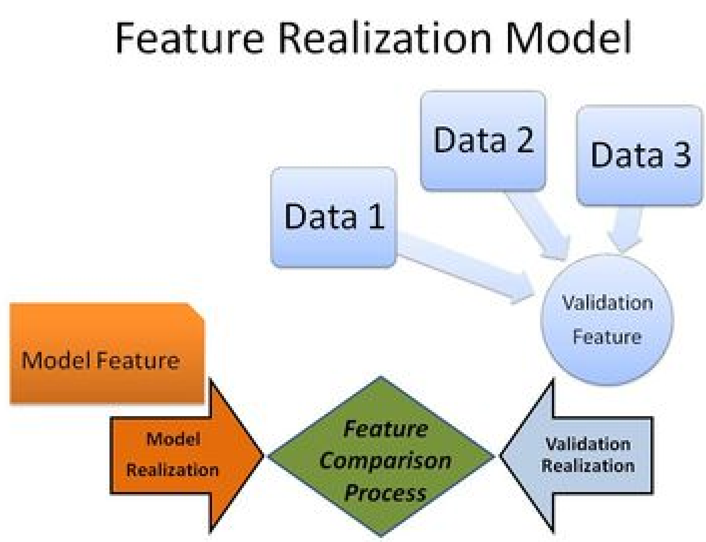

Figure 3.3. Schematic of the data flow into the feature comparison process.

The blue arrows represent the data being processed into a validation feature instantiation (blue circle). The green diamond between the model and validation features represents the *Feature Comparison* process. The feature-comparison process model consists of six operations. These are shown in Figure 3.3 and discussed on the_Model Validation Function Page. The top of the pyramid qualitatively represents the greatest impact of the feature comparison on the model currents, whereas the base reflects a lower degree of certainty. There is some leeway here for the analyst to use their experience in this determination. If it becomes necessary to use the *meteorological* comparison, it should be recognized that the ERD for the ocean response to weather is very uncertain.

Model validation (Step 4) is the kernel of the validation function (Figure 3.4). The data for the validation consist of instantiations of the geophysical features, which come from the model and the validation data. Each feature-comparison process consists of sub-processes described as evaluation guidelines. A comparison is completed when all processes have been completed and a score is determined. The output primarily utilizes the GAMES files with the addition of a *validation file* that is described in the next section. The user interface is based on ArcGIS with some additional functionality from the GAMES libraries.

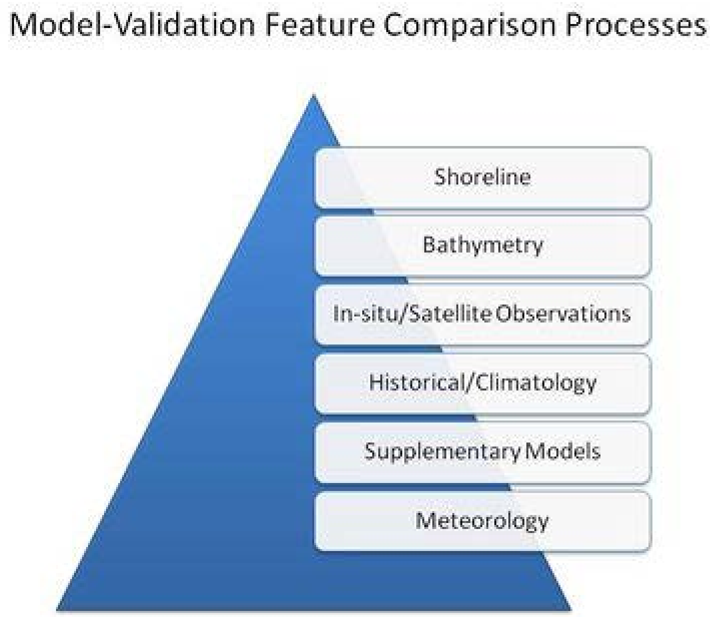

Figure 3.4. Model/Validation Feature Comparison Processes.

The minimum input required for the validation function is a file containing model fields of currents at some time. This field can be compared to the validation features. Because of the reliance of feature recognition on satellite observations, however, it is useful to have surface fields of temperature as well. The feature comparisons are completed with the *Comparison Rules*. This is an initial list that we expect to expand with experience. The desired result of the validation function is a qualified statement of the confidence in the model flow field (see the Validation Algorithm page). Experience has shown that there is no simple scoring possible for most coastal flows, so an optional scoring system is described. This score will need some qualification, which is introduced through the use of comments and supporting validation data in the *Validation File*.

We expect this validation software to be part of an ongoing learning process. Thus, each analysis is recorded in a validation file with a unique name, the contents of which will include the *digital signature* of the analyst. To avoid problems that may occur with copying files, these files will have restricted ownership to avoid duplication and deletion. This will assure that an analyst will quickly learn their own method for implementing the software and not inadvertently replicate previous analyses. Experience with using the software will demonstrate how many analyses are optimal to document the model forecast currents in a given area.

Feature Instantiation

The simulated currents can be directly validated using instantiations of the flow features, which are created from remote sensing data or *in situ* observations. A one-to-one quantitative comparison of between the model and validation instantiations is unlikely because of the difficulties in acquiring fields of surface currents. Several alternatives are used instead: (1) presence of a feature with known 3D flow regime; (2) direction of surface currents; (3) magnitude of surface currents; and (4) vertical distributions (profiles). These general guidelines are applied to the oceanographic features evaluated in this section. Such an evaluation cannot be undertaken without dealing with the problem of *Feature Extraction*. This method will can be implemented using several algorithms and thus automated but it would require an unknown amount of development. This will probably be very useful in the future but it is outside the scope of the current software project. However, features can be identified swiftly by an analyst and used to evaluate the model currents as described below.

Geographic Features

SHORELINE

This discussion for incorporating coastal data does not use an interface (e.g., ARCOAS) to ingest or analyze the model. The method is presented as general topics that can be addressed in different ways. The steps in applying a coastline are: (a) find a database; (b) produce a vector shoreline from the data; (c) process this shoreline into a compatible format for the model grid; (d) compare the validation data and model shoreline instantiations.

The first step in creating a shoreline feature is to acquire a shoreline database for the area of interest. The primary source of shoreline data is an existing vector shoreline database. There are vector shoreline databases available at different resolutions. These have been compiled from a number of sources over the years and they reflect different methods and sources themselves (WVS). However, if from a trusted source with a known error, they are the most direct approach.

The second step is to produce a vector shoreline from the shoreline database. If such a vector shoreline is unavailable, one can be produced for limited areas by digitizing from any available source, such as a navigation chart or satellite image. The georeferencing of satellite data has progressed to the point where they are probably the best data available for areas with low tidal variations. The most globally available database comes from many sources. One method of accessing this database is through Google Earth, which supplies either a standalone program for common operating systems (WinOS, Mac, Linux), or an add-on for browsers with more limited availability. This section discusses this approach. The justification is that the satellite images are generally updated frequently and thus have identified errors corrected on a more-or-less continuous basis. A vector shoreline can be produced in Google Earth by creating a path. This is done through the "Add" menu. The shoreline is produced at the desired resolution by zooming in and clicking at the required interval to capture the shoreline's variability. It can be necessary to estimate the location of the shoreline because these images are not referenced with respect to time; they are composites based on weather and image clarity. Great care must be exercised in areas where tidal flats exist. It is important to note the relative position of the shoreline from the overall image. Some images are very bad because of this. The Google Earth path is saved as a kml file, or a kmz file, which is a zipped kml file. This file can be manually unzipped using an archive tool like JZIP. The kml file is a proprietary format of Google Earth. It is based on the xml file so it is readable and, thus, it can be parsed. For this example, it was edited to remove everything but the line containing all of the input data points. This line is marked by a <coordinates> tag.

Matlab imports ascii files directly using the "importdata" function, which can be called in a script. The single line can then be parsed into latitude/longitude pairs and plotted (Figure 3.5). This process can be automated except for digitizing the shoreline data, which only takes a few minutes if the coast is readily visible.

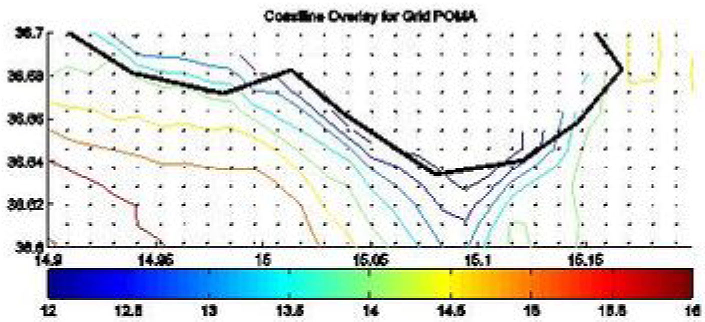

Figure 3.5. Overlay of Google Earth shoreline on SST contours from a model.

If navigation charts are available, they can be digitized by either scanning the area of interest and then digitizing with a screen method (either existing software like Google Earth or Matlab, or a digitizing progam like Data Thief), or digitized directly on a table digitizer. The second method avoids any potential problems with image warping during scanning but such digitizing tables are rare today. It is also important to place the chart precisely on the table.

BATHYMETRY

It is important to have the correct feature entity for model analysis. As with the shoreline, there are spurious errors in the higher-resolution bathymetry generated from this database because the model feature has a resolution of 3:1 over the database. The model realization to be analyzed could potentially extend from intertidal areas to ocean depths. This is the case for the southeast tip of Sicily (Figure 3.5), where water depths increase to > 1 km within 10 km of the shoreline. We recognize that the bottom currents from the model may be of greater interest than the surface currents and we will attempt to include an analysis of them in developing this method. However, when water depths exceed typical shelf depths <200 m), there are too many potential problems to be incorporated into a coastal analysis system. Thus, unless requested otherwise, this system will focus on depths less than 200 m. The exception would be surface flow within a typical shelf width (200 km).

SEAFLOOR PROFILE (2D DEPTHS)

There are a number of common seafloor profiles that recur because of the underlying topography of the continental shelf. It is probably necessary to extrapolate sparse depth data (incomplete feature realization) to the model domain using one of these common morphological models. As suggested by this section title, a bathymetry feature can be constructed from depth profiles for the continental shelf (Figure 3.6A). This is because the shelf floor tends to be the result of long-term and often relict processes associated with sealevel change and valley incision, whereas the nearshore profile is more responsive to short-term processes associated with surface waves, which change at scales form hours to years. There is thus more variability in the nearshore profile. However, the water depths are of greater interest for navigation and more data may be available. For this purpose we can identify a small number of typical profiles. We will first examine the use of depth features as represented by idealized profiles of the continental shelf.

Wave base is the determining criterion for the nearshore seafloor (Figure 3.6B). This depth is half the deep-water wavelength of incident waves. The largest waves are the ocean swell, which range widely depending on location and season. These waves can reach 700 m in length in the Pacific but they are usually much shorter. The largest waves impact sediments on the outer shelf but their rarity prevents them from sculpting the seafloor.

Figure 3.6. Schematic Seafloor Profiles. (A) Schematic of a continental margin, showing the basic geologic provinces and sub-seafloor structure. (B) Schematic of the shoreface profile, showing the concave-up seafloor.

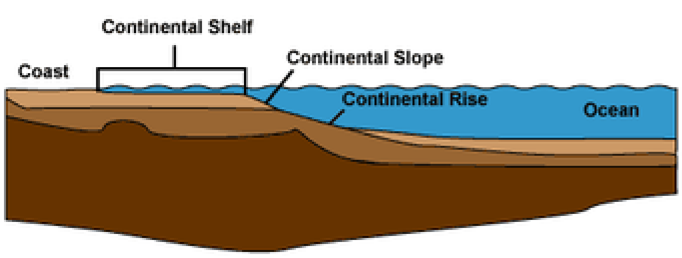

A.

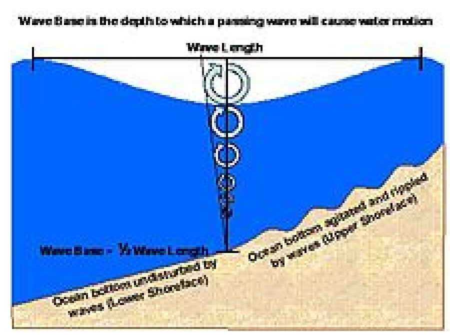

B.

Consequently, the outer shelf tends to be relatively flat (gradient ~0.001 to 0.0001) with incised canyons and mixed terrigenous and biogenic sediments. The impact of a synthetic seafloor for this area would be minimal for two reasons: (1) the water depths used to construct the model bathymetry feature will not be too different from what could be found; and (2) the models are in general not validated for bottom currents and, thus, there would be no obvious improvement in the forecast as a result of this analysis. Unless otherwise noted, the coastal bathymetry feature analysis will focus on water depths above fair-weather wave base, which can be generally taken as less than 20 m. This seafloor zone is often referred to as the shoreface. How much of a model current field could this impact? The answer to this question depends on the domain.

A typical equilibrium wave shoreface profile on a sandy beach is slightly concave up, as can be seen at the Field Research Facility at Duck, NC (Figure 3.7A), and at Santa Rosa Island, Florida (Figure 3.7B). These are different wave regimes. The Atlantic coast has waves several meters in height during the fall and winter whereas the Gulf of Mexico only occasionally sees 1 m waves.

Figure 3.7. **Measured beach profiles: (A) The Army Field Research Facility at Duck; (B) Santa Rosa Island, Florida (width = 1.3 km; depth=16 m).**

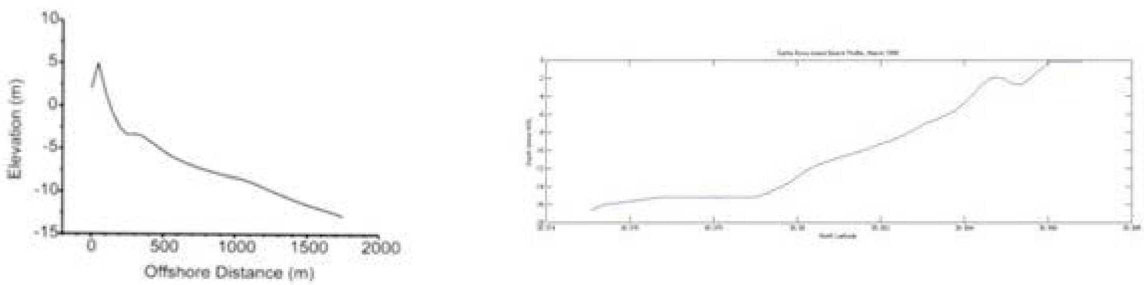

A. **B.**

This kind of profile can be used to interpolate from the 20 m isobath to the swash zone for sandy coasts subject to wave action. The slope can be reduced for lower waves. This analysis is used to evaluate the accuracy of the mean flow in shallower water by comparison to the model depth features as described above. If the model grid has a wet cell coincident with a wet point in the validation bathymetry feature, but the model water depth is too deep, the model flow is identified for further examination with respect to the likely flow structure to be seen based on other feature realizations (e.g., historical records and satellite imagery).

The east coast of S. America is a good example of a relatively straight coastline representation in a model grid (~3 km). The section of shoreline of interest borders *Lagoa Mangueira* (Figure 3.8). This section of the Brazilian shoreline has many large, shallow, estuaries with seasonal river inflow and large sediment loads. This has constructed a Chenier Plain similar to that of coastal Louisiana.

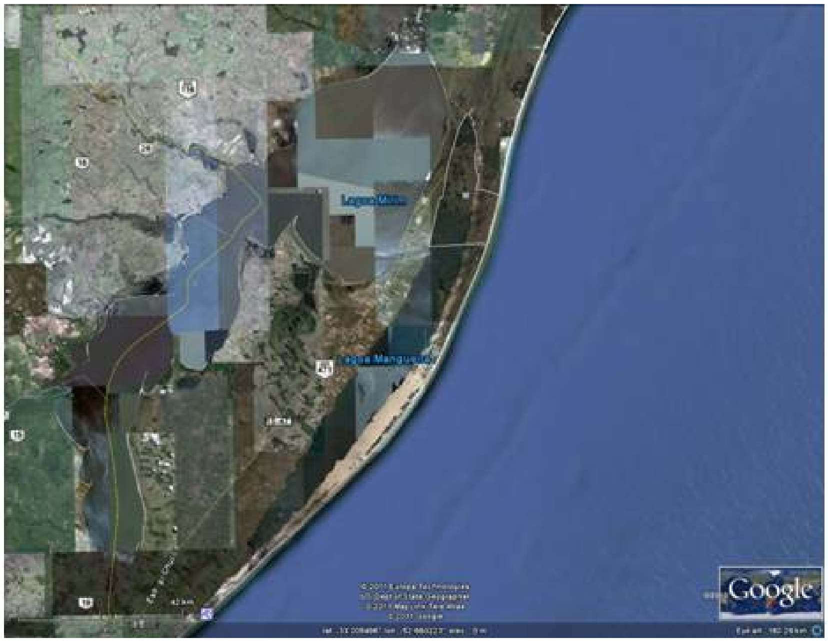

Figure 3.8. Google Earth image of the Mangueira Lagoon area.

A shoreline path was created in GE and added to this image as described above. This path can then be overlain on model bathymetry features (Figure 3.9) to show the impact of different resolution on shoreline representation. The unchanged DBDB2 bathymetry does not reach the shoreline for this particular grid (left image of Figure 3.9). This grid was generated using automated software. The image on the right has twice the resolution (~1.5 km). Now the shoreline falls inside the model wet domain.

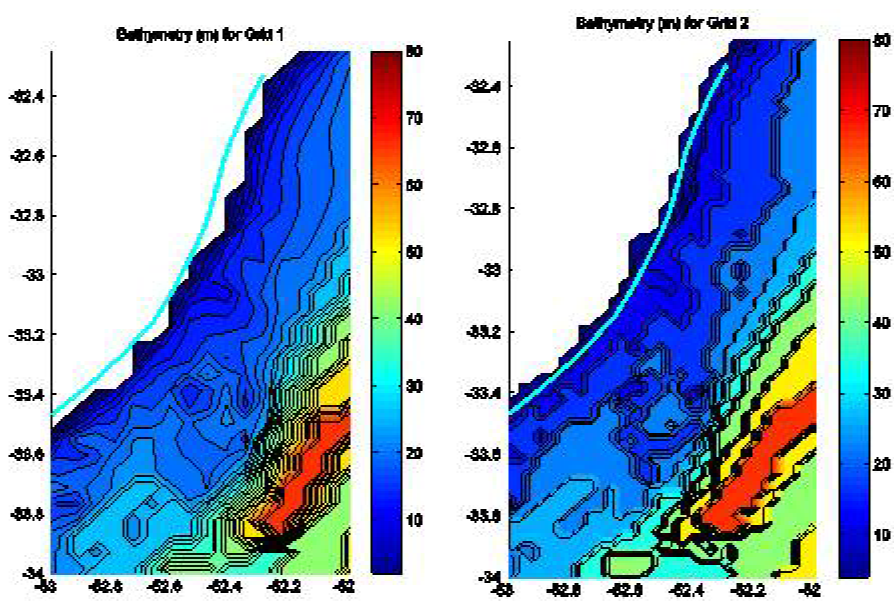

Figure 3.9. Plots of digitized satellite shoreline (cyan) on grids generated with DBDB2 bathymetry at 3 km (left) and 1.5 km (right) resolution.

The next step is to create a surface from the 20 m isobath to the coast that reflects a realistic shoreface. In a finished analysis software, this would be constructed from the shoreline feature and bathymetry feature. The model output depths would then be compared to this 3D surface and rejected if they fell below it. The exact method of generating the across-shore sections (Figure 3.10) that would comprise this surface (transects) are determined based on availability of components.

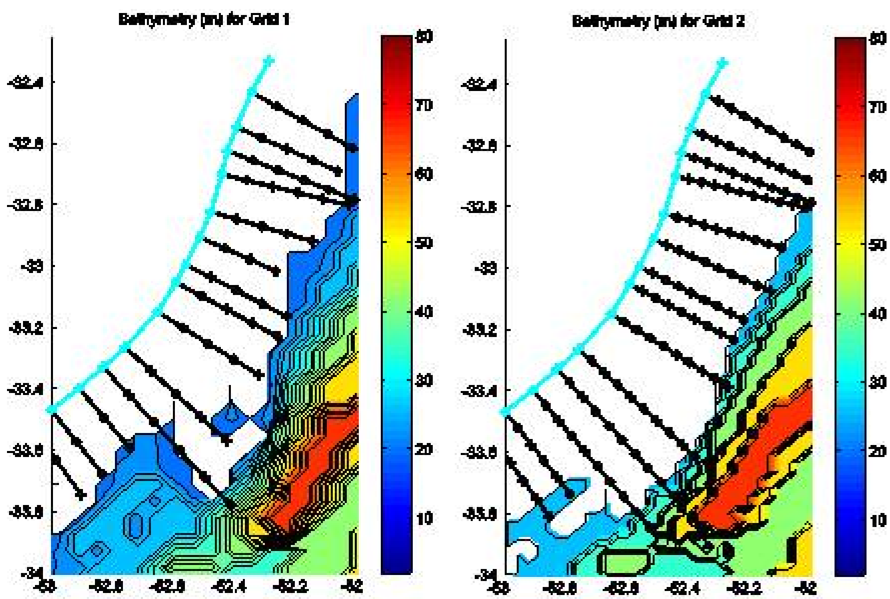

Figure 3.10. Plots of digitized shoreline and inner-shelf transects on 3 km and 1.5 km model grids.

The water depth is interpolated along the transects in Figure 3.10 using either a linear depth model or Equilibrium Profile. Here we have applied a linear shoreface for simplicity. The model bathymetry shallower than the selected value (20 m) is set to nan to simplify locating the transects. The white areas (Figure 3.10) are evaluated with this method. The resulting sections (Figure 3.11) show the wide range of variability in the width of the shoreface. The upper panel contains steep transects whereas the lower-gradient sections of the inner shelf are plotted in the lower panel.

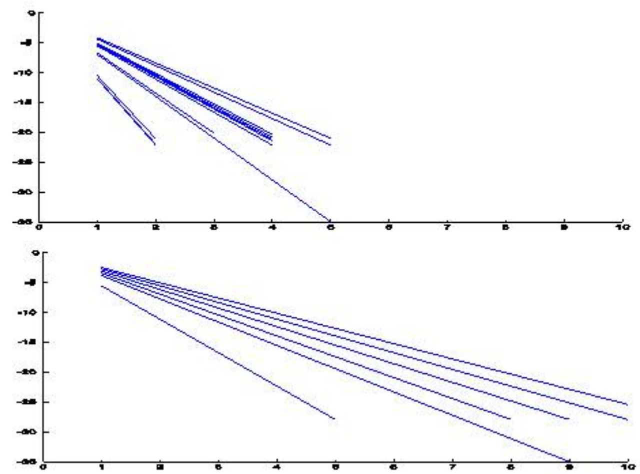

Figure 3.11. Sections from shoreline to ~20 m (right) along transects from Figure 3.10.

ESTUARIES

An estuary can be defined as "*a semi-enclosed coastal body of water, which has a free connection with the open sea, and within which sea water is measurably diluted with freshwater derived from land drainage*" (Pritchard 1967). Although this definition is general and applies to all coastal water bodies, it has been expanded; "*a semi-enclosed body of water connected to the sea as far as the tidal limit or the salt intrusion limit and receiving freshwater runoff; however, the freshwater inflow may not be perennial, the connection to the sea may be closed for part of the year and tidal influence may be negligible*" (Wolanski 2007). The definition of an estuary thus includes well-known water bodies like the Hudson River estuary as well as fjords, lagoons,river mouths, and tidal creeks. A practical definition of an estuary extends between the 1 PSU and the 30 PSU salinity isotherms.

The water depth in an estuary is most likely to be available in navigation charts where marine traffic is high. These areas tend to be small in area and not resolved by typical forecast models. This feature may not be important, but the mouths of estuaries can be significant because of the inflow of water from rivers, which can impact the hydrography of the inner shelf, including currents. Simple models like that used for the nearshore profile cannot be applied in a general manner in estuaries, although local corrections can be made where desired. These are time-consuming, however. The recommended analysis method is to apply shorelines that accurately reflect the location of morphological features at the estuary scale. These features can be used in conjunction with updated bathymetry data to construct a qualitative feature map of the region. This method is demonstrated in this section.

Estuaries are in many ways a special subregion of the coastal ocean. They include a number of unique geomorphological features as well. We can focus on a few of these features for the purpose of analyzing coastal currents within estuaries and bays. The following list includes features that will have a pronounced impact on estuary flows: (1) channels whether natural or dredged; (2) the mouths of rivers opening into the main estuary; (3) island within the estuary; (4)

shoals and flood tide deltas; (5) intertidal flats; (6) inlets through barrier islands; and (7) the ocean and bay side of barrier islands. With so many features and the expected limited data available for quantitative analysis, we can construct an estuary morphology feature data entity (instantiation) from multiple data sources (e.g., satellite images and published reports). This method is demonstrated using examples from *Lagoa dos Patos*, Brazil, and Great Bay, NJ.

Great Bay, New Jersey (Figure 3.12), exemplifies some of the problems associated with tidal flow. It also is an excellent demonstration of what can be accomplished with very high resolution (< 100 m) grids. Great Bay is a bar-built estuary ~13 km N of Atlantic City. Inflow is minimal, it has an average depth of 1.5 m, and it has extensive intertidal sand and mud flats. It has a small inlet to the Atlantic Ocean and the semidiurnal tidal range on the open coast is < 2 m.

Figure 3.12. Google Earth image of Great Bay, New Jersey.

The first feature that is apparent in Figure 3.12 is the extensive flood tide delta that bifurcates at the inlet. There are numerous tidal channels incised between islands in the western bay. These channels are < 3 m and the light-colored areas are < 1 m. There are no ship channels because this is a state wildlife refuge. The intertidal areas can be inferred to coincide with water depths < 1 m. Using this guideline, the entire southern portion of the bay is intertidal and the mouth may even become partly dry at low tide (depth ~.7 m). This interpretation is supported by the presence of large bed forms visible in newer imagery. The newest image from Google Earth (6/2/2011) shows small waves diffracting on bottom features in the inlet. Diffraction can be used to infer water depths.

Oceanographic Features

Feature extraction is a form of dimensionality reduction. This approach allows input data that has redundant information (e.g., an eddy feature) to be represented by a set of features (i.e., *features vector*). One common example of general dimensionality reduction is principal component analysis. Feature extraction is completed by the analyst using the supplied tools, thus skipping the complex step of feature detection. The features that have been identified in this manner are reduced if possible and compared to similar features extracted from the validation data. A feature to be compared is instantiated differently for the model and the validation data. The feature can be extracted completely from the model because the 3D fields are available at a number of times. The validation data will not usually have this depth of coverage, however, and the feature must be constructed from available sources.

Recognition of the feature(s) is left to the user. A feature can be delimited by drawing a rectangle around it in the feature instantiations from the model and the validation data. If an important feature (e.g, an eddy) is present in the validation data and not in the model, there is no point in analyzing the currents further because the model has not produced a valid circulation field, no matter how it does at an isolated point (e.g., mooring). There are two possible approaches to describing a feature that is present in the model and the validation data. It can be analyzed directly from the current field or inferred from another data entity like SST. In comparing the potential vorticity of a feature like an eddy, for example, it may be more appropriate to infer the current field from SST if this estimation is required for the validation data. This would permit the two realizations of the field to be based on the same entity-relationship diagram. These methods are demonstrated using examples. The current field must be identified from a scalar field for most surface data (e.g., SST). This requires some method for detecting the feature from an image of this field, if possible. This can reduce the effort by the analyst.

EDDIES AND FRONTS

One very common feature that lends itself to feature extraction is an eddy. The current field associated with an eddy is dependent on geostrophic and ageostrophic flow, but this analysis does not invoke these components because of the difficulty of isolating their contributions in a general manner for flows that span deep to shallow water depths.

The method described here uses the geometric relationships between a circular feature, the gradient of some observed characteristic (e.g., water level or SST), and the strength and direction of the currents. An eddy has a distinctive SST signature that is predicted by a hydrodynamic model and observed in several satellite products. The eddy is only a partial instantiation of the actual 3D time-dependent flow field in the ocean, however. Despite their 3D, time-dependent properties, ocean eddies have characteristic features that can be representable by a limited number of dimensions: the path, diameter, velocity, Rossby No., drift speed and depth (Casella et al., 2011).

The analyst first identifies an eddy feature in the model fields and draws a bounding box around it with the software. The analogous feature is marked in the same way in the validation data entity. We can compare the model and SST realizations in three ways: (1) size of box drawn around the eddy (diameter); (2) temperature in the center (proxy for velocity as described below); and (3) location of center of box. Other attributes can be used to construct the eddy realization using other validation data entities (e.g., depth from XBTs or drift speed from multiple satellite images). Attributes (1) and (2) can be combined into a gradient, which is a measure of the intensity of the feature.

This example from Hu et al. (2011) (Figure 3.13) uses several data entities to analyze an eddy in the Gulf of Lion. The purpose is to demonstrate the kinds of current data that could be used to instantiate an eddy from validation data. This anticyclonic eddy would have warmer water in its center and the drifter tracks indicate clockwise flow. The ADCP currents from 15 m depth indicate the strength of the circulation and its relationship to the ambient flow.

Figure 3.13. Images of SST, drifter, and ADCP data for an anticyclonic eddy.

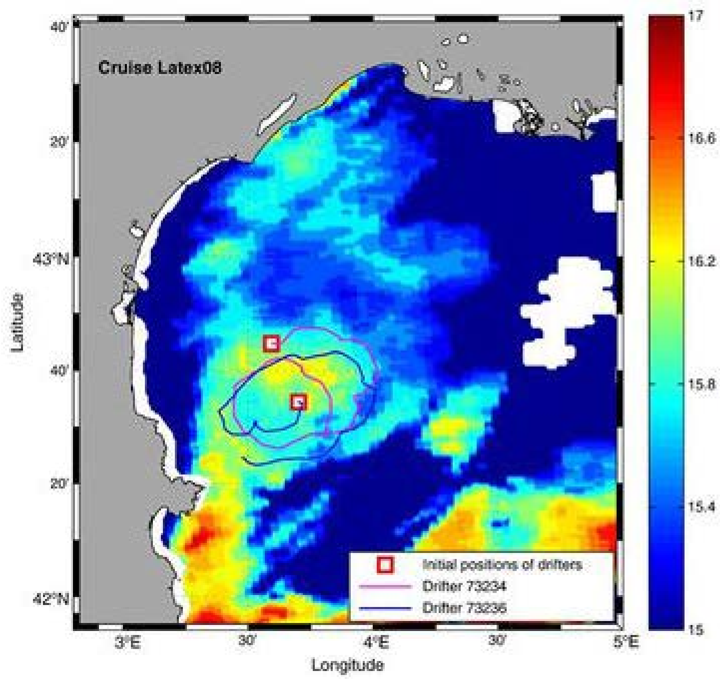

A.

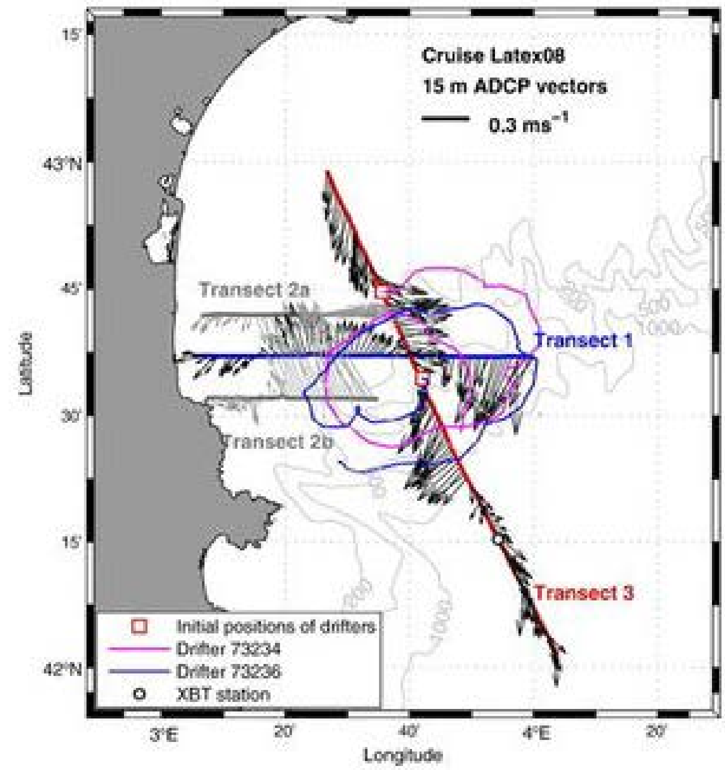

B.

These data are merged into the most complete instantiation of the eddy that can be created, but the satellite is complete in 2D only. The model should resemble this temperature field. More importantly, the surface currents from the model should show this clockwise rotation (northern hemisphere). This interpretation can also be applied to other surface characteristics such as [Chl].

An eddy can also be used to demonstrate the identification of multiple feature models. Eddies are often generated along fronts between deep-water currents like the Gulf Stream and the continental shelf water (Figure 3.14). Meanders in the Gulf Stream front produce eddies of different sizes, depending on proximity to the coast and meander size (Glenn and Ebbesmeyer, 1994). Figure 3.14 shows the spacing and size of these eddies in relation to the front. The eddies and front together comprise a *Features Vector*.

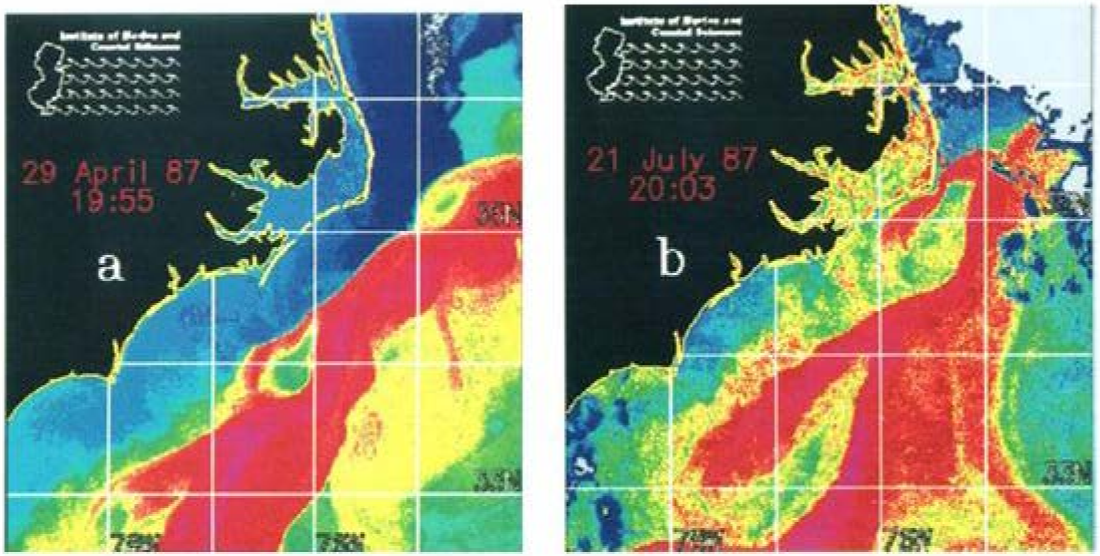

Plate 1. AVHRR images of the Gulf Stream near Cape Hatteras illustrating (a) small-meander mode on April 29, 1987 and (b) large-meander mode on July 21, 1987.

Figure 3.14. Images of eddy generation along the Gulf Stream.

UPWELLING FLOWS

When water is transported away from the coast by the wind, it is often replaced by colder subsurface water. This phenomenon can be identified in a model current field by either offshore surface flow or dominantly alongshore flow with the coast to the left (N. hemisphere). The resulting currents have a characteristic pattern O'Brien et al. (2011) (Figure 3.15). This pattern is not static in time, as seen by the rarity of upwelling flow (towards the bottom of the page). This feature is best instantiated by SST, but this is sometimes obscured by clouds this close to the coast.

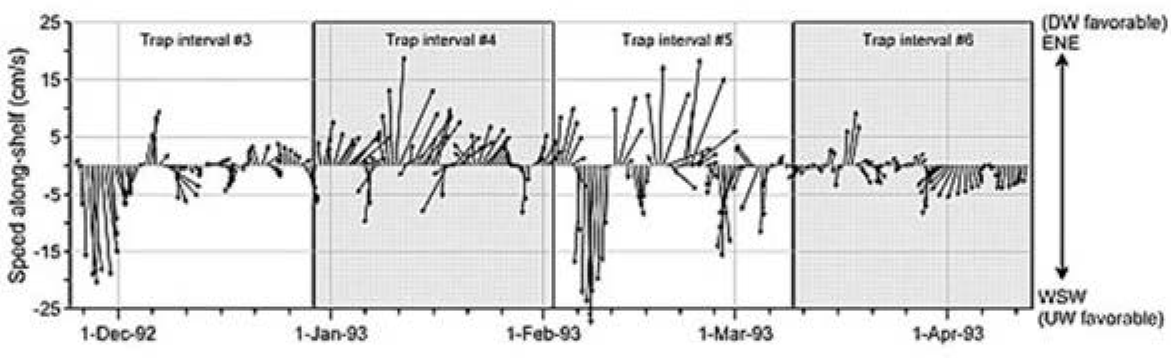

Figure 3.15. ADCP records from Arctic Ocean showing upwelling current pattern instantiation.

An identifiable pattern of cold (blue) water is visible along the NW Iberian peninsula (Figure 16). These images are easiest to interpret if there is a sequence as in this study. As with other circular features, the pattern can be used to construct geometric descriptions of the upwelling feature and inferred surface current vectors.

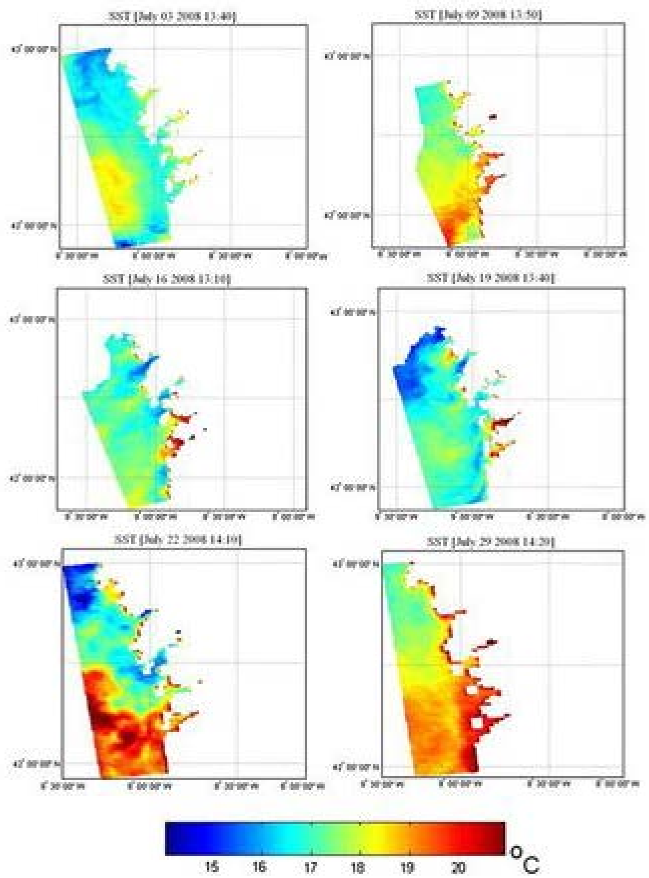

Figure 3.16. SST from MERIS for the northern Iberian Peninsula (Spyrakos et al., 2011).

RIVER PLUMES AND COASTAL CURRENTS (JETS)

The fresh and often colder/warmer water that enters the coastal sea from river mouths can be identified by satellites because it has different optically active components than ocean water. This plume has a flow field associated with it that can be inferred from its remote sensing signature. This plume in the Bay of Biscay (Figure 3.17) indicates the direction of the mean coastal flow as well as the overall strength of the river input.

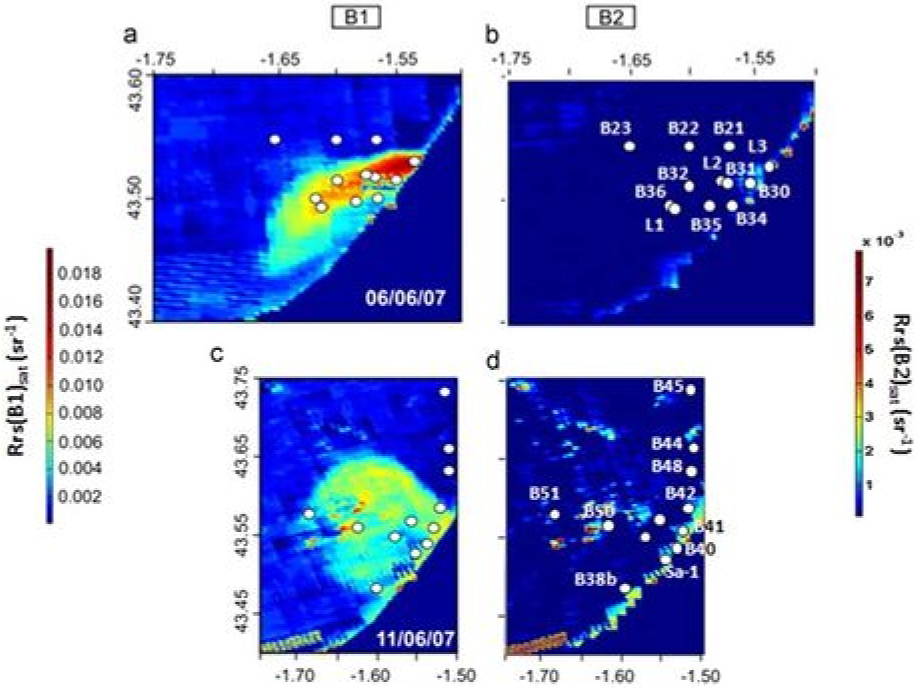

Figure 3.17. MODIS image of a plume in the Bay of Biscay.

Coastal currents can be associated with river discharge, which is often a source of different density water. Observations of these jets can also be from satellites but they have a characteristic velocity signal as well. They can also be formed by changes in shoreline orientation as in the example below. This plume (Figure 3.18) is steady because of the headland that contributes to it.

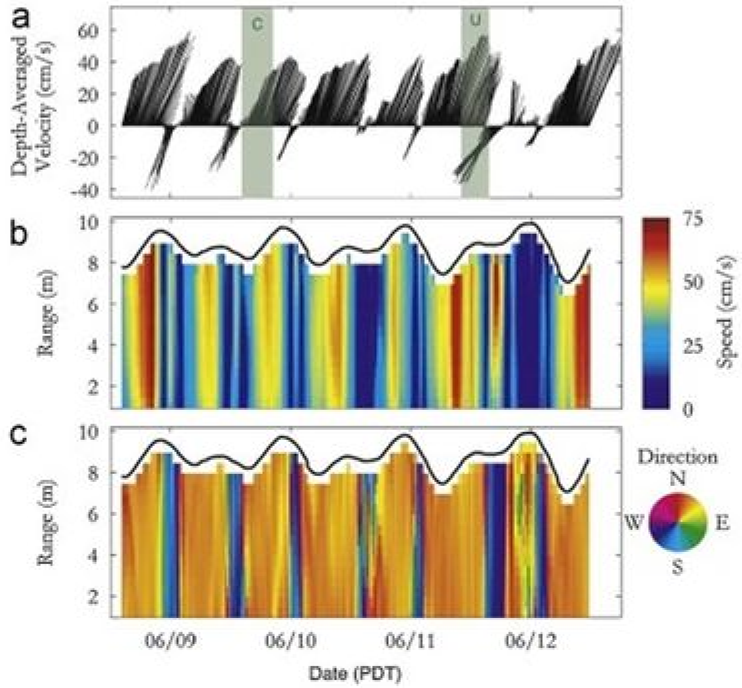

Figure 3.18. Measured currents from a coastally trapped jet (Warrick and Stevens, 2010).

TIDAL FLOWS

Tides are ubiquitous and are a critical element in evaluating the performance of a coastal model. Tidal predictions can be evaluated using several methods: (1) tidal ellipses that represent the currents over a tidal cycle; (2) time series analysis of water levels or currents; (3) harmonic analysis of mixed currents to evaluate specific tidal constituents; and (4) the residual flow over a tidal cycle or other restricted interval. These *Tidal Features* are used to validate a model. They are constructed from time series of model results and observations; the resulting feature instantiations can be compared directly.

For situations where real-time concurrent water levels and currents are available, the model skill can be quantified using speed, direction, and timing of flows. When such data are lacking, it is necessary to complete a tidal analysis using one of these methods. The approach is based on the harmonic analysis of water levels, which is the standard practice in the U.S.

The simplest tidal feature is a time series of water level or currents at a point. If the model includes subtidal flow (e.g., wind forcing), individual tidal constituents can be constructed using harmonic analysis. These are numeric data consisting of amplitude and phase for water levels, as well as currents. These constituents can then be reconstructed to predict the mixed tide from a model, or observations, that has multiple tidal forcing in addition to wind and other forcing. The resulting synthetic time series can be compared to a similar feature reconstructed from *in situ* measurements.

Model Validation

This procedure allows the analyst to compare the representations of geophysical features from two instantiations. The input instantiation is the model fields, and the second is a compound instantiation constructed from the incomplete representations inferred from multiple sources. The underlying features are never wholly represented by the instantiations. Think of these as bombed buildings; it is difficult to locate the library or the post office without a sign. Even the model fields do not necessarily fully represent the features because of uncertainties in the initial condition and boundary conditions, in addition to simplifications in the model physics (e.g., parametrization of mixing).

The operations have been kept to a minimum number. The realization of the conceptual data model consists of seven validation steps that have no particular hierarchy (although we recommend a specific sequence), but are instead dependent on data availability. These data sources are searched using a method to be partly supplied by NAVO. The analyst will complete whichever steps they feel are justified. Their determination of model performance is assisted by several decision aids that they are already familiar with (e.g., skill indices like RMS error). They can produce a quantitative index of the validation procedure if they choose.

The approach is demonstrated using example(s) from our archives. The purpose is to demonstrate the procedure and how the analyst might apply it.

The model performance should be evaluated strictly on how it handles tides separately from other flows. This evaluation should be done before a complete model setup is initiated and may not directly fit into the model validation procedures described below. If this evaluation fails, any further evaluation may just as well be curtailed. All wind stresses should be removed and the model should be run for two weeks (even in barotropic mode) just to get the tidal behaviour of the model. The tidal output should be transformed into spectral space and compared to tidal constituents which can be obtained from well known tidal database.

Components

It is not really necessary to build the analysis model from pieces but it is convenient for the purpose of demonstrating the relationships encapsulated in the data model. The components are: (1) regions or sub-domains within the model domain; (2) the representations of geophysical features both in the model and the validation data; (3) the comparison logical blocks; and (4) a quantitative score. These components are represented in the logical model as steps to be completed, but which can be skipped if desired.

ANALYSIS BLOCKS

This is an optional component. Some coastal domains consist of multiple dynamical or morphological regions; the Mississippi Bight region can be subdivided into three blocks (Figure 3.19), (A) the open sea, (B) Mississippi Sound, and (C) the Mississippi R. delta, based on nothing more than their boundaries. The open sea is impacted by the open boundary conditions more. Mississippi Sound is sensitive to land boundaries and inflow from rivers, and the delta is a complex area where the dynamics of the shallow sounds is affected by deep water directly. These blocks can be selected by the analyst for separate validation by putting a box around them. This action will then assure consistent validation of the model by subjective interpretation as well as quantitative skill assessment. The independent results can then be inter-compared or merged as desired.

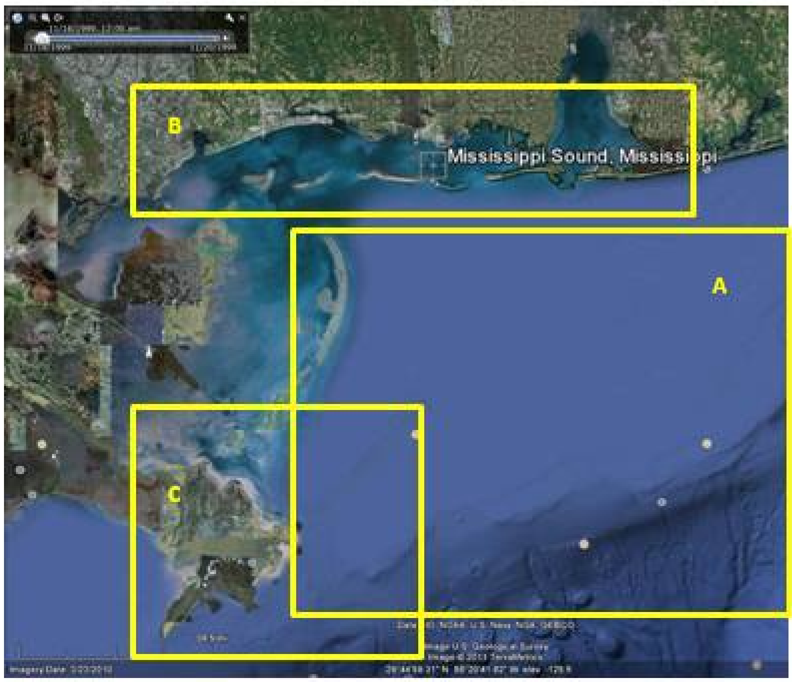

Figure 3.19. Google Earth image of Mississippi Bight, showing possible validation boxes.

FEATURE INSTANTIATIONS

It possible to complete the model validation procedure without reference to features but we believe that the analyst will find the endeavor less stressful if this component is used to some degree. This is especially true if no direct current measurements are available. Some may also be uncomfortable with the concept of a temporal feature like a tidal flow. The system is designed to work with or without this component, but this will make it simpler.

We have used the term *instantiations* consistently throughout this report to convey the fundamental problem of sampling the coastal ocean sufficiently to have a complete picture of the flow. The analysis will thus consist of comparing these incomplete pictures of the current field. The most *complete* instantiation comes from the model but this does not mean it is accurate. We can really only sample this field in pieces anyway. For example, we use time series to sample in time but only at one location. We also can use contour plots of horizontal or vertical sections. We can be creative and use time/space plots to examine the evolution of a section. We can even use isosurfaces, but none of these is a complete representation. The model output consists of the numerical grid, and gridded fields of currents, salinity, temperature, as well as the water surface anomaly. The problem of capturing the 3D flow field in the coastal ocean is simplified by the introduction of *features*, in the sense of the conceptual data model. We don't need to grasp the entire flow field at one moment to evaluate it; instead, we focus on features within our analysis block(s). The feature paradigm allows different instantiations of the flow field to be compared (Figure 3.20).

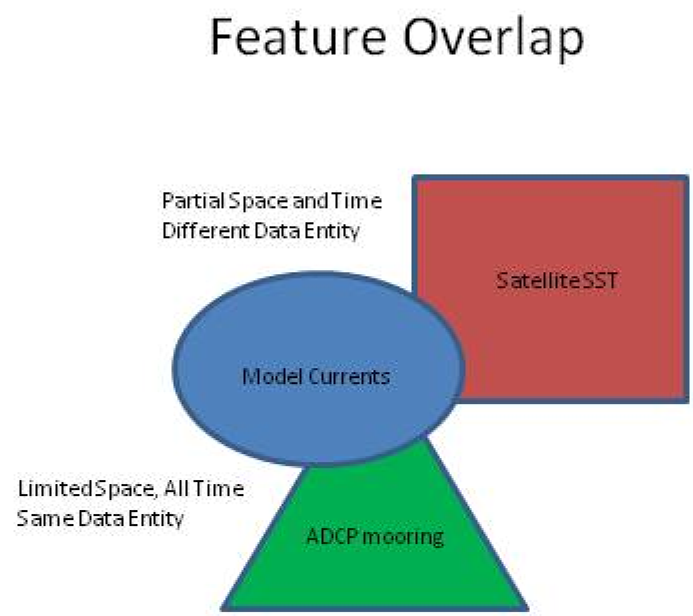

Figure 3.20. Schematic of space/time/data overlap for feature instantiations.

The current field from the model can be partly inferred from an SST image, which may not coincide exactly in space or time with the model field. We also need to rely on our understanding of the entity-relationship for this process, but we can estimate the current field related to the SST. The ADCP gives an exact match in time but only for one location; it thus cannot fully represent the feature associated with its observed flow.

We can identify geophysical features most easily from spatial representations (like satellite images). Tidal flow is a *temporal* feature, however, that can be very useful in evaluating a model. The analysis is most effective if features can be identified in one of the instantiations that are common to several, especially the model.

VALIDATION RULES

Validation is the act of comparing two instantiations of a geophysical feature to allow a conclusion to be made about the model-predicted currents. This is the definition we are using. Therefore, the statements contained in this section are always applied in a one-to-one manner, and always including the model instantiation. This component is the kernel of the analysis procedure. These statements must be applied as carefully as possible to achieve consistent results.

The process of arriving at a validation metric for the model fields is necessarily subjective because of the incompleteness of the different instantiations of the geophysical features. This does not preclude using a relatively small number of statements to represent the myriad of potential entity-relationships that exist in the ocean. The relationships introduced in this section should be considered a starting point rather than an exhaustive list. More are added on a continuous basis. It is also probable that many of them can be made semi-automatic if they are based on quantitative measures like water depth. These statements are incorporated into the logical process model as queries, decision aids, automatic procedures, and standalone actions by the analyst (e.g., go to the library/internet and look for historical data). They are listed in no particular order at this time.

These comparison are made for each analysis block. This is the reason we recommend using multiple blocks and letting the software keep track of the model performance within each.

- *Overlay the grid onto a shore*line digitized from an image. Mark cells that are over land or if the model grid does not resolve the shoreline at all.
- Compare model water depth to bathymetry. Evaluate number of levels in the model and whether a substantial fraction of the model z axis is deeper than water depth.
- Direct comparison of currents to observations. If the observations are historical, make appropriate adjustments to the result.
- Compare drifter tracks from concurrent or seasonally corrected data to simulated drifters in model output fields.
- Direct comparison of tidal heights and/or currents for different constituents from available historical tide data.
- Calculate residual currents for model results with tides and compare to seasonally adjusted results from observations, models, or satellite observations (e.g., altimetry).
- Compare surface representations of ocean features using temperature/salinity. Apply feature model(s) to evaluate the likelihood that the model flow is consistent with the validation data
- Time-dependent depth compared to observations: The water depth can be used to infer direction of movement or the relative magnitude of flow. For example, tidal maximum currents occur during ebb or flood stage. The direction can be inferred for some locations, where coastal morphology constrains flow. The peak currents can be inferred for more general cases.
- Comparison with meteorology is intended to be qualitative only. Maps of pressure systems with available wind barbs can be used to estimate surface wind direction and magnitude, which will impact surface currents.

These statements do not necessarily represent discrete steps in the analysis. One method that is under consideration is to incorporate the *source* attributes of the instantiations used in the comparisons using the steps that comprise the logical model as listed in the **Algorithm** section. This additional step would put more weight on the accuracy of the validation data.

There are three main categories of ocean feature: (1) circular features; (2) linear features; and (3) special features. These classes are based on geometry because this attribute can be used to identify distinctive characteristics that allow model and validation instantiations to be quantitatively compared. This entity-relationship attribute (representing physical cause-and-effect processes as geometric shapes) is not necessarily useful to a user, however. For the purpose of aiding in model validation, it is better to identify standard features that can be compared with traditional oceanographic knowledge. Several examples have been completed, which has contributed to an initial list of standard features. We expect this list to be supplemented as experience increases. These features can be organized in order of decreasing impact/confidence.

- shoreline
- tidal currents
- coastal currents
- eddies
- filaments
- estuarine morphology
- surface water patches
- atmospheric events

This order is based on previous examples and may be changed. It is implemented through the *physical model* as a sequential guide. The user can assign confidence based on their criteria. These standard features have key words that are stored in the *GeophysicalFeatures.FeatureType* member.

SCORING

This is an optional component that will probably become more useful as the validation procedure is applied to more cases. It is an attempt to quantify the validation procedure. At the very least, this will permit an analyst to evaluate their own performance.

Each validation step described above can be scored as pass or fail. However, a failure is not necessarily a final statement about the entire forecast because no model is completely wrong all of the time. This subjective decision might be easier if a cumulative score is kept for the forecast. This is the intent of the score.

The performance can be ranked pass (S = 1) or fail (S = 0.5). As the analysis proceeds through the recommended validation steps listed in the next section, the score is multiplied. Thus, a good forecast would result in a score of 1. If there were a wealth of validation data and the analyst had the time and inclination, a horrible forecast would have a score, $S = 2^7$ or 0.007. This is not a fraction or a percent. It is just a small number (probably not good). This score would be applicable to the entire analysis block. This is one reason to select these blocks with some consideration of their common dynamics.

An alternative scoring method is a summation, with pass = 1 and fail = 0. The maximum score would then be 7 and the minimum 0. This ranking would err on the side of conservative evaluation because a lack of validation data would be implicitly interpreted as a fail. This could be useful and it is possible to have both scores included in the logical model. This should be a topic of ongoing discussion and development.

Algorithm

The comparison statements listed above do not represent discrete steps in the model validation procedure. They are used within the validation steps listed below.

- Shoreline
- Water Depth
- Concurrent Ocean Measurements
- Surface Features
- Historical Data or Climatology
- Supplementary Models
- Meteorological Analysis

Each of these seven steps will result in a conclusion about the model's performance. The analyst will then evaluate its relative performance on applicable comparisons to rank the forecast. An optional scoring system was described in the previous section. The validation cannot be succinctly described. Instead, we will demonstrate how the algorithm can be applied to a model forecast using examples.

Ocean Feature Comparison Methods

Eddies and Fronts

The size and intensity can be combined into a gradient, which is a measure of the intensity of the feature. The location of the center as indicated by the analyst can be used to evaluate the accuracy of the eddy's position; if the model eddy has overlap with the validation data to a specified tolerance (to be determined from experience), it can be considered as accurately simulated. The intensity of the feature is analogous to the average vorticity of the eddy. We can apply this concept to the two eddy realizations by using the temperature gradient as a proxy for the *intensity* of the circulation. Both can be normalized by the model central temperature. The area of the closed flow (isentropic surface) is represented by the diameter of each representation, again scaled by the model prediction. The model always has an *average vorticity* of 1.0 and the validation data entity can range from 0 to >> 1. However, large numbers shouldn't be expected because this would imply no eddy feature is present in the model output. This can produce an estimate of the error in the eddy speed as a simple function of its diameter and temperature gradient. The current direction can also be inferred from the radial gradient of a parameter like SST or SSH, which is representative of the pressure gradient. The sign of the Coriolis force thus determines the rotation.

The model and validation instantiations of the western front can be represented by lines drawn by the analyst coinciding with the approximate location of the front in the two realizations. The analysis method will then compare the locations of the lines and the values of the data entities (e.g., SST, SSH, [Chl]) along this analysis line and produce a result similar to that for the eddy feature. It is also straightforward to calculate a gradient perpendicular to the linear feature for comparison. The two features together represent the Gulf Stream frontal system as seen in the images.

Upwelling Flows

The model SST fields can be compared directly to this kind of pattern. This will allow the 3D nature of the model instantiation to be evaluated.

River Plumes and Coastal Currents (Jets)

Plumes and coastal currents are good for validating model simulations because they have characteristic flow fields associated with them. However, they are often impacted by other coastal processes such as the wind and tides. Figure 3.21 shows the salinity fields and currents over a tidal cycle in the Yangtze River plume (Gao et al., 2009). The fresh water is trapped at the coast until the wind and tide transports it offshore. For this large plume, a jet does not form near the coast.

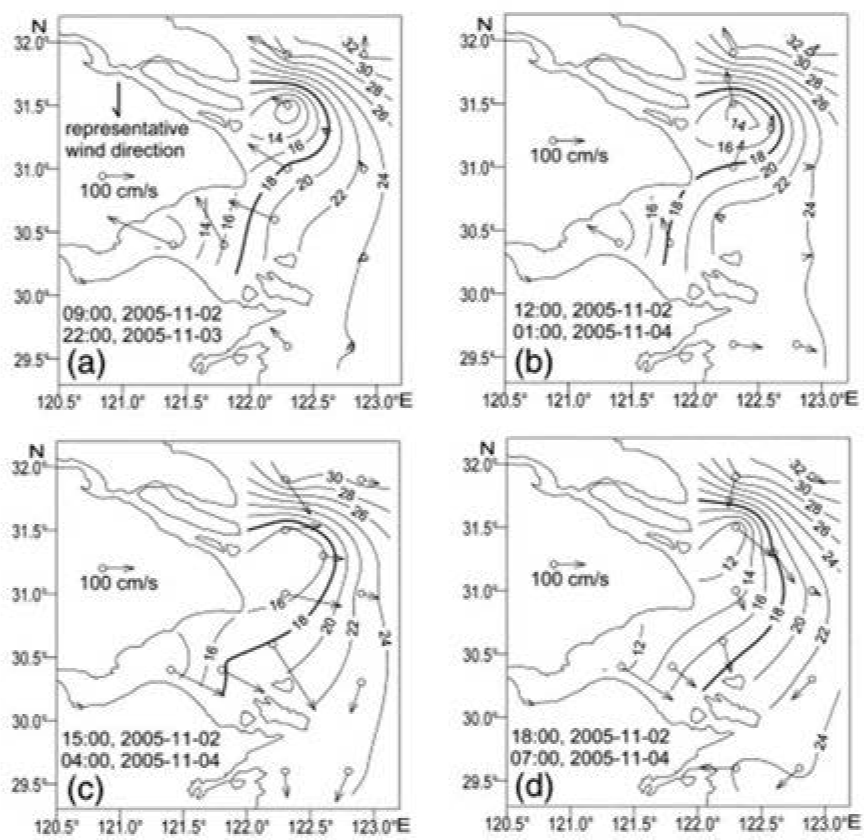

Figure 3.21. Salinity and surface currents over a tidal cycle in the Yangtze River plume.

The magnitudes cannot typically be inferred from these data but the direction is critical and the integrated movement can often be estimated from feature tracking algorithms.

Tidal Flows

The tidal analysis quantifies the model skill for predicting daily changes in water level and flow due to astronomical motion. For situations where real-time concurrent water levels and currents are available, the model skill can be quantified using speed, direction, and timing of flows. When such data are lacking, it is necessary to complete a tidal analysis using one of these methods. The approach is based on the harmonic analysis of water levels.

The deconstruction of a mixed signal to calculate the contribution to the motion of multiple astonomical forcing is accomplished by comparing different instantiations of these *features*.

- Tidal ellipses
- tidal constituent amplitude and phase for water level and currents
- residual tidal flow

This analysis was run for the model output from near the Porto Do Rio Grande IHO station (Figure 3.22) using the 29 default constituents. The result is shown in Table 3.1.

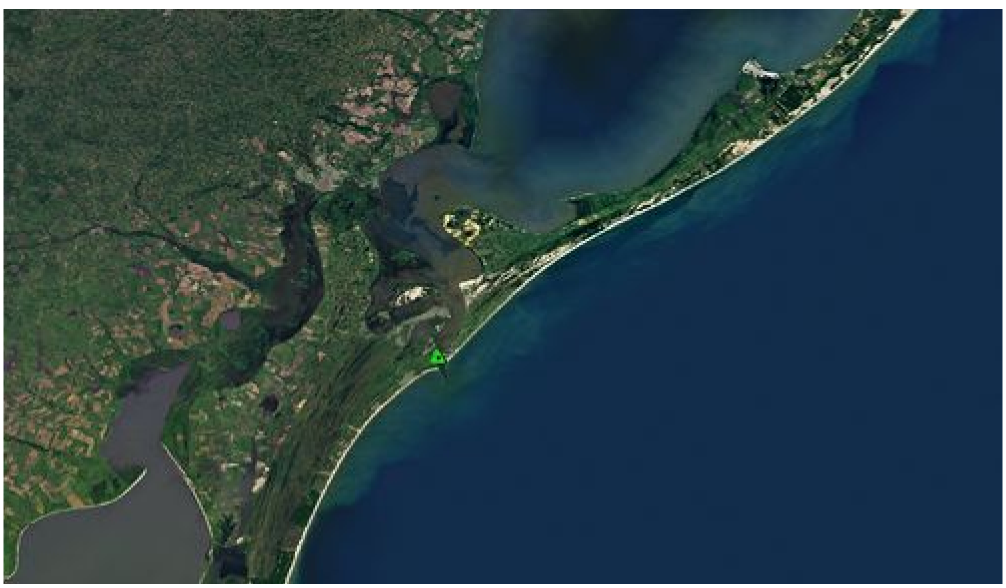

Figure 3.22. Map showing location of the sole tide gauge for the Rio Grande in Brazil. The time series are shown in Figure 3.23.

Table 3.1. Harmonic Analysis Results.

The screen output is:

```
UTide Results:
Cnstit      A      A_ci         g      g_ci
  O1     0.144    0.0222      145.       8.83
  S2     0.101    0.0259      233.       14.7
  K1    0.0908    0.0235      218.       14.8
  M2    0.0809    0.0265      196.       18.8
  N2    0.0522    0.0264      333.       29.0
 MSF    0.0383    0.0264      317.       39.5
  Q1    0.0299    0.0218      129.       41.9
 2Q1    0.0160    0.0216      122.       77.4
 NO1    0.0154    0.0337      188.       125.
 OO1    0.0146    0.0169      103.       66.1
  J1    0.0138    0.0215      336.       89.1
UPS1   0.00575    0.0156      297.       156.
 SK3   0.00446    0.0231      235.       297.
ETA2   0.00416    0.0163      223.       225.
  M3   0.00291    0.0271      344.       534.
 MS4   0.00242    0.0263      305.       623.
 MO3   0.00240    0.0227      259.       542.
3MK7   0.00209    0.0254      202.       701.
2MK5   0.00186    0.0247      193.       759.
 MK3   0.00164    0.0241      92.6       843.
  S4   0.00150    0.0254      43.4       972.
2MN6   0.00145    0.0282      282. 1.12e+003
 MN4   0.00130    0.0273      266. 1.21e+003
  M6   0.00126    0.0284      154. 1.28e+003
2SM6   0.00106    0.0264      66.0 1.41e+003
  M8  0.000723    0.0291      151. 2.30e+003
2MS6  0.000655    0.0274      338. 2.37e+003
  M4  0.000490    0.0274      31.9 3.20e+003
2SK5  0.000147    0.0230      131. 8.93e+003
 Mean (input units) =    0.0820
 Trend slope (input units per day) =   0.00503

UTide Run Description (executed 08-May-2012 11:48:08):
  Input(1D): 370 values, equispaced times, dt=2.00 hr.
    dur'n 30.8 dy; 01-Jan-05 00:00 to 31-Jan-05 18:00 GMT.
  Method: OLS.
  Conf-ints: linearized; white.
  Model: allc=29 cnstits (29 non-ref), auto (Rmin=1.00);
    trend included; no prefiltering correction;
    exact nod/sat corrections (lat=-32.157);
    g= Gwich phase lag, astr arg exact times;
    no inference.
```

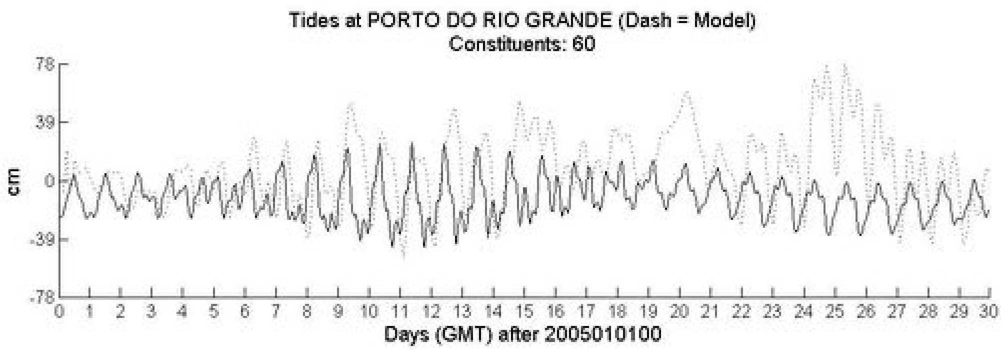

Figure 3.23. Predicted tidal elevations at Porto do Rio Grande.

These estimated coefficients from the model can be compared to the IHO values to get quantify model accuracy. Table 3.2 shows a bias in the model. The amplitude error is consistently positive (overprediction) and the phase is mostly positive, which indicates a substantial lag in timing. Note that these errors are not seen well in the timeseries because of potential subtidal signals.

Table 3.2. Comparison of the model and IHO amplitude and phase for Porto do Rio Grande for Jan 2005.

Constituent (Period, Hr)	Meas. Amp (cm)	Model Amp. (cm)	Error (Model-Meas.)	Meas. Phase (°)	Model Phase (°)	Error (Model-Meas. hr)
O1 (25.8)	10.8	14.4	3.6	72	145	4.9
S2 (12)	3.4	10.1	6.7	26	233	6.9
K1 (23.9)	4.7	9	4.3	134	218	5.6
M2 (12.4)	3.4	8	4.6	228	196	-1
N2 (12.7)	4.4	5.2	0.8	193	333	4.7
MSF (354)	3.4	3.8	0.4	256	317	60
Q1 (26.9)	3.1	3	-0.1	40	129	6
2Q1 (28)	0.1	1.6	1.5	291	122	-13.4
OO1 (22.3)	0.2	1.5	1.3	327	103	-13.7
J1 (23.1)	0.2	1.4	1.2	183	336	10

The estimated tide-only computations from the model can be reconstructed from the constituents in the same manner as the measured tides. We do not need to do this, however, because it would not be as quantitative as the skill measures in the table. The other tides have amplitudes <1 cm and are not compared. The impact of the long MSF tide (period of 15 days) is seen in the bimodal character of the tides. The tide does not rise above mean sea level except between 6 and 17 January. Of course this value of ~20 cm is due to the interaction of the multiple constituents with similar amplitudes but different phases. This is a good example of the importance of properly reproducing weaker tides in areas such as this.

Geographic Feature Comparison

Shoreline Features

This is a fundamental analysis for coastal problems. There can be no currents over land. This seemingly simple statement hides a complex decision tree in applying available coastline data, however. There are several issues that must be addressed before analyzing the model using a shoreline feature: (1) available sources of shoreline; (2) accuracy/precision of model shoreline; (3) changes in coastline with tidal activity; (4) kinds of discrepancies between the validation realization and the model (systematic versus random); (5) associated errors in water depth. This is really three problems, (5) has to do with the static water depth and (3) with the time-dependence of depth.

The most fundamental geomorphological feature is the shoreline, which is static and has an indisputable impact on the interpretation of coastal currents. As observable as the shoreline is, its position can be included in different feature entities in very different places. These differences can be systematic or random, depending on how the data points were collected to build the feature. For example, in areas with a large tidal range, it is very important to incorporate this water depth variation in constructing a shoreline. There are thus two ways in which two shoreline feature entities can be compared. Before any comparison can be attempted, however, it is necessary to determine the feature with the highest accuracy. This feature instantiation can then be used to adjust a less-well defined instantiation of a different kind. We can demonstrate this with an example. The contours of SST in Figure 3.5 show that the model shoreline does not coincide with that from a georeferenced satellite image. The overlap is as much as 2 grid points (~2 km). This discrepancy appears to be systematic, with a model shift to the NW.

A similar shift has been observed for a small tidal basin in San Francisco Bay (Figure 3.24). The magnitude of the shift was much less there but it was very significant for the scale of the study area. The model output was simply moved by the required amount using trial and error. If this method is used, however, it is important to correct all of the model data to avoid uncertainty in interpretation. The only way to correct random location errors is to mask all bad model points.

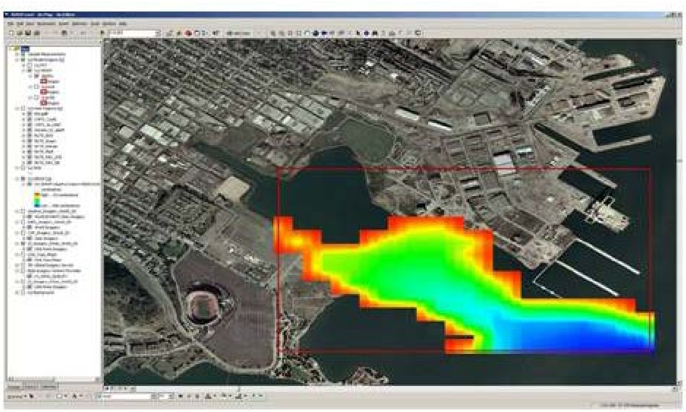

Figure 3.24. Overlay of satellite image on the model bathymetry for Hunters Point, San Francisco Bay.

The imported shoreline feature can be used to aid in interpreting the model results or to mask the model currents without evaluation. The southeast tip of Sicily (Figure3.25A) is a very low area adjacent to depths >3000 m only a few kilometers offshore. This coast consists of multiple concave bays and there are several sand spits and islands. The white line in Figure 3.25A represents the coast as digitized from a much greater distance above the earth's surface.

Figure 3.25. Satellite images and model grid for the southeast tip of Sicily. A. Image from 15 miles altitude of SE tip of Sicily. B. Model grid for Sicily. C. Contour plot of DBDB2 bathymetry and grid (+) used to construct the model grid.

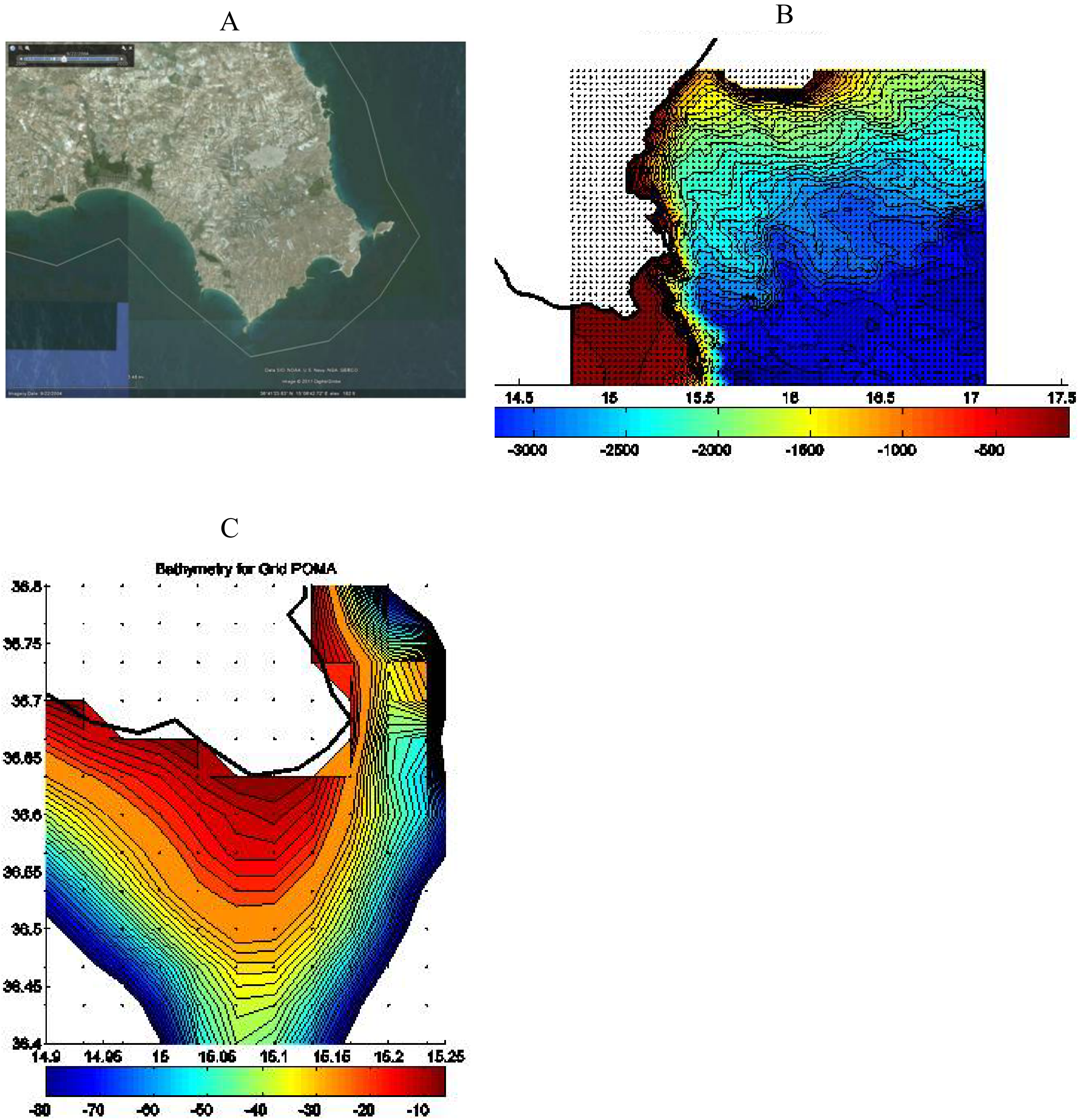

It is not always necessary to resolve these shoreline features. This is an important criterion for evaluating model-predicted currents near the coast because such an analysis is time consuming. The DBDB2 bathymetry for this area represents the general shoreline fairly well. The model grid is produced from this database. Note that the imported shoreline is a good match to this data, even though it is at a relatively coarse resolution of 2 minutes (~3700 m at equator). However, when a model grid with a higher resolution is created from this data, spurious grid cells can be produced. It is also apparent that the imported shoreline feature should be appropriate for the intended analysis.

Shelf Bathymetry

A model simulation (Figure 3.26) along the Florida coast shows significant variation of both vertical and horizontal flow, reflecting a down-welling flow that extends 10 km offshore. The maximum depth of the transect is 16 m. This would be 10 model grid cells in the Sicily grid (Figure 3.25B). If the model is being used to produce a current forecast at this resolution, it is reasonable to assume that the currents at the coast matter.

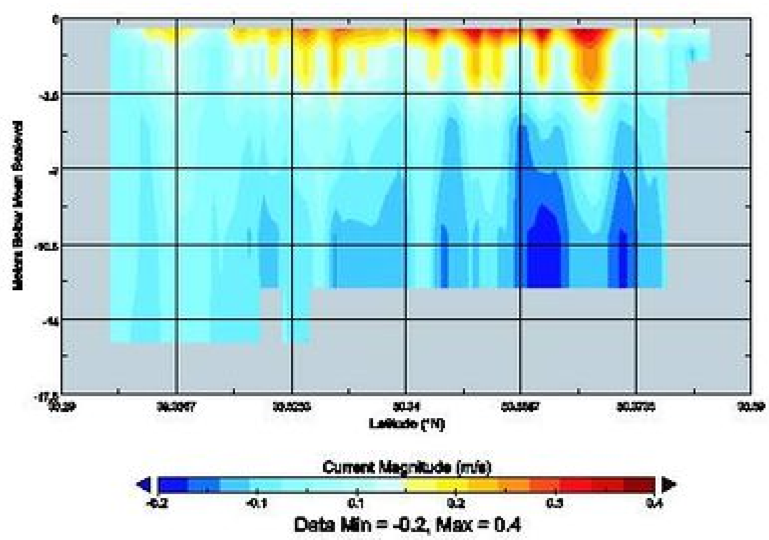

Figure 3.26. Across-shore flow from a model simulation: red = landward and blue = seaward.

The transects from *Mangueira Lagoon* (see Figures 3.10 and 3.11) can be superimposed on sections from the model's bathymetry feature (Figure 3.27) to allow the user to evaluate the currents below the surface. The analysis would then consist of determining which model depths would be valid for use. Those below the blue line would obviously be incorrect. It is also likely that the entire current profile would be incorrect because of excessive water depth, which could cause either high or low currents. Which one would depend on the physical forcing at the time.

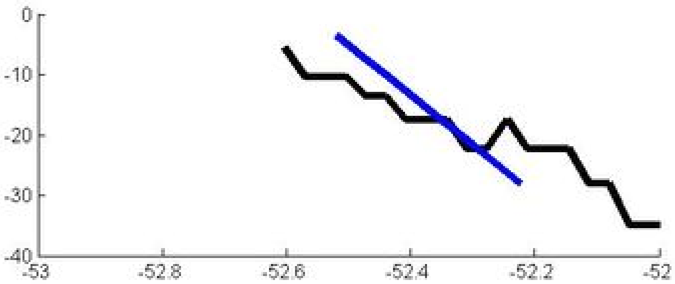

Figure 3.27. The blue line is the synthetic profile superimposed on the model bathymetry feature (black).

Estuarine Features

The composite satellite image from this region (Figure 3.28) shows the variation in the quality of data used for these images. Some of the bathymetry features are only visible in one block. Nevertheless, a great deal can be discerned from this image. The shoreline has been added as a path overlain on the model grid.

Figure 3.28. Satellite images and model grid for Mangueira Lagoon in Brazil. (A) Overlay of digitized shoreline (cyan line) on satellite image for a 3 km grid. (B) Overlay of digitized shoreline (white line) on model bathymetry for 1.5 km(left) and 3 km (right) grids.

A

B

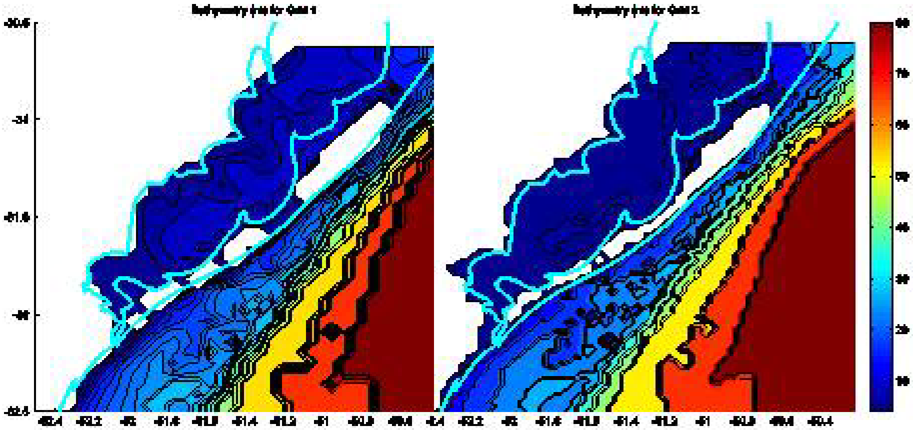

This example can be used to evaluate several of the estuary features. There are several rivers and bays connected to this estuary, none of which are reflected in the model grids. Although there are islands and shoals, we will discuss these features in the next example. Intertidal areas are not readily identified in the image (Figure 3.29A) but there are extensive areas with estimated water depths less than 1 m, which are probably intertidal. The interpretation of these areas is discussed later. The largest errors in the model currents are associated with the large channels through the barrier island in both grids. The truncation of the lagoon in the north is mostly going to impact local flow but the false openings will cause spurious exchange with the Atlantic. This is seen in the surface currents from the model (Figure 3.29B). There is uninterrupted flow into the lagoon from the north.

Figure 3.29. Currents in Mangueira Lagoon, Brazil. (A) Surface currents from the model in Patos Lagoon. (B) Measured currents from ship-mounted ADCP in main channel of Mangueira Lagoon (Marques et al., 2010).

A

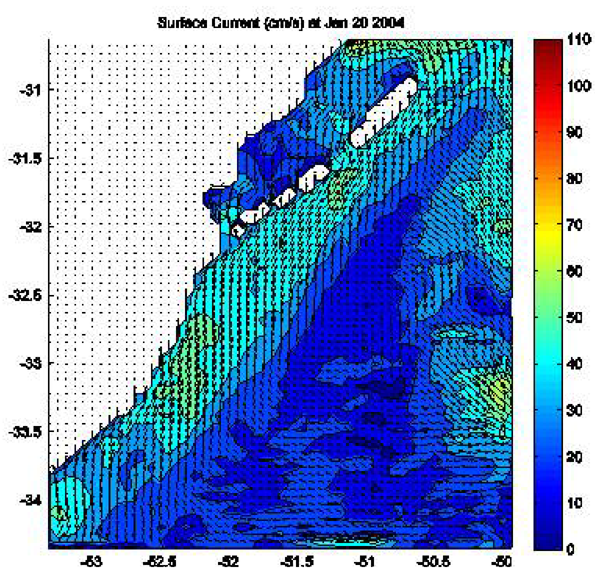

B

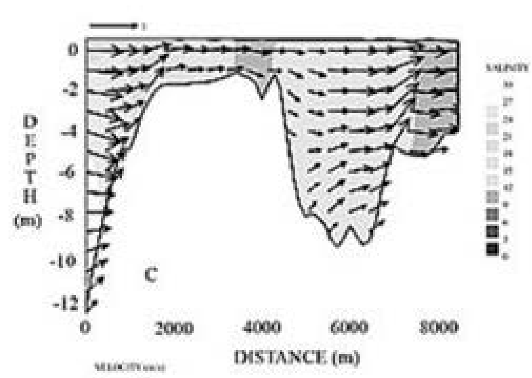

The magnitudes exceed 50 cm/s, which is obviously unreal. The superimposed shoreline can be used to mask bad areas as well as interpret flow within the area, both on the shelf and in the estuary. The satellite image can also be used to note the location of rivers, which will have a direct impact on flow as a function of their inflow rate. This is discussed later. Estuary inlet features can sometimes be constructed from historical data because of the general interest in exchange between the open sea and estuaries. A detailed transect through the *real* inlet to the lagoon shows the presence of a very shallow sill. This suggests that this inlet is relatively new, which is not surprising considering the rapid sedimentation as evidenced by the Chenier plain coastal morphology.

Compound estuary features cannot be easily digitized as discussed in previous sections. A direct comparison method can be used, however, that allows an experienced analyst to quickly determine the validity of the model currents. The general idea is to overlay an image from the model currents onto a satellite image. It doesn't take very long to get a reasonable match using trial and error. Several examples of this procedure can be seen at our gserver web server. The model current feature is then decreased in opaqueness (increased transparency) until the underlying estuary feature is visible. This method is applied to wind and tidal flow in Great Bay (Figure 3.30) as been simulated with POM on 50 m and 100 m grids generated from NOAA bathymetry data. The minimum depth in the model is 1.5 m.

Figure 3.30. Overlay from Google Earth of POM currents on Great Bay.

The islands can be seen to match well. The currents are thus in the correct direction. The channels between the islands are not resolved and the flow is therefore, too broad. The increased currents south of the islands are probably reasonable because there are no unknown features in that area and the water depth is relatively uniform and shallow. It appears, however, that the

NOAA bathymetry did not include extension of the spit from the N side of Little Egg Inlet, which has moved ~ 2 km into the inlet in the newer satellite image.

Tidal Effects on Geographic Features

Coastal water depths are subject to substantial changes because of both astronomical and meteorological tides. This changes the water depth as well as the position of the shoreline. If the tidal range is large and/or the shoreface slope is small, extreme changes in shoreline position will result. This effect is sufficiently large to warrant special treatment. This is part of the analysis for geomorphology features, however, and is part of the methods discussed above in the logical model.

The astronomical tides are repetitive and, thus, not requiring special measurements to evaluate. Furthermore, tidal models are increasing in global coverage at finer scales. In addition to these models, coastal tides have been tabulated and modeled with mathematical formulas from many years of measurements. A third source of tidal elevation (and sometimes current) data is historical records published in scientific journals and conference proceedings. For example, the measured water level in the inlet to *Mangueirs Lagoon* (Figure 3.31) shows the magnitude of the tidal variability, which includes the meteorological and atmospheric tides.

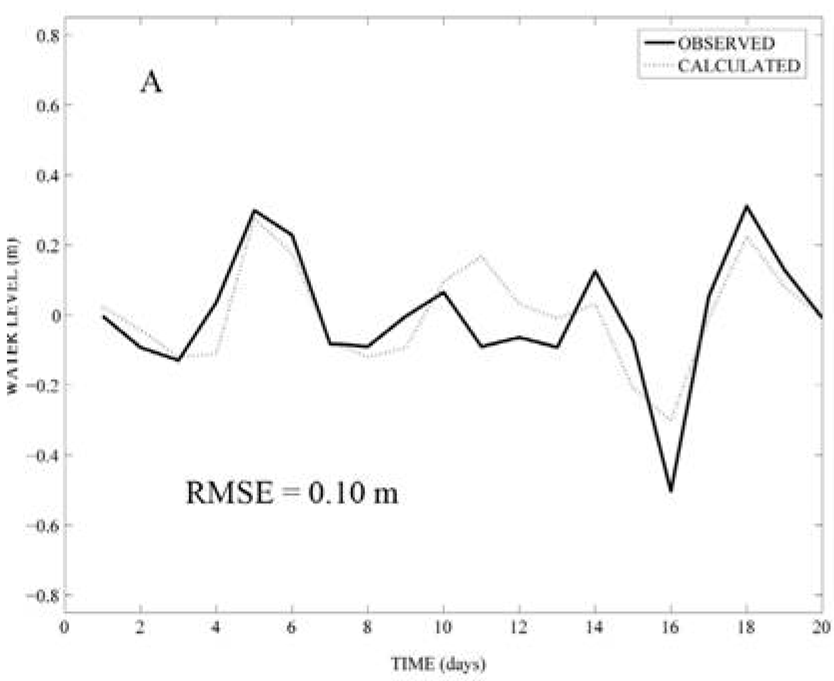

Figure 3.31. Measured water level in the inlet to Patos Lagoon.

This type of data can be used to evaluate the model with respect to both kinds of response. It looks like the astronomical tide is < 10 cm but subtidal variations can be > 50 cm. This would suggest that tidal flats would exist at synoptic scales but not daily because there are expanses of the lagoon that are < 50 cm deep. Such a timeseries of water level will need to be visible along with the morphology features during estuarine feature analysis. It is important to show these time series for both the model and the observation *instantiations* of the water level. This data could also be included in the bathymetry feature analysis above to adjust the synthetic profiles for the shoreface if warranted.

This example shows the complexity of analyzing flow features in estuaries. In order to validate the model currents with respect to the morphology sub-feature (part of estuary feature), the model water level must first be validated against any available observations or other models. The appropriate impacts of water level changes can then be used to adjust geomorphology features. If the model is accurate for magnitude but not phase, the analysis will need to be adjusted accordingly. This can be interpreted to mean that the model may still be valid if tidal flow is dominant for the estuary being analyzed, which is often the case.

The Great Bay example (see Geographic Feature Comparison section) can be used to demonstrate the use of tidal predictions such as those provided by coastal tide models. The tides at Atlantic City (Figure 3.32) are a reasonable approximation for Little Egg Inlet. This prediction can be used to adjust the water level, and tidal flat coverage, of the bay at daily time intervals.

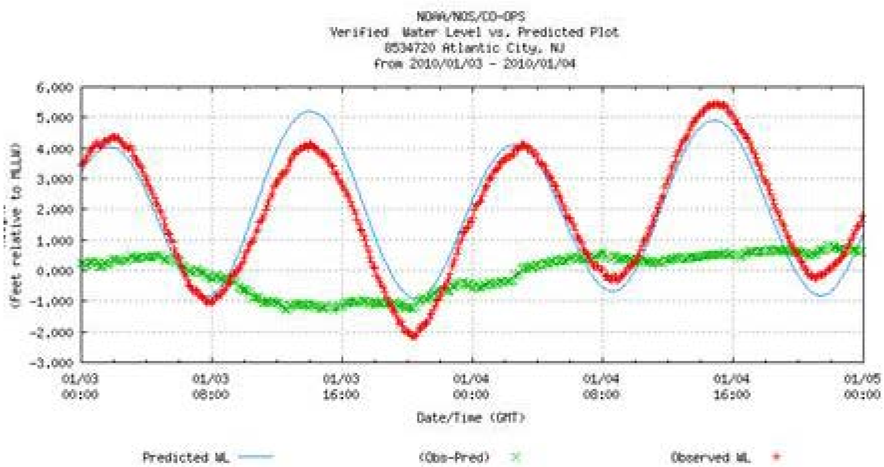

Figure 3.32. Predicted (blue) and observed (red) tides at Atlantic City. Green is inferred subtidal.

As suggested above, bathymetry data for an estuary or bay could be adjusted using this kind of data to show the *probable* location of the shoreline as it translates across the estuary bottom. This would alleviate the above-mentioned difficulty of interpreting satellite images for intertidal areas.

Statistical Methods

Long-term observations and model results are available for some areas. These are used to calculate the seasonal currents. These processed currents are used to evaluate the daily forecast features predicted by the forecast model as well as to keep a running tab on the evolving statistical behavior of the model for simulations that are continued for longer durations. The statistical and climatological currents are computed for analyst-selected boxes. A standard menu is available, consisting of surface, mid-depth, and bottom mean flow. The analyst can also specify special features like upwelling regions that may not be of long duration but which are critical for model evaluation.

Meteorological Analysis

The most general of the comparisons is between weather patterns and ocean currents.

References

Chen, Peter Pin-shan, The Entity-Relationship Model: Toward a Unified View of Data, ACM Transactions on Database Systems, Volume 1, 1976, Pages 9-36, DOI: 10.1.1.123.1085.

Marques, W. C., E. H. L. Fernandes, B. C. Moraes, O. O. Möller, and A. Malcherek (2010), Dynamics of the Patos Lagoon coastal plume and its contribution to the deposition pattern of the southern Brazilian inner shelf, J. Geophys. Res., 115, C10045, doi:10.1029/2010JC006190.

Section 4: Physical Process Model

The physical process model defines the program units and their processing logic. It also includes application and interface program units. Major program units that are critical to the model validation function are described.

Base Software Background

ArcGIS

ArcGIS for Desktop software enables you to discover patterns, relationships, and trends in your data that are not readily apparent in databases, spreadsheets, or statistical packages. Beyond displaying your data as points on a map, ArcGIS Desktop gives you the power to manage and integrate your data, perform advanced analysis, model and automate operational processes, and display your results on professional-quality maps. Three license levels are available: Basic, Standard, and Advanced (a.k.a. ArcView, ArcEditor, and ArcInfo, respectively).

ArcView consists of three applications:

- ArcMap – The application for map making and analysis.
- ArcCatalog – A tool for accessing and managing data.
- ArcToolbox – The geoprocessing environment for data management, conversion, and analysis.

Version 10.1 is the latest available version, though 10.0 is still widely used.

ARCOAS

ARCOAS version 4 was built as an add-in to the ArcView version 10 with tools requiring the spatial analyst extension (Figure 4.1). This add-in is easily installed and updated with just a few clicks of the mouse. Software development for MV&V module will leverage off of features previous built into ARCOAS and take lessons learned from ARCOAS development. Like ARCOAS, the MV&V module will also be an add-in to ArcView with the same feature for ease of installation and update.

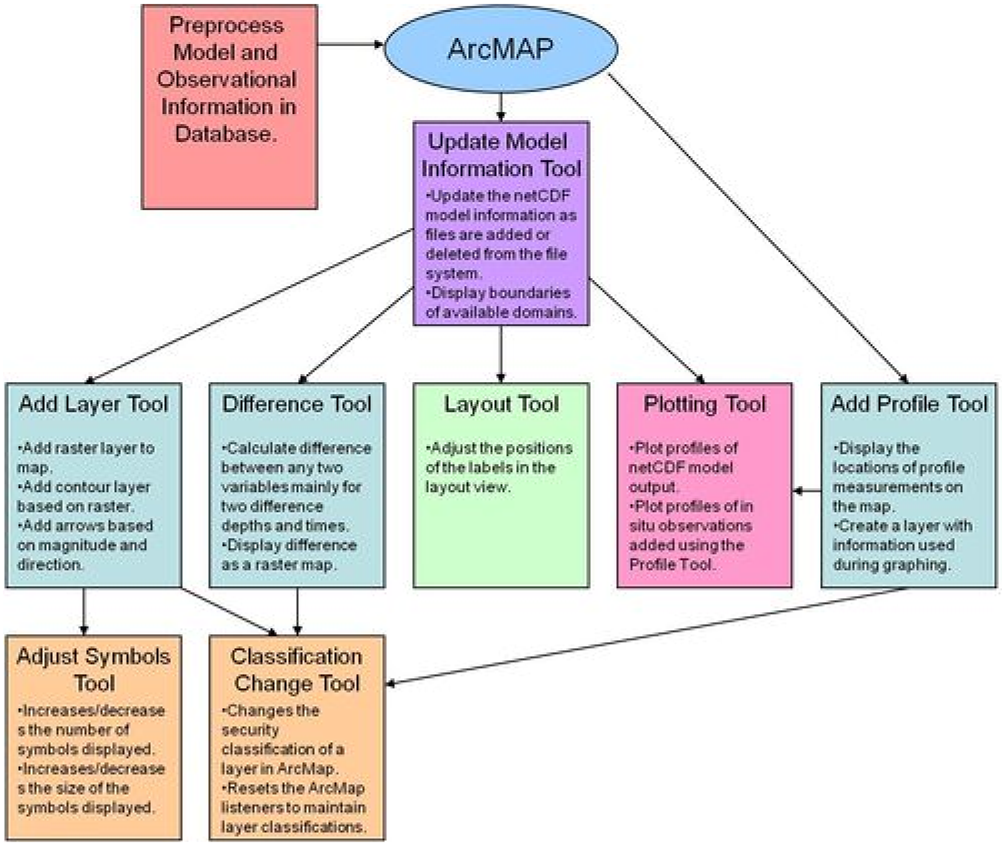

Figure 4.1. Map of groups of functions in ARCOAS.

The ARCOAS add-in extension consists of its own set of tools in a toolbar like any of the other extensions normally available in ArcMAP (Figure 4.2). Functions within the extension include tools for reading different file formats and operating on the data for analysis. Structure and functionality are described below. Along with the expected hardware and software requirements that typically exist on standard government computers, ARCOAS requires that a netCDF.dll file be installed into the Windows registry. This is a dependency for reading netCDF files, though the ArcMAP extensions and toolbox contain netCDF reader software as well. This version of ARCOAS cannot be installed in ArcMAP 9 as there is no add-in capability, a new feature of ArcGIS 10. Most programming is done in C-sharp. All these dependencies and requirements will apply as well in the MV&V module.

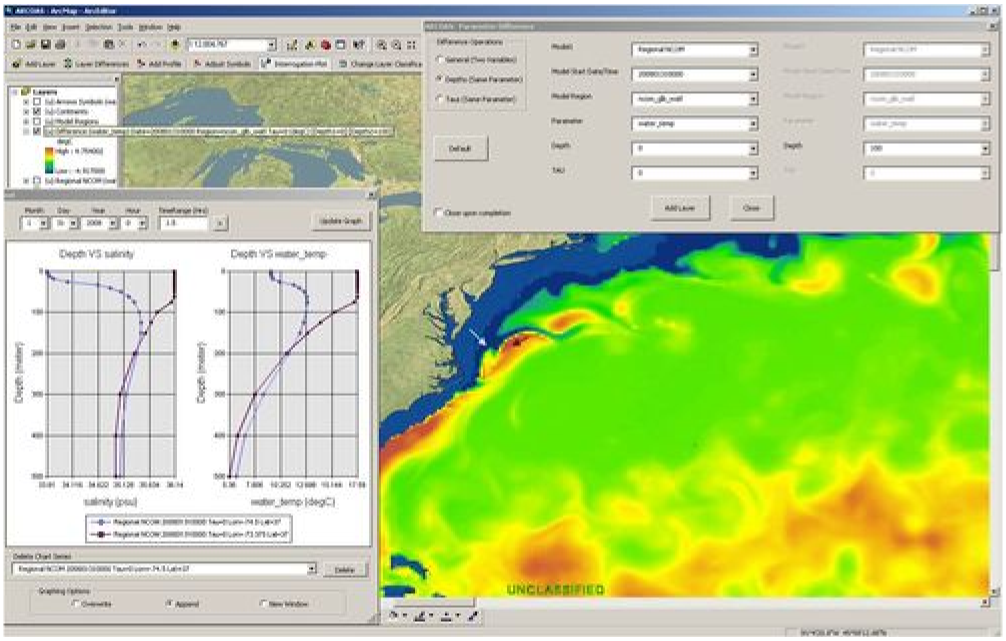

Figure 4.2. Primary functionality includes displaying an image of a raster of model output at a certain level, taking the difference between to raster layers, and manipulating arrows indicating currents direction and magnitude.

The inputs to ARCOAS (really into ArcMAP) must meet certain format guidelines and standards to be accepted. Fortunately, NAVOCEANO has already established and is using standards and conventions for the model output in netCDF as well as observational data prescribed by OcnQC and other software. The MV&V module will also benefit from these format guidelines and standards.

Model Validation (MVV) File

This is the fundamental file with the .mvv file name extension which registers all the information regarding a session using MV&V. An accompanying .mxd file is also created. Information in the MVV file forms the basis of an analysis report. Rather than containing all of the data types that are generated by the analysis, it contains information describing them and where they are located. It is not intended to be edited, but it can be as a final report. The extension was chosen because it is unknown or unassigned file extension.

The contents of this file can include:

- Model area and simulation model designations
- Date(s) opened, accessed, and saved
- Analyst digital signature
- Descriptions of all validation boxes

For each analysis box:

- Features identified

- Descriptions/links for all validation data sources
- Descriptions/links for all user-generated validation data (e.g., shorelines)
- Scores
- Comments on scores
- Recommendation

This format is shown in a sample file for Mississippi Bight (Appendix D).

Model Validation Unit Descriptions

The main class of the MV&V module (Appendix E) is ModelValidation (MV), and acts as a springboard for the instantiation of four other classes: (1) ValidationData; (2) GeophysicalFeatures; (3) ValidationAnalysis; and (4) Documentation. These subclasses are then subdivided into classes for each specific step or data type as seen in a UML class diagram. This section will describe each of these classes in sufficient detail to create the necessary code in an object-oriented programming language.

Each class is contained in a single file, with subclasses using inheritance to include the members of higher classes. The sections listed below describe the implementation of the algorithms discussed elsewhere in this report. The specific software modules will utilize existing libraries from ArcGIS and ARCOAS where possible. However, the preliminary software will use *ad-hoc* methods where necessary as required for the January 2012 deliverable.

The MV class contains members that identify the analysis and keep track of progress. Each instantiation of the MV class is associated with only one analysis. For example, a single forecast time (e.g, 21 Oct. 2011 00UT) from a regional model, which may have multiple analysis boxes selected by the analyst. The MV class thus creates a report file and an MVV file with a unique identifier contained in their names. These classes are presented to the user as tools. The most important function of the MV class is the flow module. The comparison of model and validation instantiations of geophysical features is made by the analyst rather than being automated. The *showFlow* method acts as a checklist that prompts for the next comparison, as seen in the Validation Process Model.

ModelValidation Class

MV&V Opening window (Figure 4.3) contains accesses high-level classes that complete logistical functions (Table 4.1).

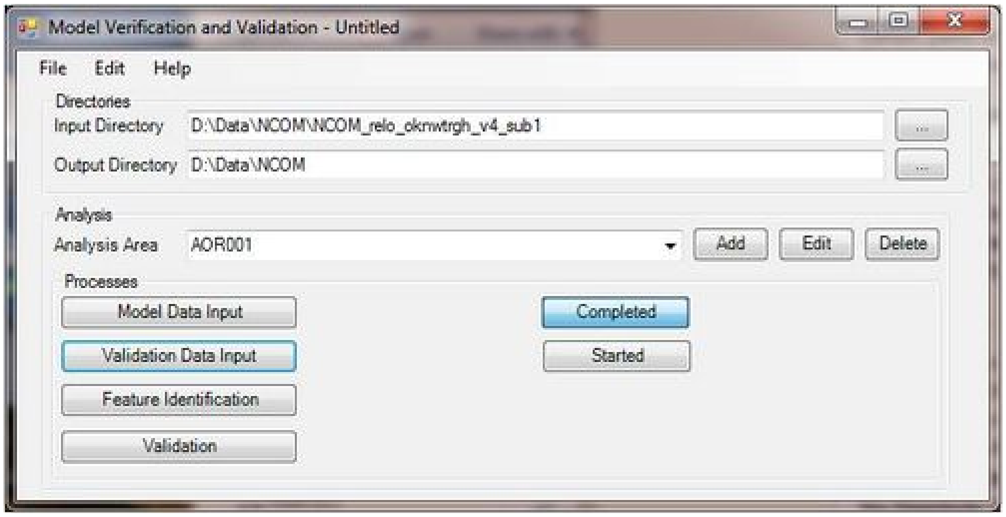

Figure 4.3. Startup window for the MVV system.

Table 4.1. ModelValidation Class Members inherited by all subclasses (accessible at the main menu)

Member Name	Description	Implementation
DateTime	Date and time of last edit of MVV file	Automatically entered in MVV file as Date type
Model	User-selected name of the model data set	ModelName entry box
Region	User-selected region box for analysis	Analysis Area drop-down with Add, Edit, and Delete buttons
Analyst	Name of the analyst based on login ID	Automatically entered in MVV file
WorkDirectory	User selected input and output paths	Browse button and drop down for each of the output and input directories
WorkFlow	Indicators on status of work flow	User controlled Boolean values to label toggle buttons indicating Started and Completed
Data	Parameter fields from the model output netCDF files	Model data of type IModel used in ArcMAP
ReadWriteReport()	A report is written to a file for delivery as a customer product. It is also to be read.	File->Create Report (Reading a report is not yet implemented)
ReadWriteMVVFile()	Current project files (.mvv/.mxd) is opened and saved	File->Save Project and File-Open Project(*.mvv into file browser)
newFlow()	New project is started	File->New Project

showFlow()	Shows the status of the work flow	Toggle buttons indicating Started and Completed
updateFlow()	Keeps track of the work flow	Toggle buttons indicating Started and Completed
getData()	User selects netCDF datesets to work with and also datasets can be deleted	Model Data Input • ->Add • ->Delete
showModel()	Data from a list of model netCDF datasets are displayed as rasters or cross sections	Model Data Input • ->Add Layer • ->Cross Section

Options in the File drop-down menu include starting a new project, opening an existing one or saving a project. Also, a report can be created which then becomes a permanent record of the analysis. "Help" allows a choice of tutorials, examples, or specialized help. Help buttons are also made available on individual dialog boxes. Within the Directories section are entries for input and output directories, which will contain the data that are used and created by this application. The output directory is the location for the analysis and validation files. The Processes section contains buttons that take you through four distinct steps, for each of which is labeled Complete as each step is accomplished. The user can move between steps or skip them as discussed in Section 3.

ValidationData Class

The validation data represent the general kinds of data that can be used: (1) "Water Depth", including shorelines; (2) "METOC", *in-situ* or sparse measurements of atmosphere/ocean variables; (3) "Models", other models; (4) "Other", user-input values that are of special interest; and (5) "Satellites", which is intended for space-based data only. Because of the wide range of file types, attributes, and availability of these data members, it is convenient to process each general type in a separate class. As each data source is collected using the appropriate class (Table 4.2), it is added to a list. The window for this class is also kept simple (Figure 4.4).

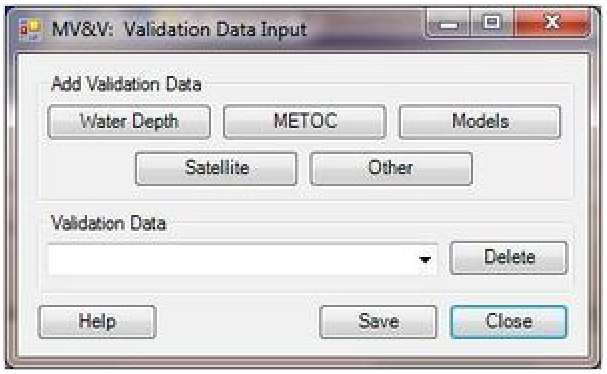

Figure 4.4. Example validation data window for the MVV system.

Any desired data can be collected by accessing its subclass using the labeled buttons. A list is generated as the data sources are collected and displayed in an editable list box, which allows the user to create a unique identifier for each data source. This is available throughout the analysis. The user can review the sources in this list and remove them using the Delete Data button if desired. The Save button will update the validation data list.

Table 4.2. ValidationData Class Members (accessible in Validation Data menu) (inherited by all subclasses)

Member Name	Description	Implementation
VariableName	Name of the variable to be validated in the model	Defined and passed on to table of contents and tables during data access and in map layer creation
Location	Geographic coordinates of data points and fields	Operates during data access and map layer interrogation
DateTime	Determined based on reference value	Operates during data access and map layer creation
shift()	A map raster layer independent of other layers is shifted along geographic coordinates of any datum	ArcMAP->Toolbox->Data Management->Projections and Transformations->Raster->Shift
import()	Data access from various file formats and services	Operates during data access and map layer creation
filter()	User-specified values for filtering out unwanted data	Operates during data access and map layer creation
interpolateTime()	Values are calculated based on user-selected points in time interpolated between available times	Not yet implemented
interpolateSpace()	Values are calculated based on user-selected points on the map interpolated from other values in that map layer	Operates during map layer interrogation
add()	Data layer addition to the map and table of contents	This is the data access and map layer creation
delete()	Removal of data from the map, table contents, and data tables	ArcMAP->Item in table of contents->Right click->Remove

The ValidationData subclasses (Appendix E) are: (1) Bathymetry (Table 4.3); (2) MetocObservations (Table 4.4); (3) ModelSimulation (Table 4.5); (4) SatelliteObservations (Table 4.6.); and (5) Other, which is intended for entering images from printed sources (e.g., publications and reports).

Table 4.3. Bathymetry Class Members (accessible via Water Depth Button)

Member Name	Description	Implementation
Projection	Geographic layout of this data	Property that is defined in the data set
Scale()	Scales the feature based on various user-controlled actions and inputs	ArcMAP->Georeferencing Toolbar->Georeferencing->Scale(Layer drop-down)
smooth()	Using a low pass option on the raster has the effect of an averaging filter	ArcMAP->Toolbox->Neighborhood->Filter using the LOW filter type
fill()	Fills sinks in a raster to remove small imperfections	ArcMAP->Toolbox->Hydrology->Fill
inputShoreline()	Imports vertices for a shoreline from a file	Feature Identification->Create(Shoreline from drop-down)->File Input(*.txt in file browser)->Save
inputDepth()	Imports data set creating a raster	Feature Identification->Create(Bathymetry from drop-down)

Table 4.4. MetocObservations Class (accessible via METOC Button)

Member Name	Description	Implementation
Type	Describes the type of METOC data to be used	Defined from input file metadata
average()	Calculates a nearest neighbour index based on the average distance from each feature to it nearest feature	ArcMAP->Toolbox->Spatial Statistics Tools->Analyzing Patterns->Average Nearest Neighbor(Input Feature Class, Distance Method, {Area})
weight()	Constructs a spatial weights matrix file to represent the spatial relationships among features in a dataset	ArcMAP->Toolbox->Spatial Statistics Tools->modelling Spatial Relationships->Generate Spatial Weights Matrix( )

Table 4.5. ModelSimulation Class (accessible in Class ModelValidation.showModel)

Member Name	Description	Action
ModelName	User-selected name of the model data set	ModelName entry box
scale()	Scales the feature based on various user-controlled actions and inputs	ArcMAP->Georeferencing Toolbar->Georeferencing->Scale(Layer dropdown)
readSimulation()	Data from a list of model netCDF datasets are displayed as rasters or cross sections	Model Data Input • ->Add • ->Delete

Table 4.6. SatelliteObservations Class (accessible via Satellite Button)

Member Name	Description	Action
Platform	Name of the orbiting satellite vehicle	Accompanies metadata of data loaded into ArcMAP
Sensor	Name of the sensor collecting data	Accompanies metadata of data loaded into ArcMAP
DataLevel	Height above or below mean sea level	Accompanies metadata of data loaded into ArcMAP
composite()	Creates a composite image from multiple sources	Not yet implemented
fill()	Fills in gaps in images due to clouds and sensor problems	Not yet implemented
transformData()	Transforms projection of layers with satellite data	ArcMAP->Toolbox->Data Management->Projections and Transformations->

GeophysicalFeatures Class

Geophysical features are identified using the Feature Identification form (Figure 4.5) if they are relevant to the performance of a model with regards to coastal currents. The first feature we should identify is the shoreline, followed by accurate bathymetry. Then, features that must be inferred from tracers (e.g., SST); such as tidal and shelf currents need to be identified along with fronts, eddies, and gyres in the coastal regions. Once these features have been identified they can be compared to the published literature and *in situ* observations, the latter brought in at the validation data input stage.

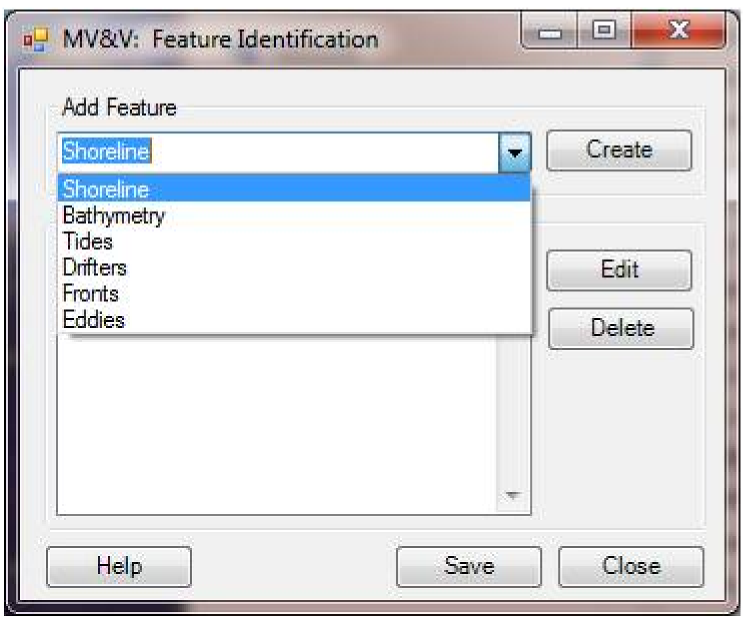

Figure 4.5. Example Feature Identification window.

There are a number of common variables and functions for all of the GeophysicalFeature subclasses (Table 4.7). Geophysical features are not to be confused with the ArcGIS terminology defining their use of the word feature as in feature class.

Table 4.7. GeophysicalFeatures Class Members (accessible in Feature Identification menu)(inherited by all subclasses)

Member Name	Description	Implementation
Location	Coordinates of the feature	Properties in the ILayer class for layers of any geophysical features
LifeSpan	Time units for which the feature occurs	Not yet implemented
FeatureName	Name for the feature (e.g., Eddy 1)	Properties in the ILayer class for layers of any geophysical features
VariableName	Name of variable (e.g, currents) is displayed in the feature	Properties in the ILayer class for layers of any geophysical features
Magnitude	Strength of signal (e.g., core temperature)	Properties in the ILayer class for layers of any geophysical features
FeatureType	Kind of feature from subclasses	Not yet implemented
locate()	Identifies the coordinates	Read-out of locations registered at bottom of map based on mouse location
create()	Generates a synthetic instantiation	A layer of class ILayer in the map is created
compare()	Compares multiple instantiations	Not yet implemented
add()	Adds the feature to the analysis block(s)	Inherent action upon creation of the feature

The GeoMorphology class (Table 4.8) is used to instantiate shorelines, water depths, and submarine features that impact currents.

Table 4.8. GeoMorphology Class Attribute and Function Members

Member Name	Description	Implementation
Type	Name of the feature type (e.g., shoreline)	Derived from name of selected class as selected from drop-down
WaterDepth	Water depth array associate with the feature	Not yet implemented
makeShoreline()	Creates a shoreline	Drop-down in Feature Identification menu->Shoreline menu
makeBathymetry	Creates a bathymetry feature	Not yet implemented

Tidal features (Table 4.9) are special in that they are typically constructed by harmonic analysis or reconstruction from harmonic constants. These functions are entry members to access lower level helper functions like plotting ellipses and harmonic analysis of mixed time series.

Table 4.9. TidalCurrents Class Attribute and Function Members

Member Name	Description	Implementation
amplitude	tidal elevation and current magnitude	Not yet implemented
phase	tidal elevation and current phase relative to Greenwich	Not yet implemented
ellipse	array of current ellipse parameters (max axis, ellipticity, angle, phase)	Not yet implemented
removeMean()	Removes the mean from a time series	Not yet implemented
adjustWaterDepth()	Calibrates mean depth	Not yet implemented
findSubTidal()	Finds long-period residual current	Not yet implemented
makeTide()	Accesses harmonic analysis and/or reconstruct a tidal signal from harmonic parameters	Not yet implemented
attachEddy()	Locates a tidal feature to an identified eddy	Not yet implemented
addMean()	Adds the mean water level	Not yet implemented

The current systems that occur along coastlines and the shelf break are complex and require more flexibility in instantiating. The class thus consists of fewer but overloaded functions (Table 4.10).

Table 4.10. ShelfCurrent Class Attribute and Function Members

Member Name	Description	Implementation
Type	Name of the flow (e.g., Gulf Stream Front)	Not yet implemented
depth	Depths of the current system, either total depth or depth at which it is located	Not yet implemented
makeCurrent()	Creates an instantiation of an idealized flow	Not yet implemented
attachToPlume()	Combines river plume and current features	Not yet implemented

Oceanographic fronts are identified from remote sensing images and thus do not give direct information on currents. Instead, they are used to create synthetic instantiations of flow regimes that are inferred from instantiations using temperature and altimetry fields (Table 4.11).

Table 4.11. Front Class Attribute and Function Members

Member Name	Description	Implementation
length	Physical length of the feature	Not yet implemented
depth	Estimated depths of front	Not yet implemented
makeFront()	Creates a synthetic front feature	Fronts can be read from a table or drawn using the Fronts menu.
addEddy()	Attaches an eddy to the front (e.g., Gulf Stream eddies	Not yet implemented

The eddy class (Table 4.12) is closely related to the front class because of their common co-occurrence.

Table 4.12. Eddy Class Attribute and Function Members

Member Name	Description	Implementation
radius	Diameter of feature	Parameter that contributes to the dimensions of the eddy
makeEddy()	Creates a synthetic eddy from minimal data	Tool that interacts with the map and the menu to draw ellipse denoted eddy feature
setGradient()	Defines the gradient of an eddy from central temperature/height and ambient field	Not yet implemented
islandWake()	Creates a set of synthetic eddies from remote sensing data	Not yet implemented

Jets and filaments (Table 4.13) are similar to fronts and their members must be loosely defined and overloaed for useful application.

Table 4.13. Jet Class Attribute and Function Members

Member Name	Description	Implementation
length	Physical length of feature	Not yet implemented
direction	orientation	Not yet implemented
makeJet()	Function to create a synthetic coastal jet	Not yet implemented

The last geophysical feature is a river plume. This class (Table 4.14) is very flexible and user dependent.

Table 4.14. Plume Class Attribute and Function Members

Member Name	Description	Implementation
Area	The estimated surface area (e.g., from SST)	Not yet implemented
makePlume()	Creates a synthetic river plume	Not yet implemented

The comparisons can be accomplished in the next step, Analysis and Validation.

Analysis Class (ValidationAnalysis)

The operation of the Analysis class is primarily described through Applications (Section 5). The physical model description is limited to the operation of the members of this class and its subclasses (Table 4.15). The parent class (Analysis) has a limited number of members because the subclasses have very different functions.

Table 4.15. Analysis Class Attributes and Functions (inherited by subclasses)

Member Name	Description	Implementation
Comment	Comments by the analysis with no particular format	Used to store and save the comments in the mvv file for each analysis area
variableName	Name of variable (e.g., COARDS standard) being used for current analysis	Not yet implemented
addComment()	Adds a comment to all related documents based on the current analysis	Text boxes are made available to input comments.

The AnalysisBlock class (Table 4.16) keeps track of all of the components of the current analysis.

Table 4.16. AnalysisBlock Class Attributes and Functions

Member Name	Description	Implementation
size	Total surface area of block	Handled by the class IEnvelope
location	Coordinates of block corners	Handled by the class IEnvelope
setBlock()	Creates a new block	Add button on the main menu with a combo box to add the new name of the block a.k.a. AreaOfInterest. Also, a tab with the named AreaOfInterest is added to the comment menu.
addToBlock()	Adds a component to a block	Not yet implemented
deleteBlock()	Removes a block and reassign any attached components (e.g., features)	Delete button in the main menu removes the selected AreaOfInterest.
mergeBlock()	Joins blocks into a composite	Not yet implemented
deleteFromBlock()	Removes a component from a block	Not yet implemented

Statistics are primarily processed by ArcMap and other components of the software system. This class (Table 4.17) is thus a wrapper for existing software but it can also be used for new statistical and analytical tools that become available.

Table 4.17. Statistics Class Attributes and Functions

Member Name	Description	Implementation
Type	Name of feature and/or variable being analyzed	Not yet implemented
rmsError()	Calculates error of the feature and/or variable/block	Not yet implemented
timeSeries()	Analyzes time dependent properties	Not yet implemented

The Scoring class (Table 4.18) tracks the analysis scores for all blocks/features/variables.

Table 4.18. Scoring Class Attributes and Functions

Member Name	Description	Implementation
score	Array of different scores within the analysis	Not yet implemented
description	General comment for the interpretation of the quantitative score	Not yet implemented
sumScore()	Adds scores in different ways	Not yet implemented
newScore()	Creates a new scoring array (e.g., new feature/block)	Not yet implemented

Documentation Class

Help system will accessible from all tools accessing the appropriate content. The documentation (Table 4.19) consists of these pages and examples from the SDP. Other guidance is included as indicated by user questions and feedback.

Table 4.19. Documentation Class Attributes and Functions

Member Name	Description	Implementation
helpRequest	String to be parsed into a help request from a box	Not yet implemented
helpType	Result parsed from the helpRequest	Not yet implemented
showTutorial()	Shows a tutorial	Not yet implemented
showHelp()	Opens window(s) for different help request types	Not yet implemented

Section 5: Applications

Two demonstration areas were examined during the design of the validation algorithm. There are also three additional areas that were used to demonstrate the software product. The first demonstration is a simulation of Mississippi Bight in March, 2005. This example is used because it has typical validation data. The second example is the Bohai Sea, within the Yellow-East China-Bohai Sea littoral. The examples will follow the general outline of this report, and demonstrate application of the Logical Process Model.

Mississippi Bight

This simulation has been described by Keen and Holland (2010). We will briefly summarize the simulation. The hindcast is for 7-11 March, 2005. The simulations used two nested models. The outer nest is examined here; it had a grid size of ~900 m and was in-turn nested to a global model (cell ~13 km). The wind forcing was from NOGAPS. Initial and boundary conditions came from the global model. Tides were introduced at the open boundary of this nest. The minimum water depth was 2 m. Several rivers were represented using available data. The model was not calibrated for this hindcast, but is treated as a forecast in an new area.

Validation Data

We have shoreline data from Google Earth but no additional bathymetry because the best available was used to construct the model grids. We have historical measurements of currents in several locations for March 1997, and imagery from Oceansat for 2005 and 2008. After searching two data bases (NRL and LSU), only two images that were comparable were identified, but these must be classified as *historical* because they are not concurrent. There are no other *Concurrent Observations* either, which includes *Surface Observations*. We have tidal heights from several IHO stations around the area.

There have been several modeling studies for Mississippi Bight. The most comprehensive was by Keen (2002) for a cold front. We have numerical model results from 1997 using POM. There are partial model results for May 2001. This collection of data can be used to instantiate features within the Mississippi Bight that are used for comparison to the model features. Storm currents and mass transport during hurricanes have also been simulated (Bentley et al., 2002; Keen et al., 2004; 2006).

Feature Identification

We can identify geophysical features that are likely to be important in this region. The satellite images show the surface chlorophyll *a* distribution in March for two years (Figure 5.1). These images show several common ocean features. The bright areas represent [Chl] > 5 mg/m^3, which are due to phytoplankton. We see filaments near the Mississippi R. delta that extend south in 2005 and north in 2008. We also note a persistent red area at the Chandeleur Islands. There are also weaker areas showing curvature offshore in both images. These resemble eddy structures. River plumes are suggested for 2005 by the seaward tongue south of Mobile Bay.

Figure 5.1. Chlorophyll images from the Mississippi River delta. (A) . March 2005. (B) March 2008.

A

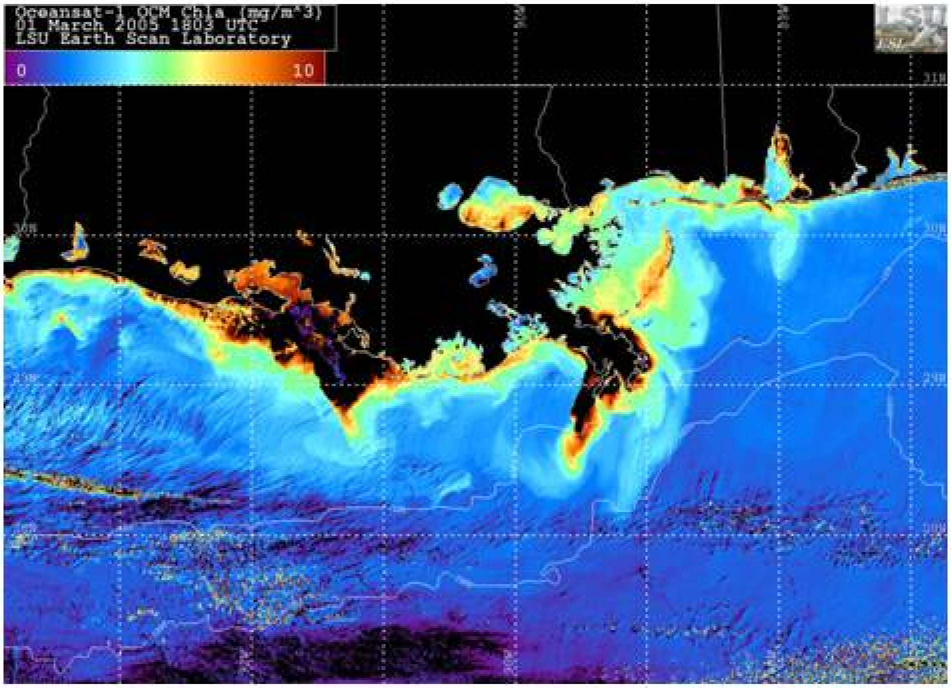

B

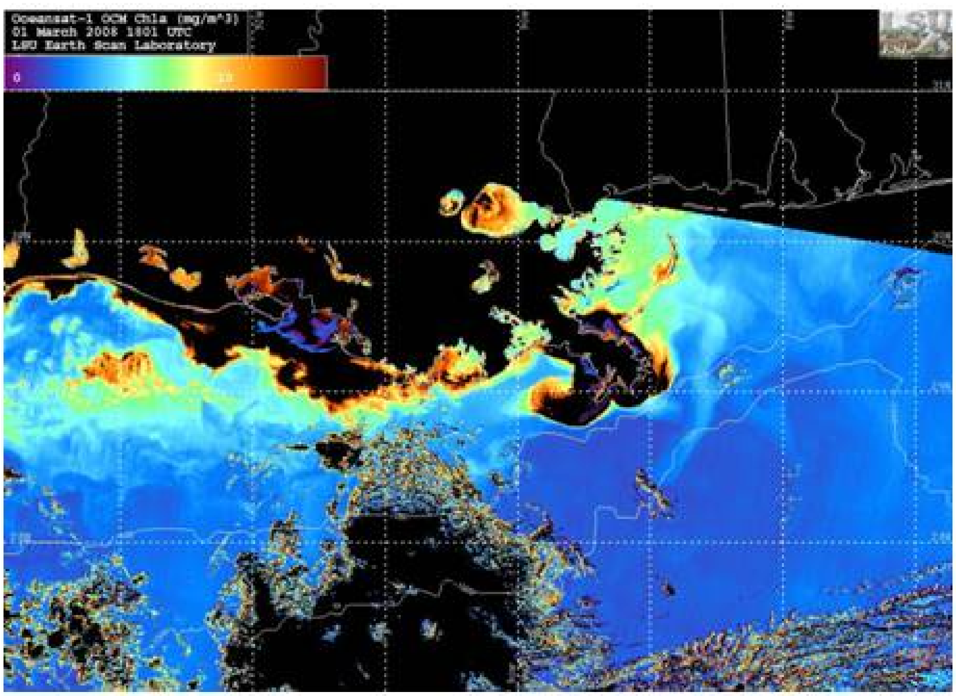

Tidal flow is suggested at the passes to Mississippi Sound. We want to look for these features in the model, which does not include [Chl] as a tracer.

- shoreline digitized from Google Earth
- tides
- filaments, eddies, and water patches
- estuary
- hurricane flow
- cold front flow

These are the features we will evaluate using the features instantiated from the available data and the simulation results.

Model Validation

This section applies the methods described in Section 3.

SELECTING ANALYSIS SUBREGIONS

The Mississippi Bight can be subdivided into three blocks (Figure 5.2), (A) the open sea, (B) Mississippi Sound, and (C) the Mississippi R. delta using their land and seaward boundaries. The open sea is impacted by the open boundary conditions more. Mississippi Sound is sensitive to land boundaries and inflow from rivers, and the delta is a complex area where the dynamics of the shallow sounds is affected by deep water directly. This will assure consistent validation of the model by subjective interpretation as well as quantitative skill assessment.

Figure 5.2. Google Earth image of Mississippi Bight, showing possible validation boxes.

Creating Features for Comparison

We digitize the relevant shoreline from a suitable image (Figure 5.3); we are using the Google Earth image (Figure 5.2). The islands need to be individually saved to guarantee their correct representation when plotted in Matlab™. We will only digitize part of the region to validate the flow in the western bays.

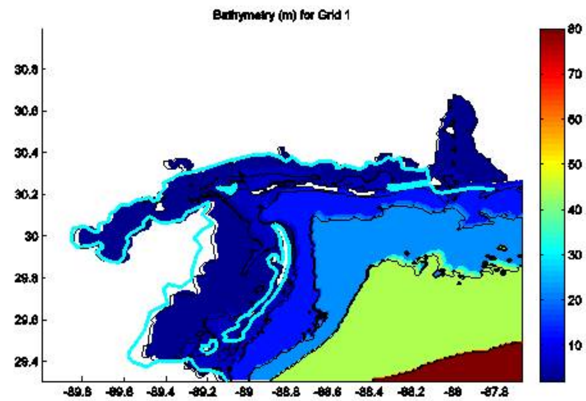

Figure 5.3. Google Earth shoreline superimposed on the model grid.

Tidal elevations can be treated as concurrent because they do not vary. Examples include the predicted water levels from the IHO stations. The time series represent a *tidal feature*. This feature is compared to the model at the appropriate location within the domain. This sample will use a qualitative comparison of the amplitude and phase of tidal elevations.

There are no concurrent data to instantiate the *filament*, *patch*, and *eddy* features that are evident in the satellite images. These are treated as typical and we can look for evidence of their occurrence in the hindcast model. We thus do not expect to find temporal overlap, but it is relevant that they occur in similar environments, such as patches in shallow water as suggested in the images. We also expect to see tidal plumes at the passes between islands, and eddies should be evident offshore.

There are two meteorological flow events that can be used to instantiate compound flows. By *compound* we refer to flows that are evidenced by different spatial and temporal signatures, which are linked physically to the atmospheric forcing. The forecast (hindcast) model instantiation of these flows is dependent on the entire forecast system rather than just the model. This is explained below.

Applying the Validation Guidelines

This section demonstrates how the validation guidelines are used to verify and validate a model simulation using the features that have been created from the model and validation data. The digitized **Shoreline Feature** is outlined in cyan in Figure 5.3. The effect of older shoreline data is evident in the Chandeleur Islands as well as the western border of Breton Sound. These are shallow and mobile areas that are morphologically sensitive to frequent tropical storms. The model grid is very good in Mississippi Sound, however.

The **Estuary Feature** is more complex because there are beaches along all of the islands, which are poorly resolved with the minimum model depth of 2 m. We can use this information to evaluate the model output for each block. The model output is at -0.5, -1.5, -2.5,...meters. The depths in Breton Sound are < 2 m, so Block C fails for z = -2.5 m. The surface flow may be okay but the satellite image suggests that large expanses are probably intertidal. However, we have defined our analysis block to further south, and the channels between the Gulf and the sound are accurate. These features are often maintained by tidal action.

Tidal features have been created at several locations in the domain (Figure 5.4A), with different performance in the analysis areas. The model has good tidal elevation phase but under-predicts the amplitude of the astronomical tides by as much as 50% near Mobile Bay. It is much better for Cat Island (area C), but poor for Breton Sound (remember the bad water depths in area B). We cannot apply the tides to block A because it contains no coastlines. A tide gauge was installed at Waveland (in St. Louis Bay) in fall of 2005 (Figure 5.4B), and this represents a combined tide/cold front feature. The model we are evaluating was run for all of 2005 and, therefore, we can make a comparison with this data as below. The model and validation features are concurrent but not for the actual time interval being evaluated. We see good prediction of the subtidal signal in this coastal bay.

Figure 5.4. Water level observations and model results. (A) Comparison of IHO and model tides in Mississippi Bight. (B) Model (blue) and measured (red) water level at Waveland in December, 2005.

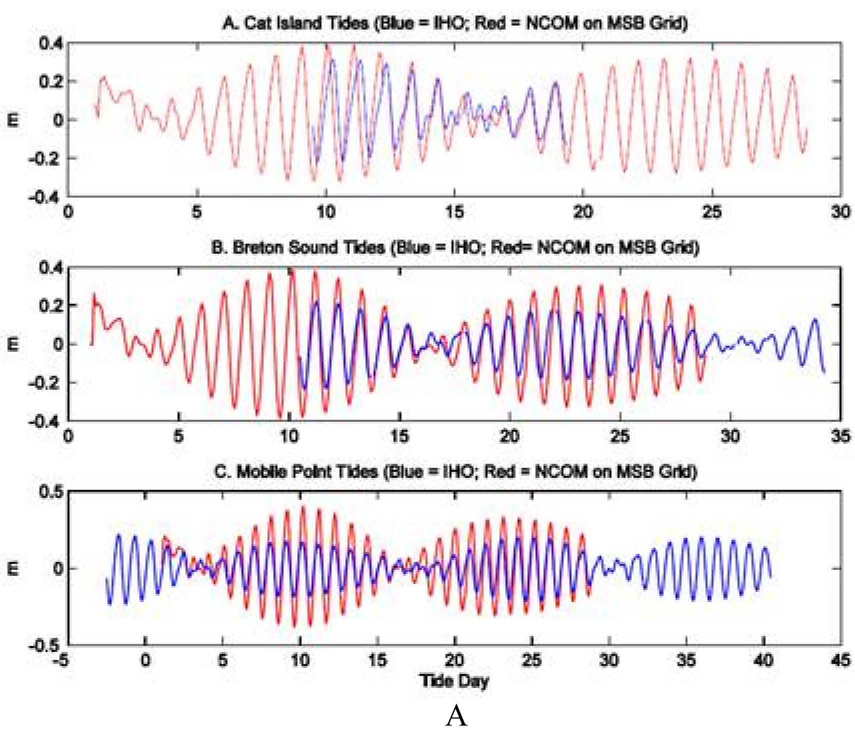

A

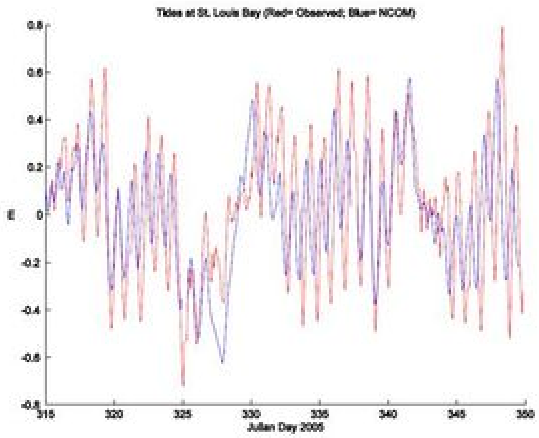

B

The **Filaments/Patches Feature** comparison is looking for evidence of filaments, eddies, or plumes associated with either the tides or wind transport. In fact, this is exactly what we see in all regions of the model SST (Figure 5.5). The model reproduces filaments in the open Gulf as well as exchange of water masses between Mississippi Sound and the Gulf. It is not as obvious for Breton Sound. However, the model clearly indicates the presence of patches of surface waters that are not mixed, which is evident in the [Chl] imagery. This comparison is with historical daily data from the correct time of year but not from the correct day. This indicates that the model flow is generally correct at synoptic time scales (~ 1 week).

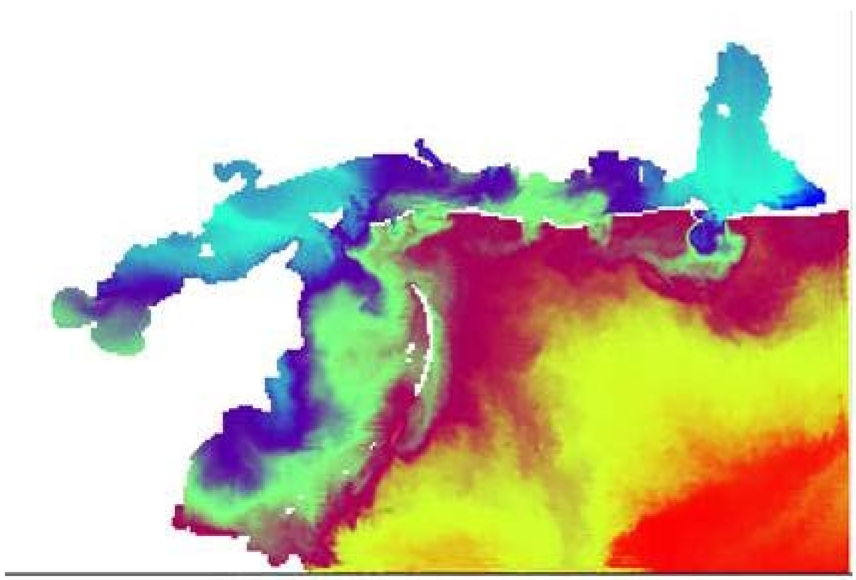

Figure 5.5. SST predicted by the model for March 2005.

The only other available historical data are currents and water levels in Cat Island Channel from March 1997. These data coincide with a cold front similar to that in March 2005, and thus should be comparable as Cold Front Flows (Meteorological) Features by examining characteristic currents during fronts. The measured water level south of Cat Island decreased by 5-10 cm after the cold front in 1997. The forecast model predicted a similar decrease in 2005 that also coincided with the shift to northerly postfrontal winds. This is only applicable to block B, however. There are no data for the other analysis blocks. The final historical data are currents measured in Cat Island Channel. These observations from March 1997 show a tidal asymmetry at this location, with mean outflow from Mississippi Sound. The speed prior to the cold front was ~30 cm/s. During the postfrontal period, the surface flow increased to > 60 cm/s. The surface currents in the channel were very similar from the forecast model in 2005.

It is possible to compare the currents from the hindcast model for Hurricane Katrina in August, 2005 to these historical examples because the model simulations were completed for the entire year, but caution must be used in interpreting the result because the storm track must be considered when comparing **Hurricane Flow Features**. Hurricane Camille (1969) approached the region from the SSE ~60 km to the east of Katrina's landfall. The ADCIRC model predicted landward flow (~ 2 m/s) into Mississippi Sound prior to landfall and reversed flow afterward, but with a slightly larger eastward component. This pattern is similar to the hindcast model for Katrina, whose magnitudes were less than 1.2 m/s during flood and 0.8 m/s during ebb. The hindcast flow also has a stronger alongshore component; however, the flow field is not discussed in detail in the earlier study. The peak currents predicted by POM for a 1947 hurricane can be used to instantiate a flow feature for a hurricane that approached the delta from the east. The peak currents were 1-1.5 m/s throughout the region. This is also higher than for the Katrina simulation. Overall, the hurricane currents are consistent with the previous studies, which earns a pass for the storm flow.

A comparison can be made between **Cold Front Flow Features** computed by the POM simulations for March 1997 (Figure 5.6A) and the hindcast model (Figure 5.6B). These are compound events with both tides and wind forcing. The currents from 1997 were southward at Ship Island because of the ebb tide, despite a southerly wind. This is also the general case for the simulation in 2005. Both models predict currents near 70 cm/s.

Figure 5.6. Surface currents during cold fronts from POM and the model. (A) Surface currents from POM for March 1997. (B) Prefrontal surface currents from the model for March 2005. (C) Postfrontal surface currents from the model for March 2005.

A

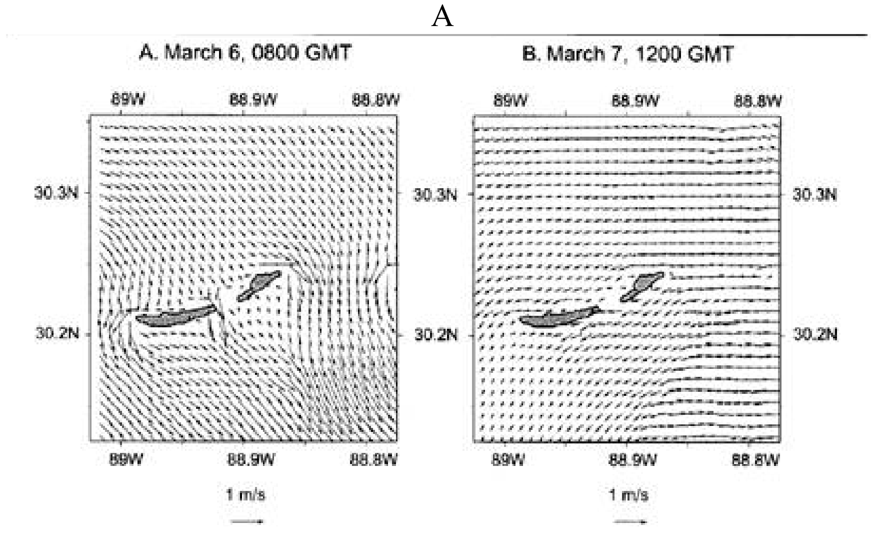

B

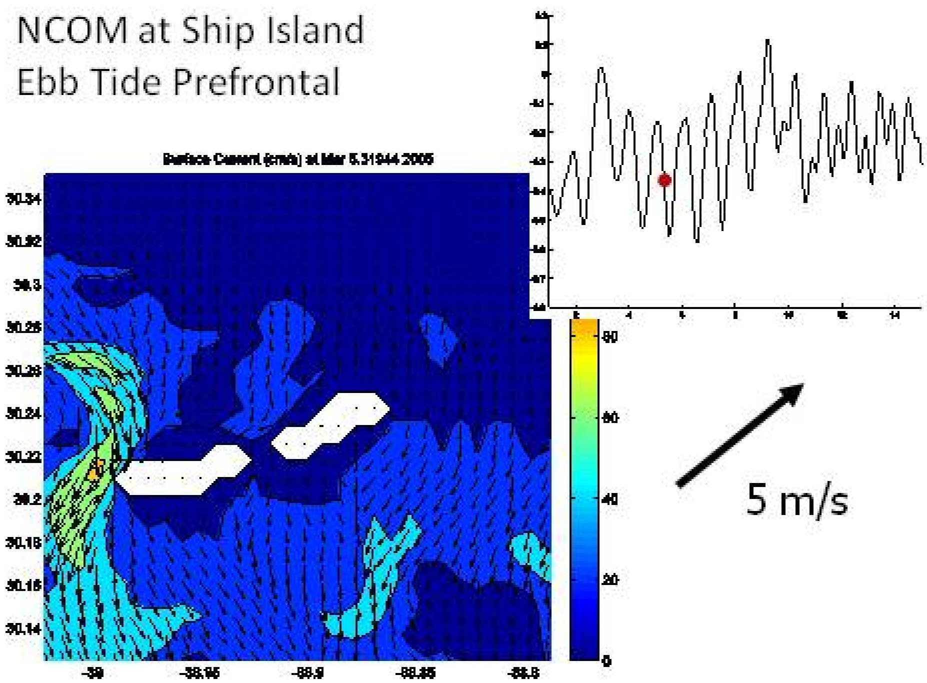
NCOM at Ship Island
Ebb Tide Prefrontal
Surface Current (cm/s) at Mar 5.31944 2005
5 m/s

C

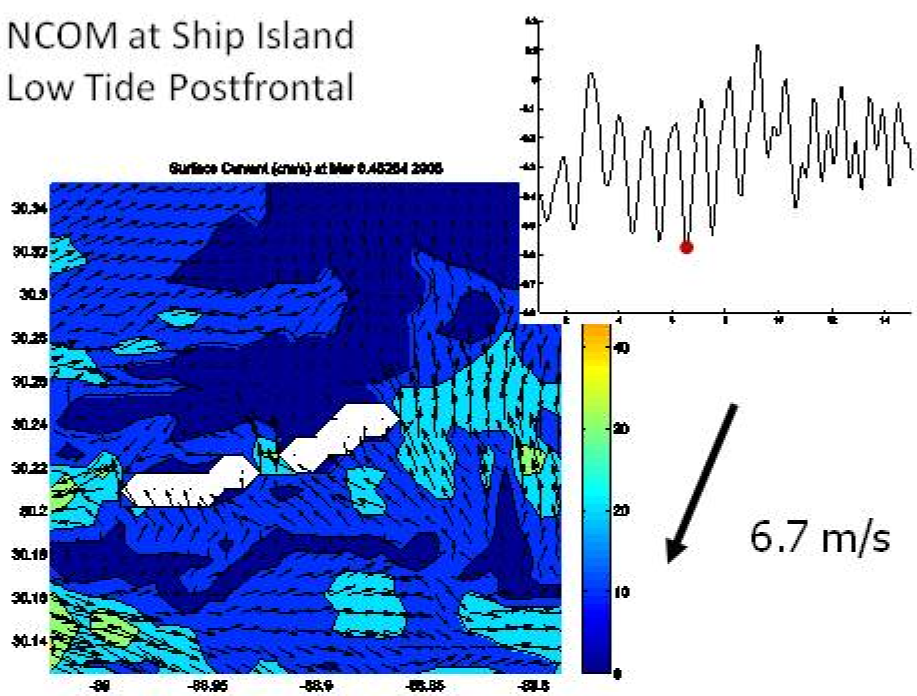
NCOM at Ship Island
Low Tide Postfrontal
Surface Current (cm/s) at Mar 6.45264 2005
6.7 m/s

The postfrontal comparison (Figure 5.6C) is not so clear. POM predicts westward flow at low tide whereas the 2005 hindcast model predicts eastward flow with northward currents to the east of Ship Island. Both cold fronts had similar wind speeds (~7 m/s) from the NE. This postfrontal flow is not consistent with the wind direction or the 1997 study. We expect some kind of westward or SW flow during the postfrontal period. It could be caused by the use of NOGAPS winds instead of buoy winds (verified by an anemometer at Cat Island) as in the earlier simulation. This comparison introduces the usefulness of meteorological data for verifying model forecasts.

Scoring the 2005 Model Simulation

Applying the analysis blocks that we previously identified, we would rate them as follows for the **Shoreline Feature**: A = P; B = P; and C = F. We give a pass to block A because the seaward margin of the Chandeleur Islands is fairly well resolved. We can tabulate the score (Table 5.1). Overall, the bathymetry for all three blocks (as defined) could be a pass, with the *caveat* that the connection between the east end of Mississippi Sound and Mobile Bay appears to be very restricted rather than open as in the older model bathymetry. Where validation data are not available, *NA* is recorded in the table.

We pass the model with respect to reproducing filaments and patches of unmixed water for all three analysis blocks because it showed a similar level of variability and structure as the satellite images. The comparison with other models suggests that the 2005 simulations are inconsistent. The model compares moderately well to concurrent data in area A only. The forecast model does not do as well as the earlier model for the postfrontal flow during a cold front, and could fail. This error could be caused by the use of the NOGAPS winds, which were not used in the other simulations. The result is a weak pass, for which we assign a score of 1.

Table 5.1. Model Verification & Validation Score

Feature Comparison	Area A	Area B	Area C
Shoreline	1.0	1.0	0.5
Tides	NA	1.0	0.5
Filaments/eddies	1.0	1.0	1.0
Estuary	1.0	1.0	0.5
Hurricane Flow	NA	1.0	1.0
Cold Front Flow	NA	1.0	1.0
Cumulative Score	1.0	1.0	0.125

References

Bentley, Samuel J., Timothy R. Keen, Cheryl Ann Blain, W. Chad Vaughan, The origin and preservation of a major hurricane event bed in the northern Gulf of Mexico: Hurricane Camille, 1969, *Marine Geology*, Volume 186, Issues 3-4, 10 July 2002, Pages 423-446, ISSN 0025-3227, DOI: 10.1016/S0025-3227(02)00297-9.

Keen, T. R. (2002), Waves and currents during a winter cold front in the Mississippi Bight, Gulf of Mexico: Implications for barrier island erosion, *J. Coastal Research*, 18 (4), 622-636.

Keen, T. R., Samuel J. Bentley, W. Chad Vaughan, Cheryl Ann Blain, The generation and preservation of multiple hurricane beds in the northern Gulf of Mexico, *Marine Geology*, Volume 210, Issues 1-4, Storms and their significance in coastal morpho-sedimentary dynamics, 15 September 2004, Pages 79-105, ISSN 0025-3227, DOI: 10.1016/j.margeo.2004.05.022.

Keen, T. R., Furukawa, Y., Bentley, S. J., Slingerland, R. L., Teague, W. J., Dykes, J. D., Rowley, C. D., Geological and oceanographic perspectives on event bed formation during Hurricane Katrina, *Geophysical Research Letters*, Volume 33, Issue 23, 14 December 2006, Article Number L23614, ISSN 0094-8276, DOI: 10.1029/2006GL027981.

Keen, T. R. and Holland, K. T. (2010). The coastal dynamics of heterogeneous sedimentary environments: Numerical modeling of hydrodynamics and mass transport in estuaries. NRL Memorandum Report NRL/MR/7320-10-9262. Naval Research Laboratory, Stennis Space Center, Mississippi, 133 pp.

Bohai Sea

This example comes from operational, unclassified, model simulations of the Yellow Sea area within the larger model domain (wpac_2_u) which is run on the unclassified HPC machines in real-time. The initial time of the model run was 2011 September 6 00 UST. The wind forcing was from NOGAPS. Initial and boundary conditions for this domain are provided by the global model. Grid spacing of the computational grid was 3 km and was reprojected to a latitude/longitude (spherical) grid as a product to the fleet. In this example a box was selected covering the western side of the Bohai Sea in the northwestern Yellow Sea (Figure 5.7). The Huanghe River flows into the Laizhou Bay via the Huanghe Delta forming a peninsula.

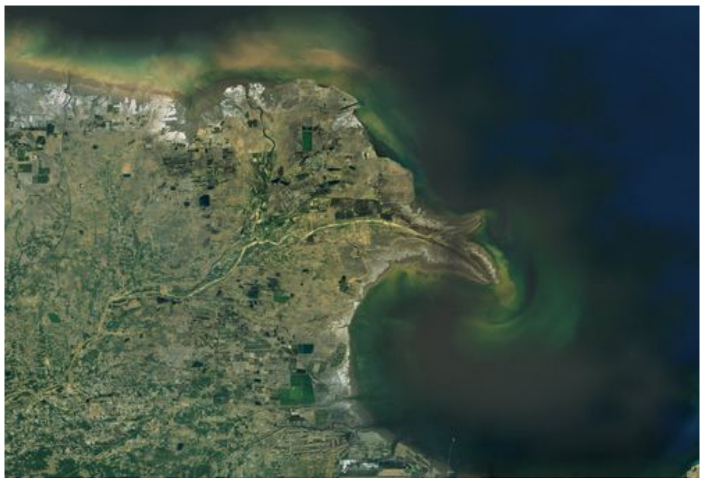

Figure 5.7. Satellite image of the Bohai Sea.

Feature Identification

As before validation data is required first. According to this imagery available on ArcMAP the shoreline is easily discernible. We assume that the best bathymetry is already the basis for the model depths, so no new information is available there. In situ observations may be available in the area historically and in real-time, but not likely to be a dense network all the time. In fact, there were no profile observations from the GODAE server throughout the first two weeks of September. Due to the high interest in the unique dynamics of the Yellow Sea and the surrounding embayments, much scientific work concerning the geophysics of this region was published.

In many papers MODIS imagery serves as a basis for analysis and yields valuable information. Bi et al. (2011) showed that field survey data and MODIS-retrieved suspended-sediment concentration (SSC) show that the sediment transport in the southern Bohai Strait has a significant seasonal variability due to alternating summer and winter monsoons. Bi et al. (2011) include observations from other papers (Figure 5.8), which show the currents that are considered in the study showing a predominate flow regardless of season. \

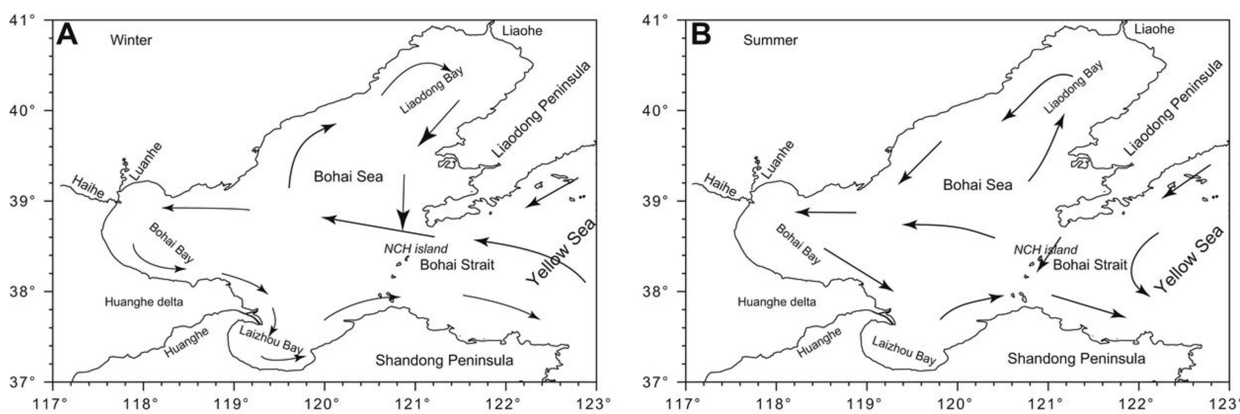

Figure 5.8. General pattern of the circulation in the Bohai Sea and the Bohai Strait in winter (Fang et al., 2000); summer circulation is discussed by Guan (1994). NCH indicates northern Chenghuang Island.

Turbidity studies (Bi et al. (2011) (Figure 5.9) are consistent with of the overall flow pattern derived from previous work.

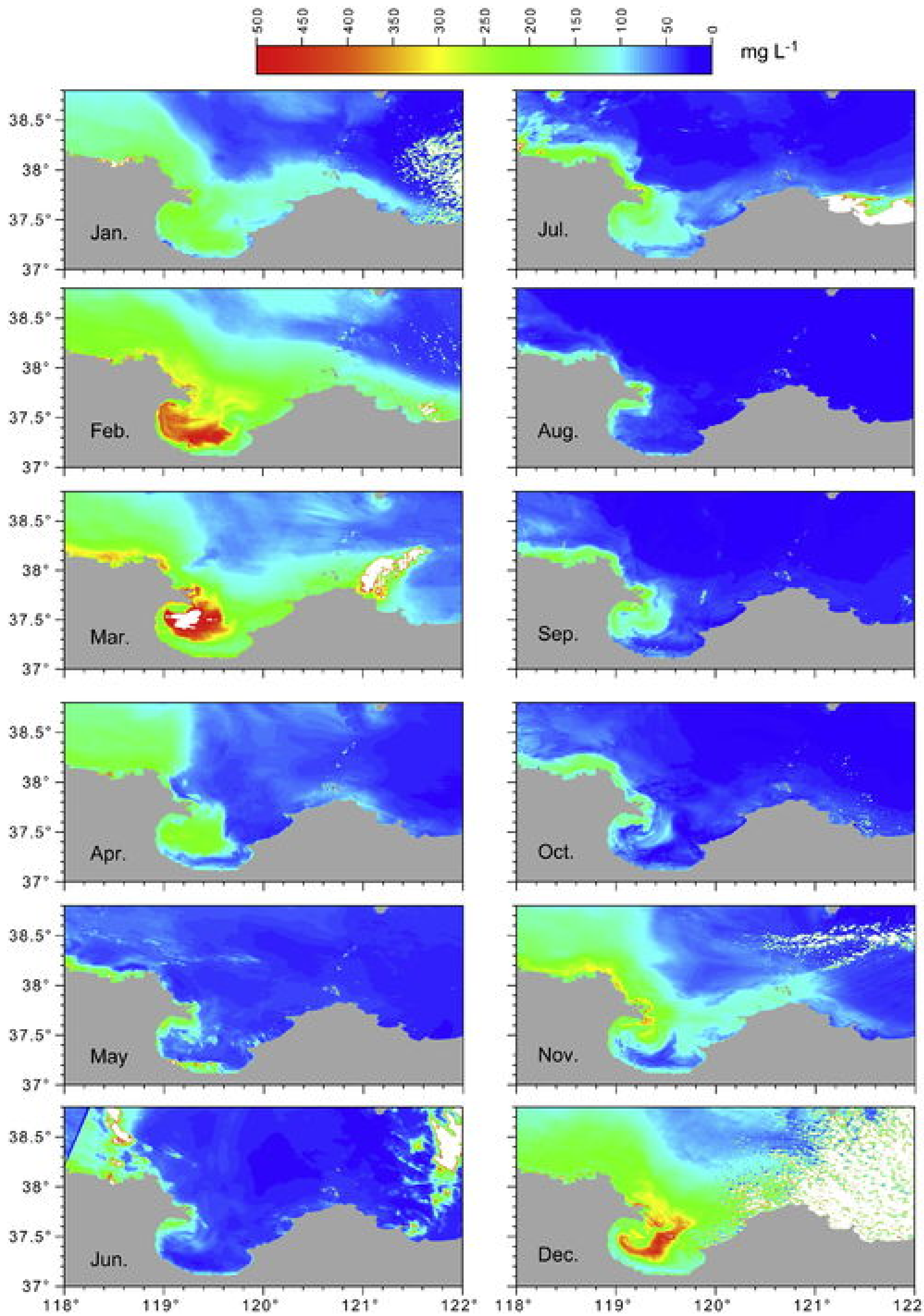

Figure 5.9. Seasonal and spatial variations of monthly averaged SSC based on the model of SSC retrieval. The white areas indicate clouds.

Geographic Feature Comparison

First the shoreline can be drawn using the ArcMAP drawing tool (Figure 5.10A). When the model field is overlain on the image (Figure 5.10B), it is clear that the Huanghe delta is entirely missing from the model grid. Stations selected on this missing land feature (Figure 5.10C) demonstrate that the model is calculating currents for water depths up to 8 m (Figure 5.10D) where there is supposed to be land. This will impact a much larger area of water than just the peninsula itself.

Figure 5.10. Using the shoreline feature to evaluate coastal currents. (A) Shoreline feature created in MV&V. (B) Model field overlain on the satellite image, showing mismatch of the shoreline on the peninsula. (C) Location of two stations used to evaluate the model water depth. (D) Profiles of salinity (blue) and temperature (red) at the stations. The deeper is more seaward.

A.

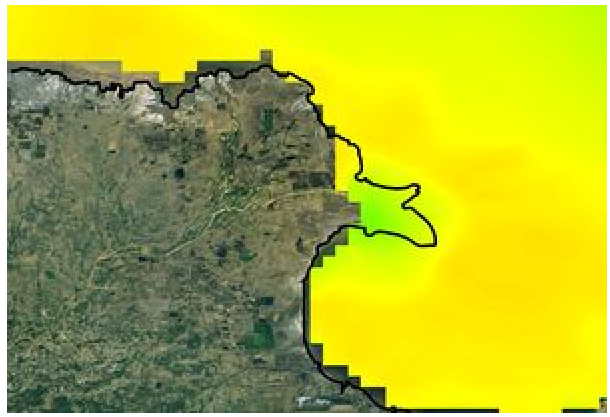

B.

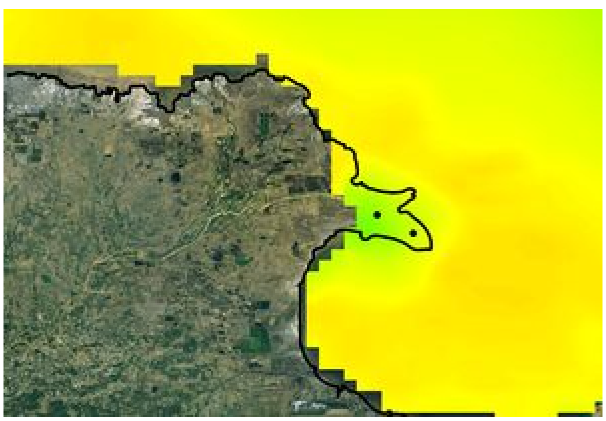

C.

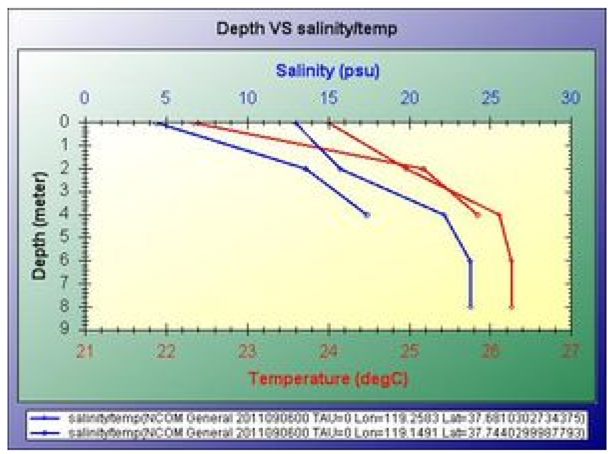

D.

References

Bi, N. S., Z. S. Yang, H. J. Wang, D. J. Fan, X. X. Sun, and K. Lei, 2011: Seasonal variation of suspended-sediment transport through the southern Bohai Strait. *Estuarine Coastal and Shelf Science*, 93, 239-247.

Fang, Y. F., G. Fang and Q. Zhang,, et al. 2000: Numerical simulation and dynamic study of the winter time circulation of the Bohai Sea. Chinese *Journal of Oceanology and Liminology*, 18, 1-9.

Guan, B., 1994: Patterns and structures of the currents in Bohai, Huanghai and East China seas. *Oceanology of China Seas*, Y. L. D. Zhou, C.K. Tseng, Ed., Kluwer Academic Publishers, 17-26.

Section 6: Appendices

Appendix A. User Guide Version 0.1

Introduction

The MV&V (Model Validation and Verification) tools are designed for the user, (geophysical subject matter expert) to validate and verify numerical ocean model output, particularly currents in shallow water and littoral regions. The suite of tools comprising the MV&V provides a user interface designed as a set of customizations of ArcMAP, a powerful software package using geographic information system (GIS) technology developed by Environmental System Research Institute (ESRI), Inc. Microsoft Visual Studio is used to develop the software and provides a rapid development path for invoking the powerful GIS functionality of ArcMAP using ArcObjects coupled with helpful classes such as ZedGraph and the netCDF library. Thus, MV&V is designed and built with an object-oriented approach that incorporates listeners, dialog boxes, interactive displays, clickable buttons all put together to offer the user a set of tools tailored to the work at hand. MV&V is made of classes and modules to make an interface that offers a certain environment and language in which the oceanographer is familiar and comfortable, while providing environmental information in a common geographic reference frame.

Implemented using a GIS display and associated GUIs, users can display geophysical data derived from observations collected in a variety of ways, their locations on the map and information about that data in tables and graphs. Geophysical parameters made available in four dimensions can be displayed on the map in 2-dimensional layers which can be enhanced for visualisation. Typically, the form of data which we will call a “dataset” but usually known as “models” comes from numerical model output intended to provide prediction information and typically comes in the form of netCDF files in the COARDS convention.

The next section will provide guidance in setting up and installing MV&V to get the user started. Then a substantial section describes each of the user tools in detail. Along the way in this manual are associated notes, tips, and comments that explain behind-the-scenes concepts, indicated by "NOTE", "TIP", and "BTS", respectively. Included is an Appendix with tips and section with frequently asked questions.

Setup

SYSTEM REQUIREMENTS

- Microsoft Windows XP Operation System (32-bit) Professional Edition with SP3 or Microsoft Windows 7.
- ArcMAP version 10.0 with Spatial Analyst License
- ArcMAP Toolboxes
    - Conversion Tools

- Data Management Tools
    - Multi-dimension Tools
    - Spatial Analyst Tools
- Latest netCDF.dll in the system directory
- Hardware
    - 1.6 GHz recommended or higher
    - Intel Core Duo, Pentium or Xeon Processors
    - 1 GB minimum RAM
    - 24-bit colour depth display
    - Screen resolution 1024x768
    - Swap space 500 MB minimum
    - Disk space 3.2 GB

INSTALLATION

The installation process is user-oriented, i.e. it is controlled by the user and alters only user's environment and files. No administrative help is required.

- Click on the ModelVV.esriAddin file to install MV&V using a window (Figure A1).
- If the installation fails, verify that ArcMAP is installed on the computer by starting ArcMAP. Close ArcMAP then attempt to install MV&V again using the same file.

Figure A1. MV&V Add-In Utility Window. Tip: Whenever you install an updated add-in, save your work and close ArCMAP before installing.

STARTING MV&V

To get started with the MV&V process, the main procedure box is opened in the following way:

- Start ArcMAP with a new empty map. Opening some other .mxd file may be a way to quickly add data in a new project. Otherwise opening a project file as described below will open a previously saved .mxd file, and clear out data from any previous work.
- If the MV&V Tools button is not visible, right click on the ArcMAP menu bar and select ModelVV Tools from the list (Figure A2)

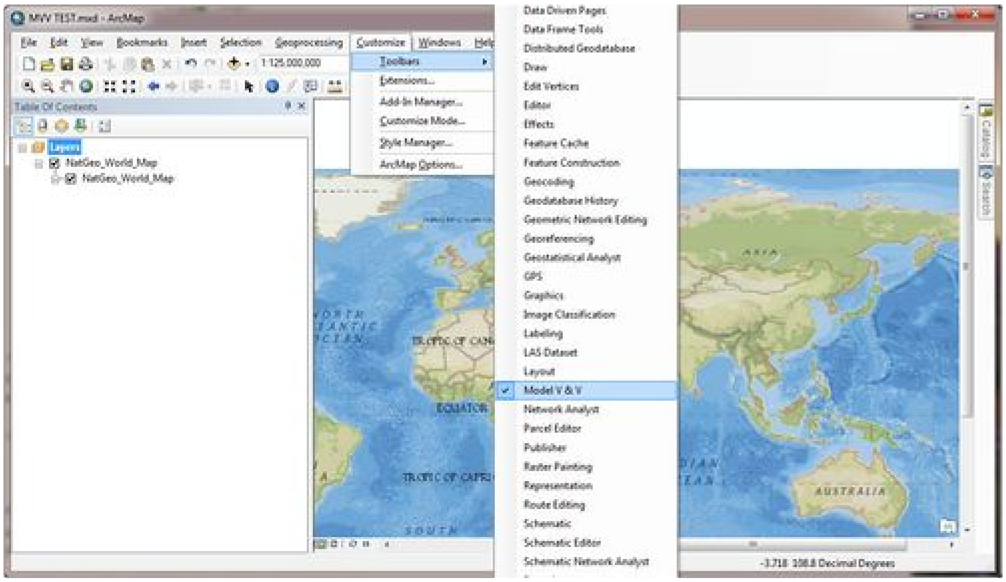

Figure A2. Selecting MV&V from the customizing list of tools.

- Start MV&V by clicking the MV&V button in the MV&V toolbar. This will open the MV&V main procedure box (Figure A3) and present you blank entries and subdued buttons.

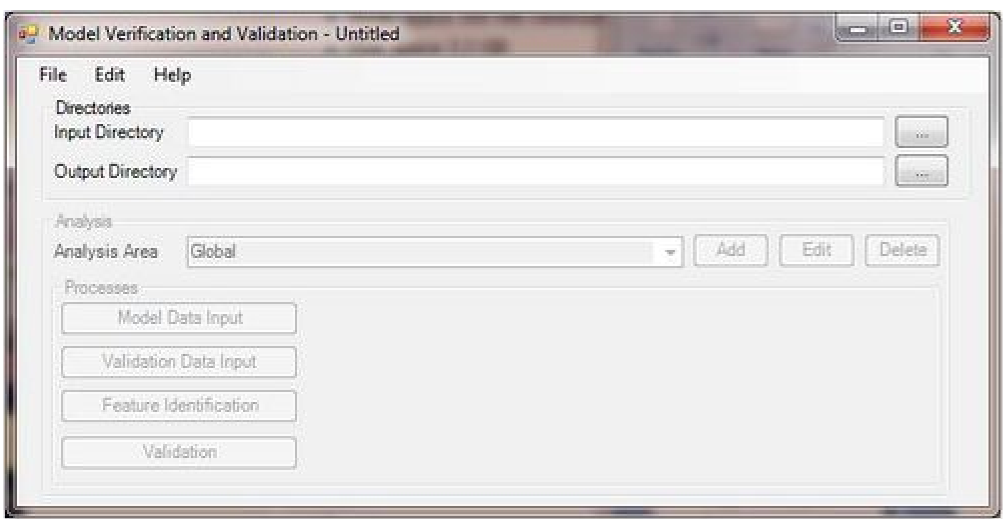

Figure A3. Model V&V main procedure box before starting the analysis.

- A companion window call the MV&V Analysis box for user entries will also open (Figure A4). Entries can be made in any of the available tabs at any time. This companion is gone forever once you click the X button. You'll have to restart ArcMAP, a situation that is being looked at. In other words, don't push the red button.

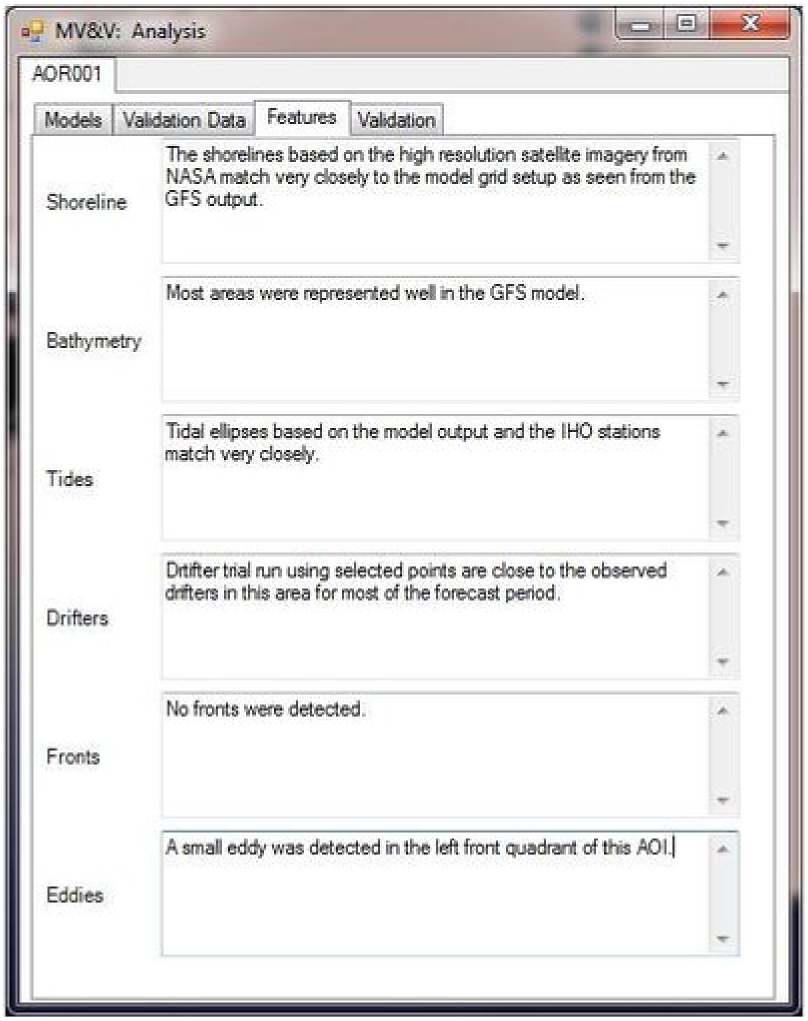

Figure A4. ModelV&V analysis entries are made in this box.

MV&V MENU ITEMS

The top left three menu items are described as follows:

- File: Start a new project; open an already saved project; save a project; create a report; and exit the MV&V module. Project files are saved with the .mvv extension and has human readable information. BTS: An accompanying .mxd file is also saved with the project file. Creating the report is still work in progress.

- Edit: Properties on the overall behaviour of MV&V; adjusting symbols such as arrows of a feature layer; and adjust the colour scheme of a raster layer.
- Help: Self-explanatory. NOTE: Work in progress.

MV&V Properties

Properties for the overall behaviour of MV&V include directory locations for for executables; map projection of this session; and netCDF file data handling behaviour (Figure A5).

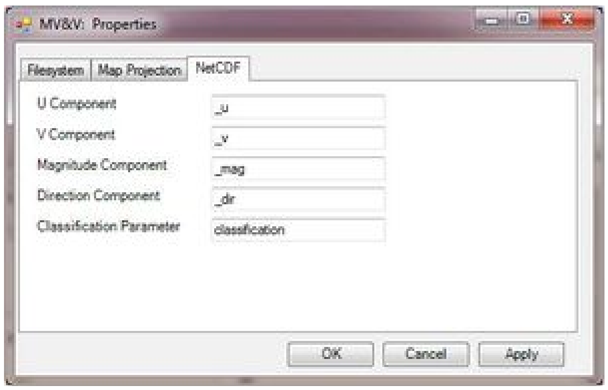

Figure A5. Model V&V properties.

FILE SYSTEM

Certain paths to files are specified here. At this time just the location for the key executable for the Drifter tool, *opie.exe*, is specified.

MAP PROJECTION

One radial button can be selected for the desired projection. Geographic coordinates are normally selected at first, but others might be more appropriate. For instance, Polar coordinates should be used for analysis in the polar regions, and Mercator for the equatorial. In the latter case when the international date line runs through the analysis area, the Data Location should be set to something like -180 to shift the map so that this area is covered in a connected way.

NETCDF FILE

Configures how certain components or read. The NetCDF File settings include those options associated with the variables and attributes in the netCDF files. The settings are used to search the netCDF files for specific information. The U Component and V Component settings are used to search the netCDF file for two variables which are identical with the exception of the u- and v-components. If these two variables are located, the Add Layer tool will use them to calculate magnitude and direction so that a vector layer can be added to ArcMAP. Similarly, the Magnitude Component and Direction Component are used to find two variables which are identical with the exception of the magnitude and direction components so that a vector layer can be added to ArcMAP; however, this layer is directly connected to the netCDF file. The Classification Parameter is used to locate the attribute for the security classification of the netCDF file. This security classification is used as the security classification for the layers created from the netCDF file.

MV&V INPUT AND OUTPUT DIRECTORIES

First thing is to establish the connections to the data in a file system. Once done, the process buttons below as shown on Figure A6 are ready to go and you will then be able to select additional analysis areas besides the global default. Also, as you procede through the various procedural items another button besides the procedure will appear labeled Started. This is a toggle button that the used can click to label it Completed as an aid to the user.

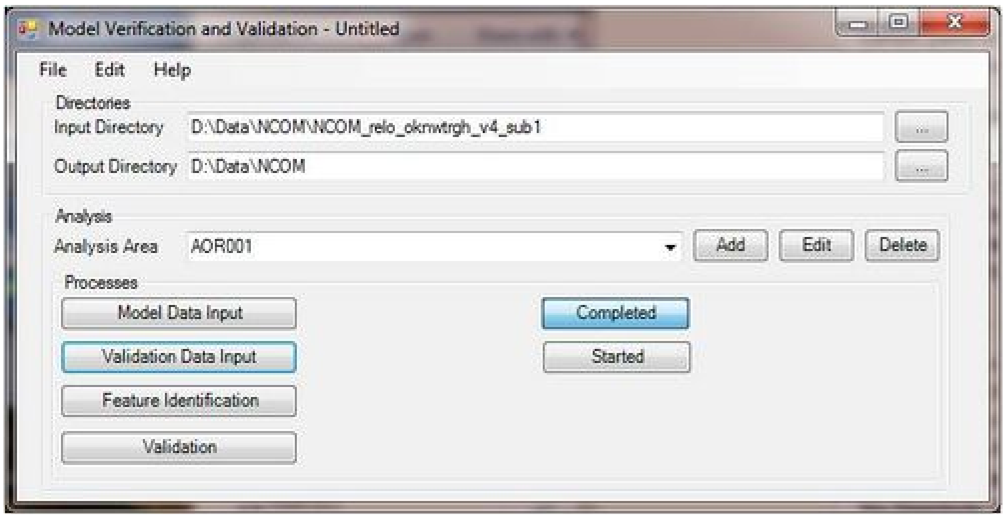

Figure A6. ModelV&V main procedure box with input and output directories entered making ready for analysis.

Analysis Procedure

Other analysis areas may be specified, but it may be prudent to display the model output to be analyzed on the map first for reference.

MODEL DATA INPUT

Clicking on the Model Data Input button opens the menu box where you enter a name of your choice in Model Name and then click the Add button to select the set of netCDF output model files for this analysis. Once this is done, click on Save and some of the buttons within the Prcedures section are made available (Figure A7).

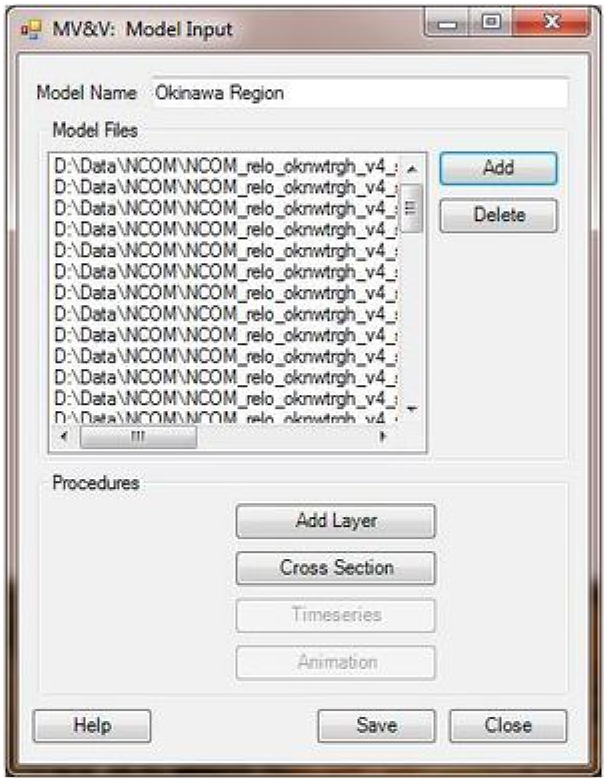

Figure A7. Model V&V Model Input after a name and a group of files are selected.

Add Layer . This tool window allows the user to select a field from the added NetCDF files and display a raster layer and for directional data also a feature layer on the map (Figure A8).

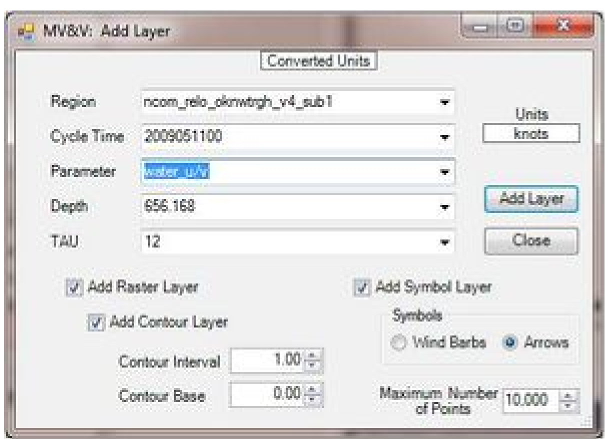

Figure A8. Add Layer window for selecting fields for display.

Cross-Section Form. This tool window allows the user to select a line on the map along which a cross section is created with the user-selected field (Figure A9).

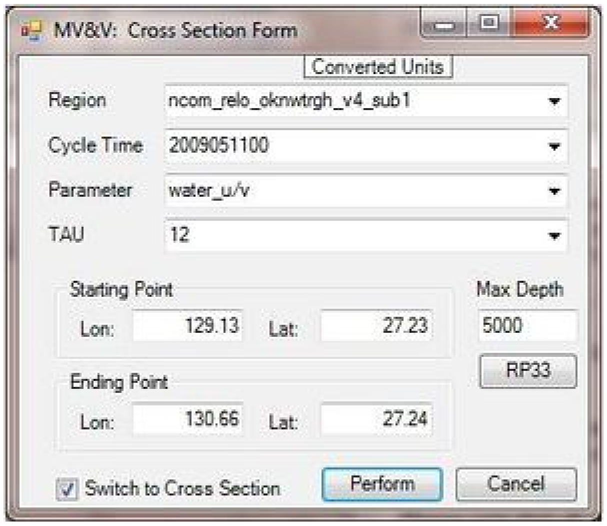

Figure A9. Cross section form window for selecting fields for display in a cross section.

ANALYSIS AREA

Now that model netCDF data has been selected for input and a layer can be added for reference, additional sub areas may be selected for analysis. Referring back to Figure A6, clicking the Add button opens a box (Figure A10) where a Name can be entered and boundaries can be specified. In conjuction with typing the values in, actions with the mouse on the map with a rubberband bounding box can also be used in specifying the values. The Edit button allows new areas (other than the global default) to be changed, whilst the Delete button is available for removing these new regions.

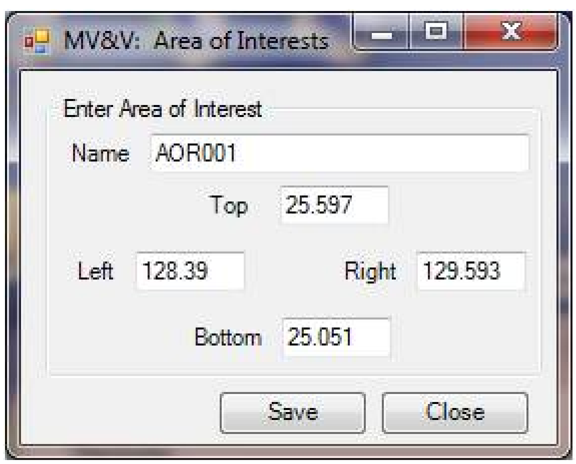

Figure A10. Area of interest selection box in conjuction with mouse action of a rubberband bounding box on the map helps select that values for the bounding box.

VALIDATION DATA INPUT

This step is the user's oportunity to load different types of data for validation. This data can be measurements, in situ or remotely sensed, or other model output. The Validation Data Input menu (Figure A11) offers buttons to several tools for adding layers to the map and thus to the table of contents (TOC). NOTE: The only active buttons are METOC and models.

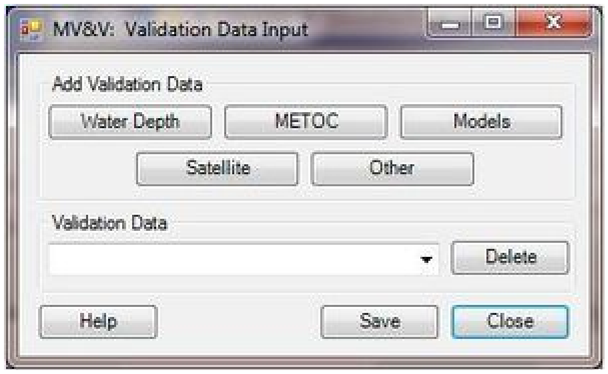

Figure A11. Add validation data with this menu.

FEATURE IDENTIFICATION

Here we implement tools to help us identify features that are relevant in helping as verify the model performance (Figure A12).

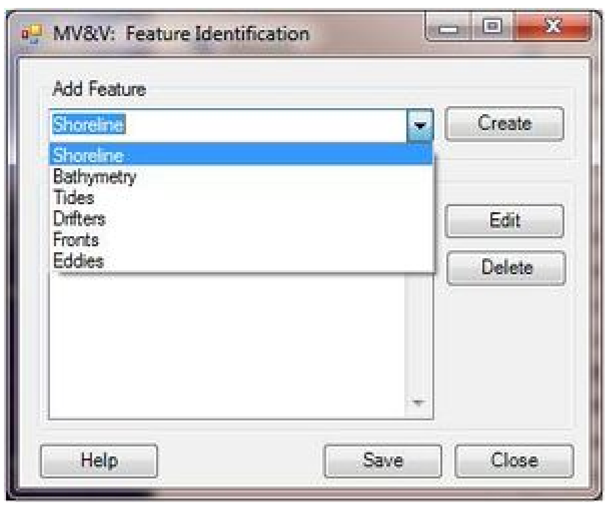

Figure A12. Feature Identification menu for selection various tools to aid in this identification.

The first important aspect of the model performance is the location of the shoreline. The shoreline tool allows us to draw the shoreline based on high resolution imagery or other sources of information on the map. The bathymetry tool helps us to match that bathymetry based on currently available data to what the model considers bathymetry.

In the littoral regions, tides are a very important feature to identify. In many cases the currents are predominantly influenced by the tides. The tidal ellipses tool will help us draw ellipses for selected locations to give us an indication of the tides from the model output. These results can be matched to the results of analyses based on published data. Tidal water levels are an indication of tidal flow; these can be evaluated using the time series tool for comparison to available data bases (e.g., IHO tide tables).

The drifter tool allows us to draw drifter trajectories selected points on the model output for a user selected period of time. These then can be compared directly to observational drifters on the map.

Fronts can be drawn on the map whether they be based on temperature gradients from the model output or from observation of data measurements such as remotely sensed data in the form of multi channels sea surface temperature. Qualitative comparisons can then be made.

Eddies can be indicated on the map by drawing a rectangular box around the feature resulting in an ellipse that has eccentricity based on the shape of the rectangle. You could indicate either cold or warm core. The indices for these rectangular boxes can also be file input.

Validation. Based on your analysis of the features and how they compare between the model and other sources of information, you then provide here your assessment of the model performance.

Appendix B. Comma-Separated File Format

The drifter data was made available in the following format:

Column	**Data**
1	ID Number
2	Year
3	Month
4	Day
5	Hour
6	Minute
7	Second
8	Latitude
9	Longitude
10	Unknown code
11	Unknown value
12	Unknown value

Appendix C. Sample Model Validation File (*.MVV)

A sample validation file for this analysis could look like this, *msb20110927.mvv*:

```
Mississippi Bight;
NCOM;
2005030700;
96;
27 September 2011;
27 September 2011, 28 September 2011;
28 September 2011;
Tim Keen;
3;
A -89.5 26.4 -88.5 29.1;
historical observations;
"\d\My Documents\PROJECTS\MODEL_VALIDATION\SLIDES\esl_chl_1.jpg",
"\d\My Documents\PROJECTS\MODEL_VALIDATION\SLIDES\esl_chl_2.jpg";
1.0;
surface filaments are present offshore as in noncoeval imagery;
1.0;
okay because there are no coastlines or other important features in error,
sensitive to wind errors;
B -90.1 26.5 -88.7 30.1;
shoreline;
"\d\My Documents\PROJECTS\MODEL_VALIDATION\GOOGLE_EARTH\msb_cat.xyz",
"\d\My Documents\PROJECTS\MODEL_VALIDATION\GOOGLE_EARTH\msb_coast.xyz";
1.0;
good coastline from ngli project;
tidal observations and water level;
"\Z\ARCHIVE\DATA\TYPE_OF_DATA\tides\CatIsland.dat",
"\Z\ARCHIVE\DATA\TYPE_OF_DATA\tides\MobilePoint.dat",
1.0;
good phase with some underprediction of amplitude;
historical observations;
"\Z\ARCHIVE\DATA\TYPE_OF_DATA\tides\BAY_ST_LOUIS_2005.dat";
"\d\My Documents\PROJECTS\MODEL_VALIDATION\SLIDES\esl_chl_1.jpg",
"\d\My Documents\PROJECTS\MODEL_VALIDATION\SLIDES\esl_chl_2.jpg",
"\d\My Documents\RESOURCES\MY_REPRINTS\2002_Keen_JCR_MB.pdf";
1.0;
water level at bay st louis yacht club from dec 2005 has good subtidal
comparison,
plumes evident through tidal passes between islands,
water level at cat island similar to march 1997 cold front,
surface currents in cat island channel similar to march 1997,
tidal asymmetry at cat island channel reproduced;
model comparison;
"Marine Geology 186 (2002) 423-446",
"Marine Geology 210 (2004) 79-105",
"Journal of Coastal Research 18 (2002) 622-636",
"Geophysical Research Letters 33 (2006) L23614 doi:10.1029/2006GL027981";
1.0;
similar flow as in other hurricane models from region (katrina),
similar prefrontal flow as predicted by pom in march 1997 cold front,
some discrepancy in postfrontal flow;
weather pattern;
0.5;
```

postfrontal flow in wrong direction could be due to nogaps wind error;
C -90.1 26.2 -89.0 28.1;
Up to date shoreline used;
shoreline;
"\d\My Documents\PROJECTS\MODEL_VALIDATION\GOOGLE_EARTH\msb_chandeleur.xyz",
"\d\My
Documents\PROJECTS\MODEL_VALIDATION\GOOGLE_EARTH\msb_chandeleur_south.xyz",
"\d\My Documents\PROJECTS\MODEL_VALIDATION\GOOGLE_EARTH\msb_coast.xyz";
0.5;
Old position of western shore;
bathymetry;
"google earth";
0.5;
okay in area defined by box,
large intertidal areas will influence model;
tidal observations;
"\Z\ARCHIVE\DATA\TYPE_OF_DATA\tides\BretonIsland.dat";
1.0;
good phase but weak amplitude;
historical observations;
"\d\My Documents\PROJECTS\MODEL_VALIDATION\SLIDES\esl_chl_1.jpg",
"\d\My Documents\PROJECTS\MODEL_VALIDATION\SLIDES\esl_chl_2.jpg";
1.0;
patches of high [chl] in breton sound match similar images;
0.25;
bathymetry errors will influence coastal flow in this area;

Appendix C. Class Diagram